



This is to certify that the

dissertation entitled

High Pressure Multi-Phase Equilibrium
of Carbon Dioxide with Organic Solids
in Binary and Ternary Systems

presented by

Gary Leon White

has been accepted towards fulfillment
of the requirements for

Ph.D. degree in Chemical Engineering

Major professor

Date 10/16/91

LIBRARY
Michigan State
University

PLACE IN RETURN BOX to remove this checkout from your record.
TO AVOID FINES return on or before date due.

DATE DUE	DATE DUE	DATE DUE
_____	_____	_____
_____	_____	_____
_____	_____	_____
_____	_____	_____
_____	_____	_____
_____	_____	_____
_____	_____	_____

MSU is An Affirmative Action/Equal Opportunity Institution

c:\crl\datedue.pm3-p.1

**HIGH PRESSURE MULTI-PHASE EQUILIBRIUM
OF CARBON DIOXIDE WITH ORGANIC SOLIDS
IN BINARY AND TERNARY SYSTEMS**

By

Gary Leon White

A DISSERTATION

Submitted to
Michigan State University
in partial fulfillment of the requirements
for the degree of

DOCTOR OF PHILOSOPHY

Department of Chemical Engineering

1991

ABSTRACT

HIGH PRESSURE MULTI-PHASE EQUILIBRIUM OF CARBON DIOXIDE WITH ORGANIC SOLIDS IN BINARY AND TERNARY SYSTEMS

By

Gary Leon White

To test and improve predictive models for multi-component systems, the loci of the phase boundaries must be known. Such data for systems involving solids in contact with supercritical fluids are still relatively scarce. The objective of this work is to address that shortage by acquiring new data from equilibrium measurements in new systems and by modeling the observed phase behavior using an equation of state.

An apparatus capable of providing phase equilibria data for solid/SCF systems was designed and constructed. The system consisted of a view cell to permit visual observation of the phase behavior, a mechanism for sampling fluid phases within the cell, and the equipment to control the pressure and temperature in the cell. P-T-v-x-y data for the CO₂+naphthalene system and P-T data for the CO₂+phenanthrene system were measured along the SLV lines. P-T data were obtained along the SSLV lines for the CO₂+naphthalene+ τ ternary systems where the third component τ = biphenyl, phenanthrene, acenaphthene, or anthracene. Seven sets of P-T-v-x-y data were obtained in the three phase regions of the CO₂+naphthalene+biphenyl ternary system. As expected,

the binary systems studied exhibit melting point depressions of the solids along the SLV line with temperature minimums before terminating in upper critical end points. The phase behavior of the CO₂+naphthalene+biphenyl and CO₂+naphthalene+phenanthrene systems was different than expected. Both exhibit eutectic melting point depressions along their respective SSLV lines, but each intersects an invariant point of undetermined type at a pressure much lower than the upper critical end points of the constituent solid/supercritical fluid binaries.

The data were used to test a modification of the Peng-Robinson equation of state to determine if improving the volume predictions for the pure components could also improve the phase equilibrium predictions for mixtures of these components. The results of the modeling indicate that improving the predictions of the pure component volumes by volume translations can sometimes improve the equilibrium phase predictions for mixtures. The improvement is most dramatic when the translations are largest.

To Sunshine

ACKNOWLEDGMENTS

I wish to thank Dr. Carl T. Lira for the considerable time and effort he has spent teaching me and advising me on this project. I am especially appreciative of his patience when the work was going slow or when family duties diverted my attention temporarily from research.

I also wish to thank Dr. Victoria McGuffin and her students for helping me resolve difficulties in the GC analysis necessary for this work.

Partial support for this work by NSF Grant No. CBT10705 is gratefully acknowledged.

I would like to thank the Michigan State University and the Gerstacker Foundation for their financial support during this work.

I am thankful to my parents for their emotional support as well as for loaning me the funds to support myself and my family during my last term at MSU.

Most of all I want to thank my wife Kathy who has endured 7 1/2 years of married student life while I completed three college degrees.

TABLE OF CONTENTS

LIST OF TABLES	viii
LIST OF FIGURES	ix
CHAPTER 1: INTRODUCTION	1
CHAPTER 2: BACKGROUND ON MULTI-PHASE EQUILIBRIUM . . .	5
Phase Diagrams for Supercritical	
Fluid-Solute Mixtures	5
Historical Perspective	14
Experimental Studies of Solid-SCF Systems .	14
View Cells	19
Composition Determinations	21
CHAPTER 3: EXPERIMENTAL APPARATUS	24
View Cell	24
Temperature Control	26
Pressure Control	26
CHAPTER 4: EXPERIMENTAL PROCEDURE	30
Melting Point Curve Determination	30
Sampling	36
Composition Analysis	47
Materials	47
CHAPTER 5: EXPERIMENTAL RESULTS	49
Melting point experiments	49
Composition measurements	52

CHAPTER 6: PREDICTIVE MODELING	58
Phase Equilibrium	60
Solid Fugacities	61
Liquid Fugacities	62
Vapor or Supercritical Phase Fugacities . .	64
Peng-Robinson Equation of State	66
Translated Peng-Robinson Equation of State	67
Calculations and Comparison of Results . .	69
CHAPTER 7: CONCLUSIONS AND RECOMMENDATIONS	83
Conclusions	83
Recommendations	86
APPENDICES	
APPENDIX A: GC CALIBRATION	91
APPENDIX B: SAMPLE LOOP VOLUME DETERMINATIONS	94
APPENDIX C: ITERATION SCHEME FOR SLV AND SSLV LINE	
DETERMINATIONS	96
APPENDIX D: COMPUTER CODE FOR CALCULATING SLV AND SSLV LINES	
.	99
APPENDIX E: ITERATION SCHEME FOR ISOTHERMAL SLV LINE	
DETERMINATIONS IN TERNARY SYSTEMS	124
APPENDIX F: COMPUTER CODE FOR CALCULATING ISOTHERMAL SLV	
LINES IN TERNARY SYSTEMS	128
APPENDIX G: EQUATION OF STATE PARAMETER DETERMINATIONS	138
APPENDIX H: RAW COMPOSITION DATA	146
BIBLIOGRAPHY	155

LIST OF TABLES

Table 2.1	Previously Investigated Type F SCF + Solid Systems	17
Table 2.2	Ternary Systems	19
Table 4.1	Purity of Materials	48
Table 5.1	Experimental Pressure-Temperature Data Along the SLV and SSLV Equilibrium Lines for 6 CO₂+Hydrocarbon Systems	50
Table 5.2	P-T-v-x-y Data for the CO₂+Naphthalene System.	53
Table 5.3	P-T-v-x-y Data for the CO₂+Naphthalene+Biphenyl System.	53
Table 6.1	Pure Component Triple Points	75
Table 6.2	Binary Eutectic Temperatures	75
Table B.1	Data for volume determination of sample loop 1	95
Table B.2	Data for volume Determination of sample loop 2	95

LIST OF FIGURES

Figure 2.1	Six types of binary fluid phase behavior. . .	7
Figure 2.2	Type F fluid phase diagram.	8
Figure 2.3	P-T traces in a ternary system with discontinuous critical locus.	11
Figure 2.4	Ternary composition diagram at fixed pressure and temperature.	13
Figure 3.1	Cross-sectional diagram of the view cell. . .	25
Figure 3.2	Constant temperature bath.	27
Figure 3.3	Pressure control.	28
Figure 4.1	Depression of eutectic melting point by a supercritical fluid in an A-B-SCF system where A, B are immiscible solids and $P_1 < P_2 < P_3$. . .	31
Figure 4.2	Methods for finding first melting points along SLV or SSLV phase boundary.	35
Figure 4.3	Sampling system.	38
Figure 4.4	Sampling positions for the 10-port HPLC valve.	39
Figure 5.1	S-V region beyond the end point of the CO_2+naphthalene+phenanthrene SSLV line. . . .	51
Figure 5.2	Comparison of liquid composition measurements along SLV line for the CO_2+naphthalene system.	55
Figure 5.3	Comparison of data from this work and that of Lu and co-workers.	56

Figure 6.1	Predicted and measured SLV P-T traces for the CO₂+naphthalene system.	70
Figure 6.2	Predicted and measured SLV P-T traces for the CO₂+biphenyl system.	71
Figure 6.3	Predicted and measured SLV P-T traces for the CO₂+phenanthrene system.	72
Figure 6.4	Predicted and measured SLV P-T traces for the CO₂+naphthalene+biphenyl system.	73
Figure 6.5	Predicted and measured SLV P-T traces for the CO₂+naphthalene+phenanthrene system.	74
Figure 6.6	Predicted and measured P-x-y plot along the SLV line for the CO₂+naphthalene system.	78
Figure 6.7	Predicted and measured P-x-y plot along the SLV line for the CO₂+biphenyl system.	79
Figure 6.8	Predicted and measure P-x-y plot along the SLV line for the CO₂+phenanthrene system.	80
Figure 6.9	Comparison of equation of state phase equilibrium predictions to experimental data.	81
Figure G.1	Comparison of fits of the SLV P-T trace for different values of k_{ij} in the Peng-Robinson equation for the CO₂+naphthalene system.	140
Figure G.2	Comparison of fits to the P-x-y plot along the SLV line for the CO₂+naphthalene system.	141
Figure G.3	Comparison of fits of the SLV P-T trace for different values of k_{ij} in the Peng-Robinson equation for the CO₂+biphenyl system.	142

- Figure G.4** Comparison of fits to the P-x-y plot along the SLV line for the CO₂+biphenyl system. . . . 143
- Figure G.5** Comparison of fits of the SLV P-T trace for different values of k_{1j} in the Peng-Robinson equation for the CO₂+phenanthrene system. . 144
- Figure G.6** Comparison of fits to the P-x-y plot along the SLV line for the CO₂+phenanthrene system. . 145

CHAPTER 1

INTRODUCTION

A supercritical fluid is defined as a component or mixture of components above its critical temperature and pressure. The first experiments demonstrating the ability of a supercritical fluid (SCF) to act as a solvent were reported over a century ago by Hannay and Hogarth (1879). For some time this observation remained little more than a scientific curiosity, but in the last twenty years, supercritical fluids and their unusual solvent properties (such as strongly pressure dependent solvating power) have been applied to an ever widening spectrum of processes. Most current uses are in the petroleum industry for such processes as deasphalting heavy crude oils and enhanced oil recovery and the food processing industries for decaffeination of coffee and extraction of flavors and aromas. Some applications in the areas of chemical and polymer processing and waste treatment are now in research and development. Supercritical fluid chromatography (SFC) has also emerged as a valuable analytical tool. Full development of these processes, however, will require a more thorough understanding of the thermodynamics of high pressure systems involving supercritical fluids.

In general, the better a process is understood, the more fully and effectively it is utilized. Distillation, for example, has been studied and employed for centuries as

a separations method. It is now arguably a very well characterized operation. Engineers continue to improve the technology of distillation, but most improvements are now relatively incremental.

Less well understood but potentially valuable technologies, such as supercritical fluid phase operations, remain underutilized. Full exploitation of the potential of these emerging processes will require the acquisition of additional fundamental data, and the development and testing of models to accurately interpret these data and represent the underlying thermodynamics.

One notable area in which knowledge is still deficient is the thermodynamics of multi-phase systems involving solids and supercritical fluids. (In this dissertation, the term "solid" refers to compounds which are solid at atmospheric pressure and room temperature.) As noted by McHugh and Krukoniš (1976):

"... high pressure phase-behavior can be complex even for simple binary mixtures in which the components are chemically similar but have different molecular sizes ... "

In supercritical fluids, the molecules are likely to be packed nearly as densely as in a liquid. Interactions based on molecular shape, size, polarity, polarizability, or even relative orientation can have a profound effect on the phase behavior of such systems.

To test predictive models for multi-component systems, the loci of the phase boundaries must be known. Such data

for systems involving solids in contact with supercritical fluids are still relatively scarce.

The goals of this work were: 1) to construct an apparatus capable of providing phase equilibria data for solid/SCF systems, 2) to expand the existing data base with new measurements on both previously studied systems and new systems for which little or no data existed, and 3) to test a modification of the Peng-Robinson equation of state to determine whether improving the volume predictions for the pure components could also improve the phase equilibrium predictions for mixtures of these components.

The system assembled for this work consisted of a view cell to permit visual observation of the phase behavior, a mechanism for sampling fluid phases within the cell, and the necessary equipment to control the pressure and temperature in the cell. This apparatus proved suitable for obtaining the desired phase equilibria data. Several recommendations will be made at the conclusion of this dissertation, however, which would improve its capabilities.

In this work, P-T-V-x-y data for the CO₂+naphthalene system and P-T data for the CO₂+phenanthrene system were measured along the SLV lines. P-T data were obtained along the SSLV lines for the CO₂+naphthalene+r ternary systems where the third components r = biphenyl, phenanthrene, acenaphthene, or anthracene. Four sets of P-T-V-x-y data were also obtained in the three phase regions of the CO₂+naphthalene+biphenyl ternary system. These systems were

chosen for reasons of safety, availability, and the likelihood that they would form the type of systems of interest for this work. The systems did form the desired type of binary systems, but the phase behavior of some of the ternary systems was a little different than expected.

The results of the modeling of the systems in this work indicate that improving the predictions of the pure component volumes by volume translations can improve the equilibrium phase predictions for those components in mixtures. The improvement is most conspicuous when the translations are largest.

The remaining chapters in this dissertation discuss in more detail the phase behavior being studied, the methods and models used to study them in this work, and how this work relates to corresponding work done elsewhere.

CHAPTER 2

BACKGROUND ON MULTI-PHASE EQUILIBRIUM

To put the work reported in this dissertation in perspective and clarify some of the terms necessary to describe the observed behavior, a short discussion of phase diagrams is presented. To simplify this discussion, the phase diagrams for mixtures of a single SCF with a single solute will be used to provide a basis for understanding and explaining the phase behavior of multi-component SCF-solute mixtures.

Phase Diagrams for Supercritical Fluid-Solute Mixtures

According to the Gibbs phase rule, the degrees of freedom in any non-reacting system may be determined by the relation:

$$F = 2 + C - P \quad (2.1)$$

Where F is the degrees of freedom (number of independent intensive variables), C is the number of components, and P is the number of phases. In a binary system, this means that when three phases are in equilibrium, such as a solid, a liquid and a vapor, specifying a single intensive variable will fix the values of all other intensive variables. Alternatively, if a critical phase is present, two of the degrees of freedom are used by equations which define a critical condition. Where four phases are in equilibrium or

a single phase is in equilibrium with a critical phase, all variables are fixed, resulting in an "invariant point". These lines and points are shown in Figure 2.1 as projections on pressure-temperature (P-T) diagrams to illustrate the types of phase behavior which may be encountered. The letter classification scheme shown in this figure is that given by Luks (1986) and will be used in this dissertation when referring to the different classes of binary phase behavior.

Mixtures where the two components have very similar triple points and critical points tend to form type A systems. As molecular disparities increase, the triple points and critical points become more dissimilar and regions of liquid-liquid-vapor (LLV) immiscibility appear. When two components are sufficiently dissimilar, the binary mixture will form a type F system with two distinct branches separated in temperature by a solid-vapor region. This type of behavior is typical of systems where one component is a light gas such as ethane, ethylene, or CO_2 (which are commonly used SCF's) and the other component is a heavy compound which is normally solid at room temperature.

Figure 2.2 illustrates a portion of the type F P-T diagram in more detail. The light component (or SCF) is denoted by the subscript "a". Component "b" is the heavy component. C_a and C_b indicate the critical points of the respective pure components. The triple point of the pure solid is designated by the triangle. On the lower

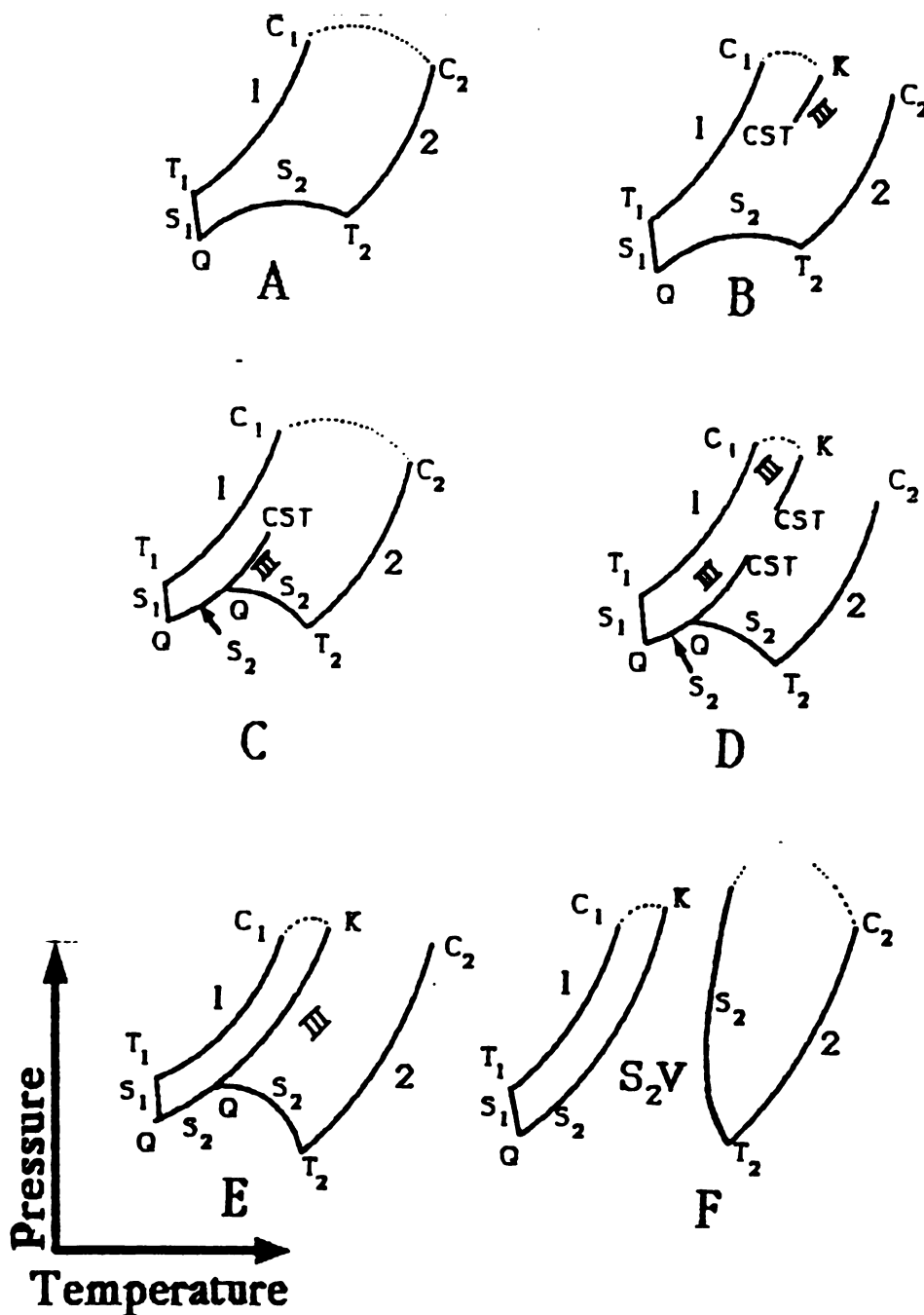


Figure 2.1

Six types of binary fluid phase behavior. T_1 and T_2 - components 1 and 2 triple points, C_1 and C_2 - component 1 and 2 critical points, S_1 and S_2 - S_1 LV (solid component 1 + liquid + vapor) and S_2 LV equilibrium lines, III - LLV equilibrium, K - critical end point, Q - quadruple point, CST - critical solution terminal point.

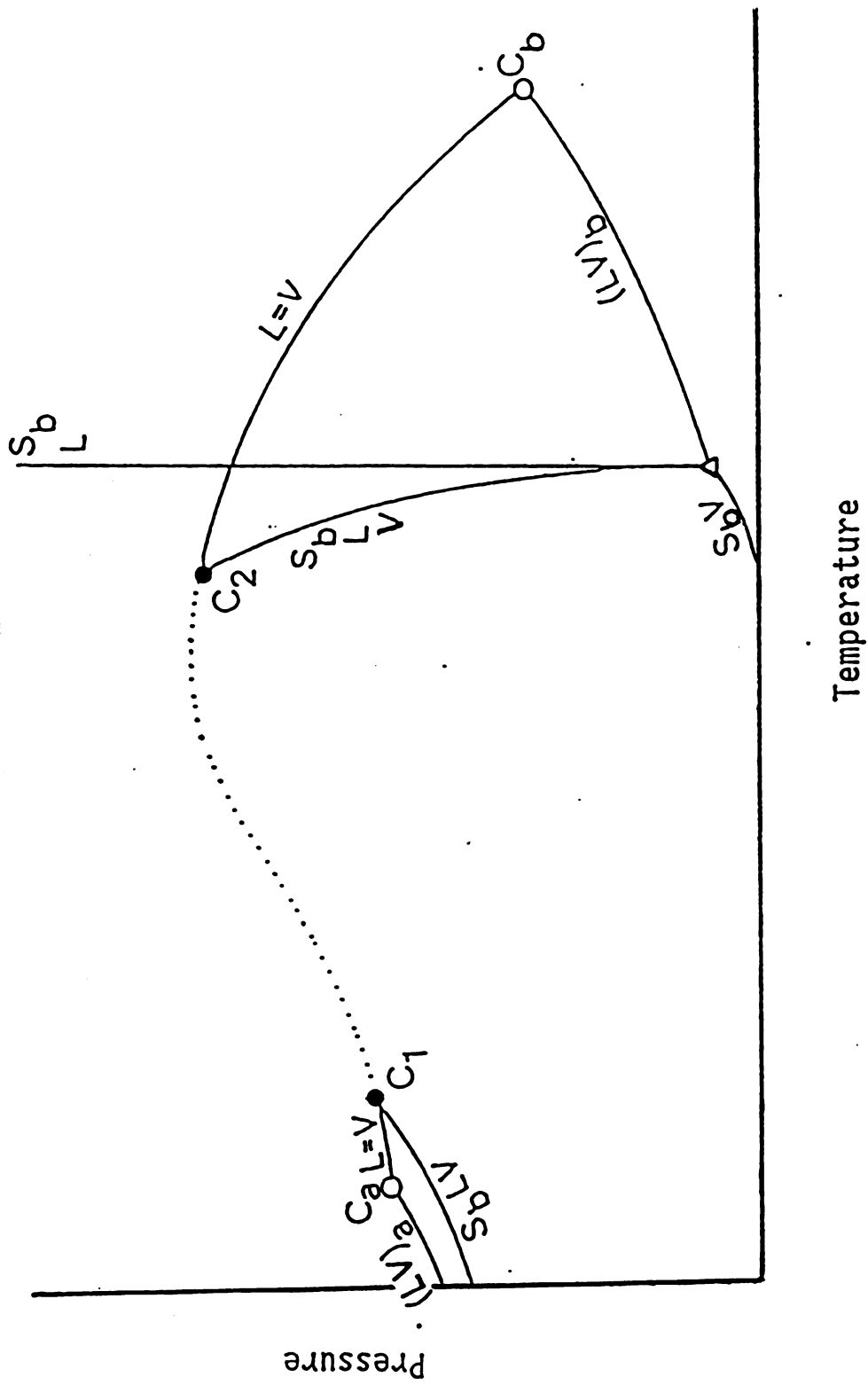


Figure 2.2 Type F fluid phase diagram.

temperature branch, the solid-liquid-vapor (SLV) line intersects the critical mixture curve at the lower critical end point (LCEP), which is denoted in Figure 2.2 as C_1 . The SLV line of such a system often lies very close to the VLE curve of the light component, and is very difficult to distinguish on a P-T plot of experimental data. The SLV line of the upper branch intersects the critical mixture curve at the upper critical end point (UCEP), which is denoted in Figure 2.2 as C_2 . This was the branch studied for the binary systems in this work. It may be noted that as more of the lighter component dissolves into the liquid with increasing pressure along this line, the melting point of the solid is initially depressed. For many systems, the slope of the upper branch SLV line on the P-T diagram remains negative until it intersects the critical mixture curve. However, for other binary systems of organic solids with CO_2 , including those studied in this work, the SLV line reaches a minimum in temperature and then begins to curve gradually back up in temperature until it reaches the UCEP.

Phase behavior in ternary systems is more complex, but analogous to that in binary systems. According to the Gibbs phase rule (eqn. 2.1), four phases may co-exist along a line on the P-T diagram. Invariant points occur where either five phases or one critical phase and two additional phases are in equilibrium. In work with a ternary mixture of ethylene, naphthalene, and hexachloroethane, van Gunst et

al. (van Gunst 1953b) observed a temperature depression of the SSLV ternary eutectic line. As shown in Figure 2.3, such systems may exhibit two ternary critical end points, designated as the "p" (lower temperature) and "q" (higher temperature) points. Ternary systems may display such an interruption of the critical locus if the binary mixtures of the individual solids with the solvent gas also have interrupted critical loci. The existence of the LCEP and UCEP for each of the SCF-solid binaries does not, however, mandate such an interruption of the ternary critical locus, i.e. type F behavior by the binaries does not always lead to type F analogue behavior for the ternary. Most of the measurements done on ternary systems in this work were carried out along the upper branch SSLV line beginning at the binary eutectic of two solids.

It can also be helpful to plot the compositions of the phases in equilibrium along the binary system SLV and ternary system SSLV lines. When a system has a critical end point the compositions of the liquid and vapor phases will meet at the critical end point. For the binary systems, all component compositions are fully represented by a single plot on a pressure vs. composition (P-x-y) diagram.

In a ternary system, a ternary or triangular diagram is needed to represent the mole fractions of all components simultaneously. Compositions may be plotted along the SSLV line, SLV isotherms, or SLV isobars. At fixed pressure and

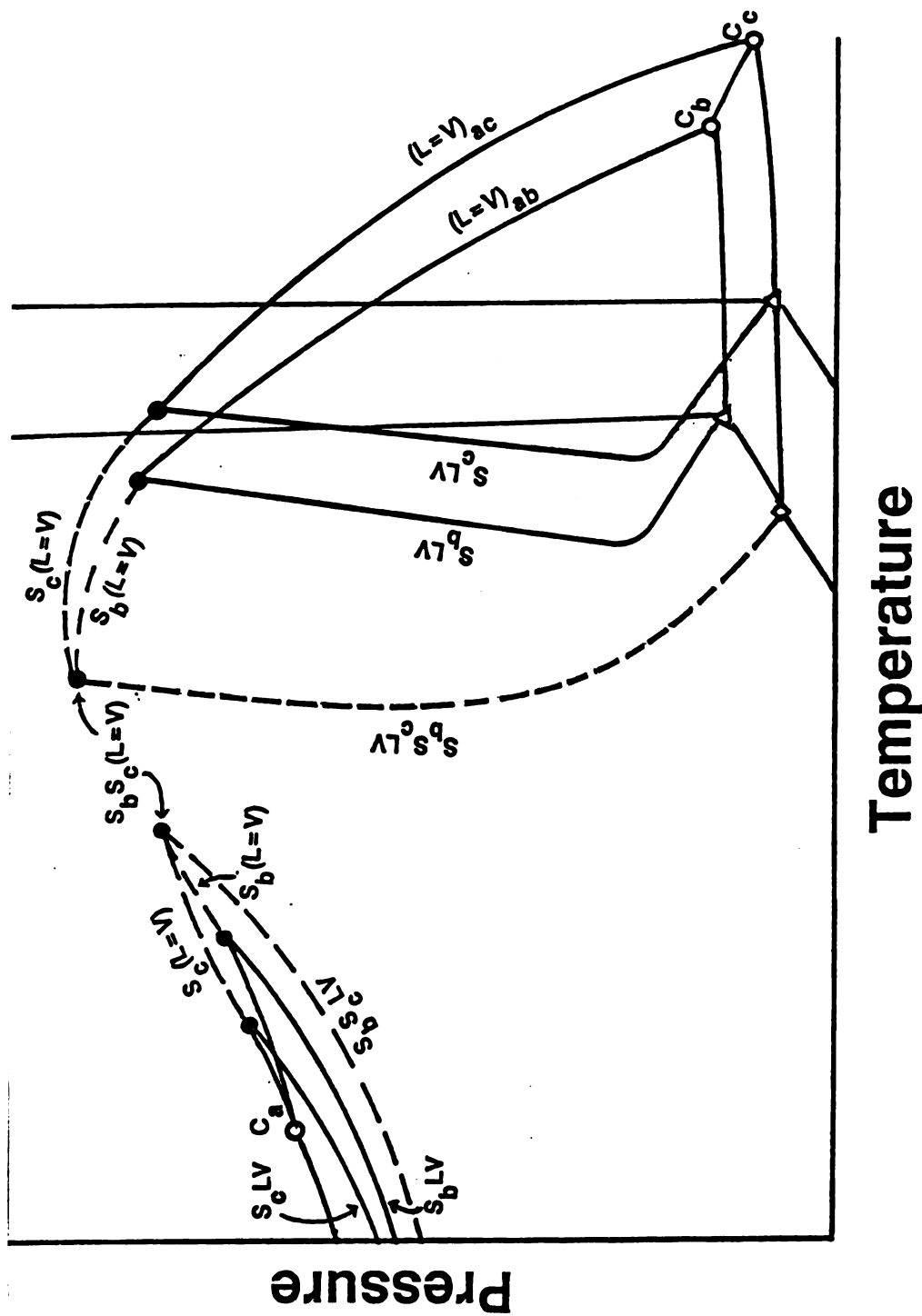


Figure 2.3 P-T traces in a ternary system with discontinuous critical locus.

temperature, phase compositions and tie lines may also be plotted on a ternary diagram.

Figure 2.4 illustrates this type of diagram for a ternary system at a pressure and temperature between the first melting and first freezing points for the two solids. This corresponds to a region in Figure 2.3 between the S_bS_cLV line and the S_bLV and S_cLV lines. Figure 2.4 shows the different types of phase behavior which would be observed at different overall compositions. In some composition regions, a single phase of variable composition will exist. For example, at high SCF solvent mole fractions, only one vapor phase will exist. In regions where two phases may coexist, tie lines specify the compositions of the equilibrium phases. The diagram also has regions where three phases will coexist at fixed compositions but in variable quantities. The circles and triangles on the diagram indicate the compositions of the vapor and liquid phases respectively at SLV conditions. Changes in pressure or temperature change the appearance of the diagram in a systematic manner. As the SSLV line is approached, the region between the circles and the triangles becomes compressed until the left and right sides merge to form a line with one circle and one triangle (which represent the equilibrium vapor and liquid compositions). As the ternary UCEP is approached, the region collapses to a single point.

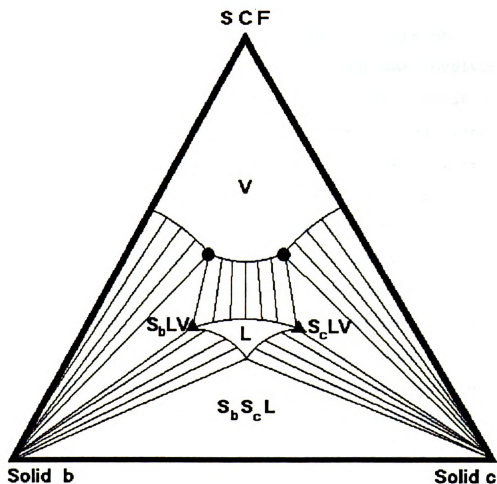


Figure 2.4 Ternary composition diagram at fixed pressure and temperature. **S** - solid, **L** - liquid, **V** - vapor, subscripts **b** and **c** refer to the two solids.

In order to put the research reported here in perspective, the remainder of this chapter is devoted to discussing the related work of other researchers.

Historical Perspective

Researchers have compiled considerable data on solubilities and phase behavior in many systems involving supercritical fluids. Much of the available information has been reviewed by McHugh and Krukonis (1986). Additionally, the two authors compiled a list of most of the reviews on the topic published up through 1985 (Paulaitis et al. 1983a, Randall 1982, Johnston 1984, Brunner and Peter 1981, Williams 1981, Irani and Funk 1977, Paul and Wise 1971, Valertis 1966) and symposium proceedings (Königstein 1984, England 1983, Paulaitis et al. 1983b, Schneider et al. 1980, Penninger et al. 1985, Charpentier and Sevenants 1987, Johnston and Penninger 1989). Since many excellent review papers and books have already been published on the subject, completely duplicating their information for this dissertation would be superfluous. The focus of this research was on phase equilibria of organic solids with carbon dioxide, so only previous work directly related to that topic is noted here.

Experimental Studies of Solid-SCF Systems

The first report of the ability of supercritical fluids to dissolve solids came in 1879 at a meeting of the Royal Society of London. Hannay and Hogarth presented the results of experiments in which they observed that changes in

pressure caused several inorganic salts to dissolve into or precipitate from supercritical ethanol (Hannay and Hogarth, 1879 and 1880). In 1896, Villard, published a review of supercritical fluid solubility phenomena including a description of the depression of the melting point of pure solid camphor contacted with ethylene at elevated pressures (Villard, 1896). E. H. Büchner also reviewed the literature in 1906, adding his own data and observations of SCF-solute systems. He reported cloud points, freezing points, and number of phases in his solubility studies (Büchner, 1906). Not long thereafter Prins studied phase behavior of naphthalene with supercritical carbon dioxide and ethylene (Prins, 1915). His experiments included determination of three-phase border curves and critical end points for naphthalene in both gases.

Most additional work on phase behavior of solids in supercritical fluids until the late 1940's was concerned with inorganic solutes and fluids such as water. In 1948 Diepen and Scheffer published a study of phase behavior of binary systems involving organic solids and supercritical ethylene (Diepen & Scheffer, 1948). In their article, they reported P-T (pressure-temperature) data along phase boundaries and critical loci for eleven systems. Nine of the systems were type F. This is the class of binary systems into which the binary systems studied in this work fall. The P-T traces of the SLV lines in those nine systems exhibit melting point depressions of the solids. Two papers

by van Gunst, Scheffer and Diepen (1953a,b) presented additional P-T phase boundary data for seven binary systems of ethylene and organic solids and one ternary system of ethylene with naphthalene and hexachloroethane. A series of papers by van Welie and Diepen in 1961 detailed the SLV boundary for the ethylene+naphthalene system including pressure, temperature, volume and phase compositions along the SLV line up to the upper critical endpoint of the line (van Welie and Diepen 1961a-e).

Additional studies by several individuals and groups have explored type F phase behavior of mixtures of solids with supercritical fluids. Table 2.1 lists researchers and systems studied. Studies involving ternary systems where the supercritical fluid forms a type F system as a binary with one of the two solutes are listed in Table 2.2. At the time the work reported in this dissertation was initiated, little phase behavior data other than solubilities of solids in supercritical fluids existed for ternary systems where both heavy components formed type F systems with the light component. (Van Gunst et al. (1953b) gave P-T trace data but no composition data along SSLV lines were available.)

All the studies listed in Tables 2.1 and 2.2 include SLV or SSLV P-T trace data or solid solubilities in the supercritical fluid. A limited number include composition measurements along the SLV lines in binary systems. Cheong (1986), Zhang (1988), and Lu (1989) report upper branch P-T trace data and liquid compositions along the upper branch

Table 2.1

Previously Investigated Type F SCF + Solid Systems

Smits (1903-04a,b; 1904-05; 1905-06a,b; 1909-10)	$(\text{CH}_3\text{CH}_2)_2\text{O} +$ Anthraquinone
Smits and Treub (1911-12a,b)	$(\text{CH}_3\text{CH}_2)_2\text{O} +$ Anthraquinone
Verchoyle (1931)	$\text{H}_2 + \text{CO}$
Diepen and Scheffer (1948)	$\text{CH}_2=\text{CH}_2 +$ 1,3,5-Trichlorobenzene p-Chloriodobenzene p-Dibromobenzene Octacosane Hexatriacontane Naphthalene Biphenyl Benzophenone
van Gunst et al. (1953a)	$\text{CH}_2=\text{CH}_2 +$ Anthracene Hexaethylbenzene Hexamethylbenzene Stilbene m-Dinitrotoluene Naphthalene
van Welie et al. (1961a-e)	$\text{CH}_2=\text{CH}_2 +$ Naphthalene
Diepen and van Hest (1963)	$\text{CH}_4 +$ Naphthalene
Rodrigues and Kohn (1967)	Ethane + Octacosane
Streett and Hill (1971)	Ne + Ar
Streett and Erickson (1972)	He + Ar
Kuebler and McKinley (1976)	$\text{CH}_4 +$ Benzene $\text{CH}_4 +$ Toluene

Table 2.1
(cont.)

Kohn et al. (1977)	CH ₄ + Octane CH ₄ + Cyclohexane
Tiffin et al. (1979a)	Ethane + Naphthalene
Kohn et al. (1980)	CH ₂ =CH ₂ + n-Eicosane CH ₂ =CH ₂ + n-dotriacontane
Tsang et al. (1980)	H ₂ + CH ₄
Tsang and Streett (1981a)	H ₂ + CO ₂
Tsang and Streett (1981b)	H ₂ + CO
McHugh (1981)	CO ₂ + Naphthalene CO ₂ + Biphenyl
McHugh et al. (1984)	CO ₂ + Octacosane
McHugh and Yogan (1984)	Ethane + Biphenyl Ethane + Octacosane CH ₂ =CH ₂ + Biphenyl CH ₂ =CH ₂ + Octacosane CO ₂ + Naphthalene CO ₂ + Biphenyl CO ₂ + Octacosane
Krukoniš et al. (1984)	Xe + Naphthalene
Cheong et al. (1986)	CO ₂ + Naphthalene CO ₂ + Biphenyl
McHugh et al. (1988)	Xe + Naphthalene
Zhang et al. (1988)	CO ₂ + Phenanthrene
Lemert and Johnston (1989)	CO ₂ + Naphthalene CO ₂ + 2-Naphthol
Lu and Zhang (1989)	CO ₂ + Naphthalene CO ₂ + m-Terphenyl
Yamamoto et al. (1989)	CO ₂ + Indole CO ₂ + Quinoxaline

Table 2.2

Ternary Systems

Verchoyle (1931)	$H_2 + CO + N_2$
van Gunst (1950)	$CH_2=CH_2 + \text{Naphthalene} + \text{Hexachloroethane}$
van Gunst et al. (1953b)	$CH_2=CH_2 + \text{Naphthalene} + \text{Hexachloroethane}$
Tiffin et al. (1979b)	$CH_4 + \text{Ethane} + \text{Benzene}$ $CH_4 + \text{Ethane} + \text{Cyclohexane}$
Zhang et al. (1988)	$CO_2 + \text{Naphthalene} + \text{Biphenyl}$ $CO_2 + \text{Naphthalene} + \text{Phenanthrene}$
Lemert and Johnston (1989)	$CO_2 + \text{n-Pentane} + \text{Naphthalene}$ $CO_2 + \text{Methanol} + \text{2-Naphthol}$

for the binaries they studied. Lu and Zhang (1989) also determined P-T-x values at three temperatures along the critical locus near the UCEP (upper critical end point) for the CO_2 +naphthalene system. Using these data, they determined the pressure, temperature and composition at the UCEP. Yamamoto et al. (1989) measured vapor phase composition along the three phase lines in their study. Zhang et al. (1988) report liquid phase compositions along what they believed was the four phase line (SSLV) for the two ternary systems they studied. However, their method used a first freezing method, which actually provided only three phase equilibrium.

View Cells

A view cell in which phase changes can be observed is requisite for any study of melting points. To contain the

pressures in supercritical fluid studies, these view cells generally fall into two categories: thick walled glass tubes and metal cells with windows. Each type has inherent advantages and drawbacks.

The apparatus used by Hannay and Hogarth (1879) consisted of a thick walled, small i.d. glass tube attached to a pressure generating device. Van Welie (1961a), Luks et al. (Fall and Luks 1984, Jangkamolkulchai et al. 1988), McHugh (1981), and Lemert (1989) also used thick walled glass tubes in their phase equilibria studies. These view cells are relatively inexpensive to construct and have no blind spots in viewing. On the other hand they are limited in the pressures they can contain and tend to fail unpredictably.

Kohn (1956), Lu et al. (Cheong et al. 1986, Zhang et al., Lu and Zhang 1989) and Yamamoto et al. (1989) used high pressure liquid level sight gauges in their investigations. Custom made steel optical cells are also commonly used by researchers. (Lentz 1969, Brennecke and Eckert 1989, Johnston et al. 1989, Smith et al. 1989, Beckman et al. 1989) A custom built optical cell was used for the work reported in this dissertation. Such cells can be constructed to hold very high pressures. The high thermal inertia of the metal (usually steel) walls can also be an advantage in maintaining an isothermal environment for the enclosed system. Flat windows in windowed cells aide studies using ultraviolet spectrophotometry or other

non-invasive analytical techniques where uniform optical pathways may be advantageous. These cells are, however, usually much more expensive to construct than the glass tube type. The metal walls may also obscure portions of the cell, thus creating blind spots which cannot be monitored.

Composition Determinations

Phase compositions in high pressure systems have been determined by three different methods: 1) flow system sampling, 2) quasi-static sampling, and 3) synthetic methods. Each method has inherent limitations.

Sampling near a solid/fluid phase boundary tends to be very difficult due to the potential for solidification of some components in the sampling lines. The problem is worst for liquid phases, which are much richer in the components which solidify. There is also the likelihood of depleting the solid solutes during sampling. Synthetic methods usually require custom made cells (which are expensive) and can easily leak if not machined with sufficient precision. Since these methods rely on accurate determination of the amount of each component charged to the cell before the experiment begins, any leakage introduces error by allowing unknown quantities of the components to escape.

Direct sampling can be done either in a flow system, or by a quasi-static method. Although several different flow methods are described in the literature, (Prausnitz and Benson 1959, Simnick et al. 1977, Van Leer and Paulaitis 1980, Johnston and Eckert 1981, Kurnik et al. 1981, Schmitt

1984, Krukonis & Kurnik 1985), they all embody the same basic features. In a typical flow system, a solid sample is first placed in the system, the system is flushed and pressurized with the solvent gas, and the system is then brought to equilibrium. Once equilibrium has been established, a sampling valve is opened and a continuous supply of the solvent gas is pumped through the system, becoming saturated with solutes as it passes through. This method is usually limited to sampling the vapor phase. If a liquid phase is also present, care must be exercised to prevent entrainment of the liquid in the vapor which would produce errors in the composition determination.

Quasi-static sampling methods involve taking small samples from an otherwise closed system. The research group of Dr. C. -Y. Lu (Cheong et al. 1986, Zhang et al. 1988) constructed an apparatus which samples the liquid phase using a three way valve which is evacuated and then turned to connect it with the view cell. The pressure in the cell pushes the liquid into the evacuated valve. The sample thus obtained is expanded to atmospheric pressure and the composition analyzed. Legret et al. (1981) constructed a high pressure sampling micro-cell which could be used to take a sample directly from the vapor phase and inject it, still under pressure, into a gas chromatograph for analysis. In this work, a method was developed for sampling both phases. Details of the method are contained in Chapter 4.

For a synthetic method, phase compositions are determined by introducing known amounts of the components into the cell and adjusting the pressure or temperature until phase transitions occur. Van Welie and Diepen (1961 a-e) used this method in their studies of the ethylene+naphthalene system. By doing multiple determinations over a range of temperatures or pressures for each fluid (liquid or vapor) phase, and extrapolating the constant composition lines on a P-T diagram to their intersection with the previously determined P-T trace of the three phase (SLV) line, they determined the equilibrium phase compositions along the SLV phase boundary. A similar technique has also been used by McHugh et al. (1984) to measure solid solubilities in supercritical fluids. Their apparatus included a piston which allowed variation of the total cell volume in addition to the system temperature and pressure.

With the necessary explanation of the phase behavior to be studied provided and the relevant work of other researchers discussed in this chapter, the work done for this dissertation can now be presented.

CHAPTER 3

EXPERIMENTAL APPARATUS

The experimental apparatus allows for control of the pressure and temperature within the experimental cell, observation of the phase of the cell contents, and sampling of the contents of the cell.

View Cell

Figure 3.1 shows a cross section of the view cell. This cell is fabricated from 316 stainless steel. The interior of the cell is illuminated through the window at the top of the cell by a fiberoptic light. The state of the contents is observed through the side window by means of a closed circuit color camera connected to a borescope. The internal volume of the cell is about 30 cm³. Although view of the upper region of the cell is restricted, any additional phase formed in this region must have a mass density less than the mass density of the supercritical phase. Such behavior is not anticipated with the systems studied here. The windows are 3/4 inch x 3/4 inch quartz. A triangular magnetic stir bar at the bottom of the cell stirs the lower phase in the cell. A rectangle of stainless steel wire mesh on a shaft epoxied into the magnetic stir bar stirs the upper phase. During melting point determination experiments, the solid sample rests on a stainless steel wire mesh platform at the level of the side window of the view cell. During sampling experiments, the platform is replaced with a narrow stainless steel mesh cross

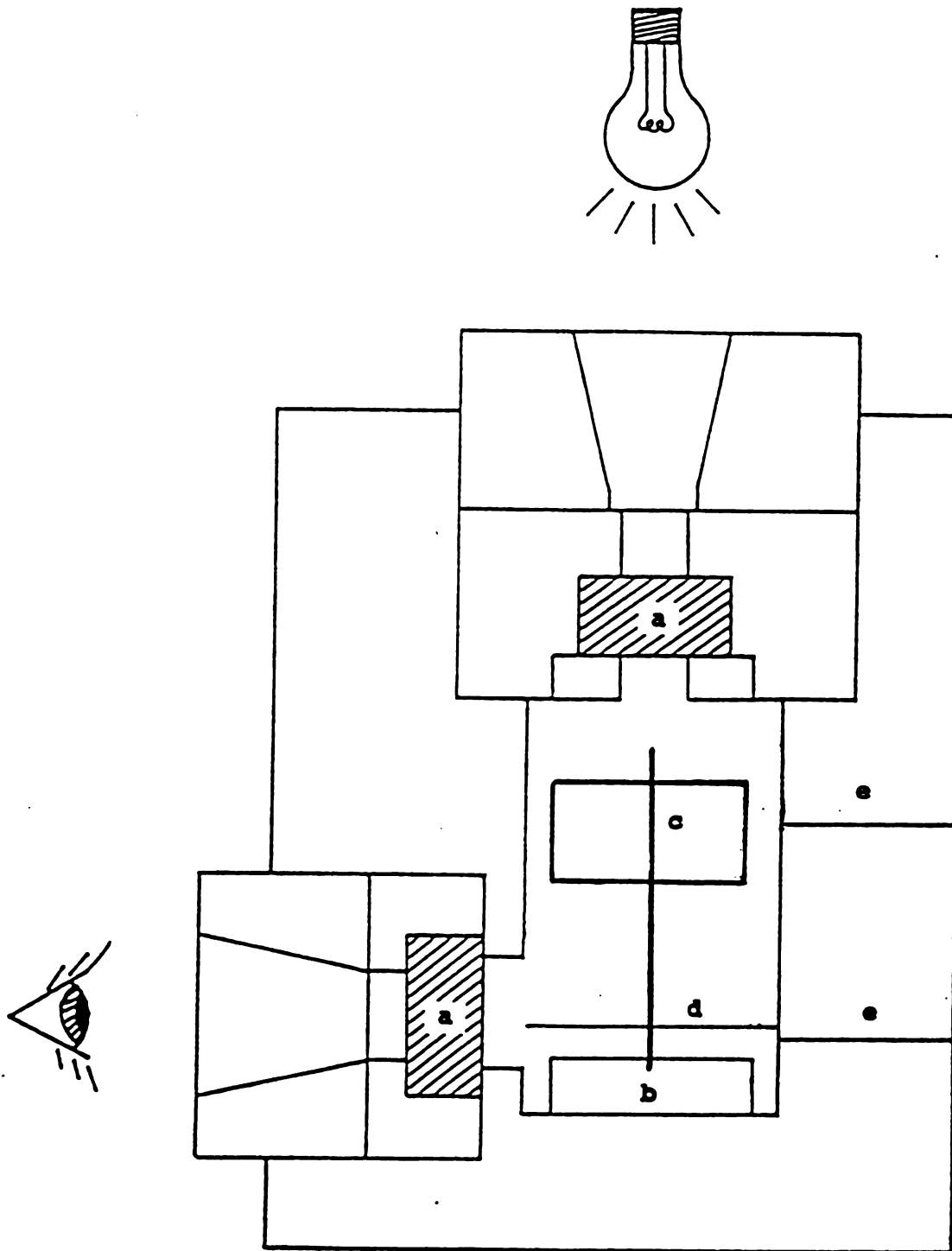


Figure 3.1

Cross-sectional diagram of the view cell. Components are labeled as follows: a - quartz windows, b - magnetic stir bar, c - wire mesh flapper, d - sample platform, e - sampling ports.

piece which keeps the vertical shaft axially centered in the cell during stirring. Two ports through the wall of the cell opposite the side window permit samples of each phase to be withdrawn for analysis of composition.

Temperature Control

A schematic is given in Figure 3.2 of the portions of the apparatus used to control the temperature in the view cell. The cell is immersed in a water bath. Temperature control components consist of 1/4" nominal diameter copper cooling coils (c) (supplied with cold tap water), a 300 watt copper clad Ni-Cr resistance heater (base heater) (d) controlled with a type 3PN1010 Staco Energy Products Co. variable transformer, and a Bayley Instrument Co. Precision Temperature Controller (model 123) (e) connected to a 500 watt quartz heater. The temperature within the bath is measured with ASTM thermometers which were checked against NBS traceable thermometers and verified to be accurate to ± 0.05 °C. The temperature within the cell is measured with a calibrated thermistor (Omega Engineering, model THX-400-GP) which passes through a compression fitting into the cell. The water in the bath is stirred with a T-Line model 105 stirring motor (with a shaft and propeller) attached to a T-Line model 115 Adjusta-Speed controller (both from Talboys Engineering Corp.). The motor was usually run at full speed, i.e. 1550 rpm.

Pressure Control

Figure 3.3 shows the portions of the apparatus used for control of the pressure. Carbon Dioxide (Linde bone dry

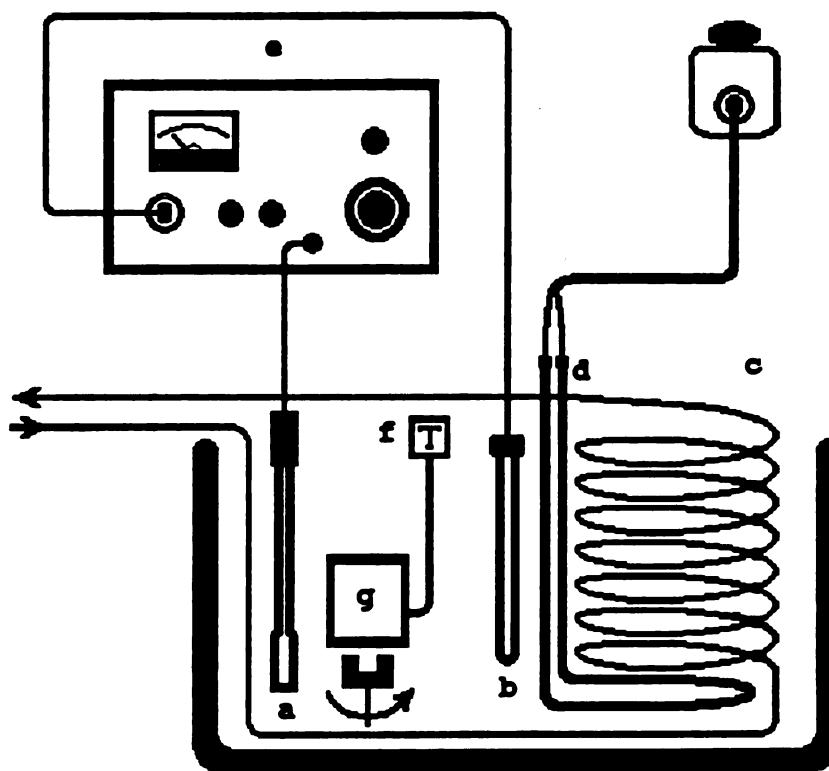


Figure 3.2

Constant temperature bath. Components are labeled as follows: a - controller temperature probe, b - quartz makeup heater, c - cooling coils, d - base heater (connected to variable voltage transformer), e - temperature controller, f - thermistor, g - view cell.

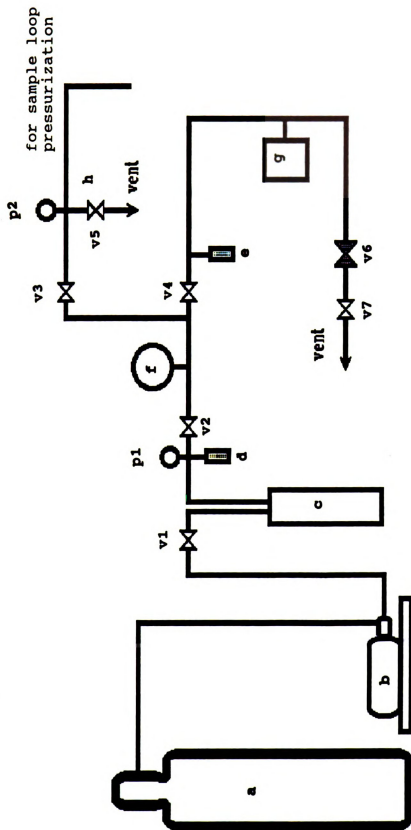


Figure 3.3

Pressure control. Components are labeled as follows: a - CO₂ supply tank, b - gas compressor, c - ballast/pressure reservoir, d - reservoir rupture disk, e - view cell rupture disk, f - 10,000 psi Heise pressure gauge, g - view cell, h - sample loop pressurizing branch, p₁ and p₂ - pressure gauges, v₁ through v₇ - valves.

grade) from a supply cylinder (a) is supplied to an air driven gas compressor (Haskel model AG-152) (b). The pressurized CO₂ is fed to a High Pressure Equipment Company model OC-11 reactor (c) which serves as a reservoir or ballast. Valves v1 and v2 allow isolation of the reservoir. A Heise model CMM 63457 pressure gauge (f) is used to determine the system pressure. Valves v4 and v6 allow isolation of the view cell (g). Safety relief heads (d and e) are installed at the indicated points to prevent accidental overpressurization of the system. System pressure is raised by carefully cracking open valve v2. System pressure is lowered by opening valve v6 and adjusting valve v7, an HIP model 60-HF11-MTS metering valve, to bleed off gas at a controlled rate. Ashcroft 10,000 psi pressure gauges (p1 and p2) are used to monitor pressures in the reservoir and in the sample loop pressurizing branch. The four lines extend from a high-pressure cross (h) comprise the sample loop pressurizing branch. Clockwise from the top, these lines connect to: 1) a pressure gauge, 2) an open line which can be connected to the sampling line, 3) a venting valve, and 4) valve v3. The function of this branch is explained in the next chapter as part of the sampling procedure.

CHAPTER 4

EXPERIMENTAL PROCEDURE

Two types of experiments composed the experimental portion of this work. The first experiments were designed to determine the P-T traces of the melting point curves in binary and ternary systems. The CO_2 +phenanthrene, CO_2 +naphthalene, CO_2 +naphthalene+biphenyl, CO_2 +naphthalene+phenanthrene, CO_2 +naphthalene+anthracene, and CO_2 +naphthalene+acenaphthene systems were studied in these experiments. None of the solids used in this work form solid solutions with naphthalene so all solid phases are pure. The second set of experiments was designed to determine the phase compositions along the phase boundaries. The systems examined in these experiments were CO_2 +naphthalene and CO_2 +naphthalene+biphenyl.

Melting Point Curve Determination

According to the Gibbs phase rule, binary systems with three phases (SLV) and ternary systems with four phases (SSLV) have one degree of freedom. This may be chosen to be the system pressure or temperature. Both first melting and first freezing methods have been used to study melting point depressions. Both may be used in binary systems, but only the first melting method is suitable for studying the SSLV line in ternary systems. Figure 4.1 is useful to illustrate this. The figure is drawn on a solvent free basis and represents the shift in the pure solid melting points and mixture eutectic with changes in pressure. For a single solid the first

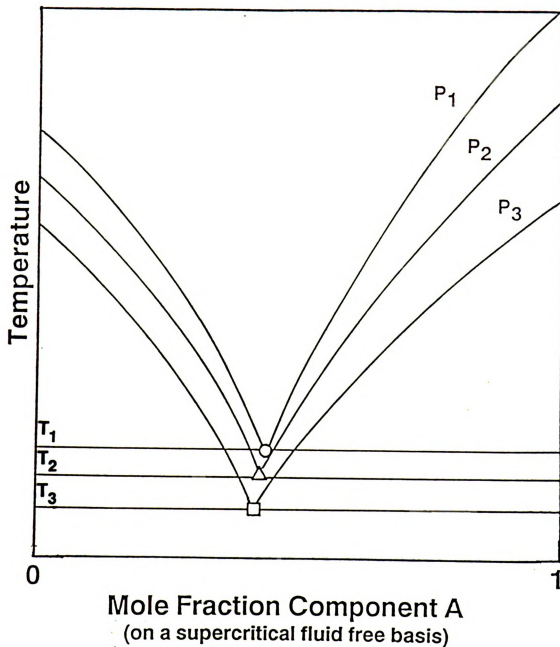


Figure 4.1

Depression of eutectic melting point by a supercritical fluid in an A-B-SCF system, where A, B are immiscible solids and $P_1 < P_2 < P_3$. The upper lines represent first freezing and the lower lines represent first melting. T_1 is the eutectic temperature at pressure P_1 .

freezing point will be identical to the first melting point, although changing the pressure will shift this point. First melting and first freezing experiments correspond to approaching this melting/freezing point from above and below respectively. In contrast, in a mixture of solids melting and freezing will occur over a range of temperatures at fixed pressure. Consider the equilibrium line at pressure P_1 with eutectic temperature T_1 . For a composition between a pure component and the eutectic composition, if melting is approached from below (the solid side), the first melting will occur at the eutectic temperature T_1 and the first liquid will be at the eutectic composition. Above this temperature, no more than one of the components in the binary system may remain solid. Increasing the temperature will continue to melt the remaining solid phase (changing the liquid composition) until the equilibrium curve is reached. The temperature at which the last solid melts corresponds to the first freezing point for the liquid at that composition. Unless the solid/solid ratio is precisely that of the eutectic, using a first freezing method in a ternary system would yield points on a three phase surface, not along the SSLV line. From the Gibbs phase rule, a ternary system with three phases will have two degrees of freedom so fixing either the pressure or the temperature alone will not uniquely determine all other variables of the system, hence a surface is defined rather than a line.

In this work, sample preparation is similar for both the binary and the ternary systems. For binary system measurements, some of the solid is melted and drawn into a section of capillary tubing of 2 mm i.d. or smaller using a small pipet bulb. The upper (non-sample) end of the tube is quickly sealed with a fingertip to prevent the liquid sample from draining out and the tube is removed from the liquid container and allowed to solidify. A 3/4 inch section of this filled tubing is placed on the wire platform and serves to hold the portion of the sample being studied in a constant position and prevent it from draining away completely when melting occurs.

For ternary measurements of the SSLV line, the two solids to be used in the study are first mixed to provide intimate contact. The minimum melting point for the solid-solid binary at atmospheric conditions occurs at the eutectic composition. A solid mixture of this composition is prepared in the expectation that a similar ratio of the components will be present in the liquid phase at the first melting point in the ternary mixture. The solid mixture is melted in a test tube and stirred to obtain a homogenous liquid. Some of the liquid is drawn into a capillary tube. The remaining liquid is poured out onto a clean sheet of aluminum foil. After the binary liquid cools and solidifies, the thin sheet of solid material is broken up into "flakes" for loading into the view cell.

Once the sample is prepared, adequate solid (1 to 2 grams) is loaded into the view cell to ensure the presence of excess solid at all conditions to be studied. The capillary tube is placed on the wire mesh platform as close as possible to the side window and parallel to it. With the sample loaded, the cell is sealed, placed in the temperature control bath, and connected to the high pressure gas reservoir. The cell is purged with the solvent gas and then pressurized with enough of the solvent fluid to bring it near the desired final pressure. The bath is also heated or cooled to near the desired temperature. The contents of the cell are stirred at least 20 minutes to ensure that thermal and composition equilibrium have been achieved before initiating measurements. Thermal equilibration was confirmed using the thermistor installed in the cell wall.

Measurements are made by two methods. Method A (see Figure 4.2) is used in the initial lower pressure region where the decrease in melting point with increasing pressure is most rapid. The temperature of the bath is held constant and the pressure in the cell is varied by adding and releasing small amounts of the vapor phase. The pressure at which the first melting occurred within the capillary tube (near the ends) is recorded as the melting point. Accuracies for these measurements are ± 0.35 bar and ± 0.05 K.

In the higher pressure region where the P-T curve becomes almost parallel to the pressure axis, method B (Figure 4.2) is used. The pressure of the cell is raised to near the desired

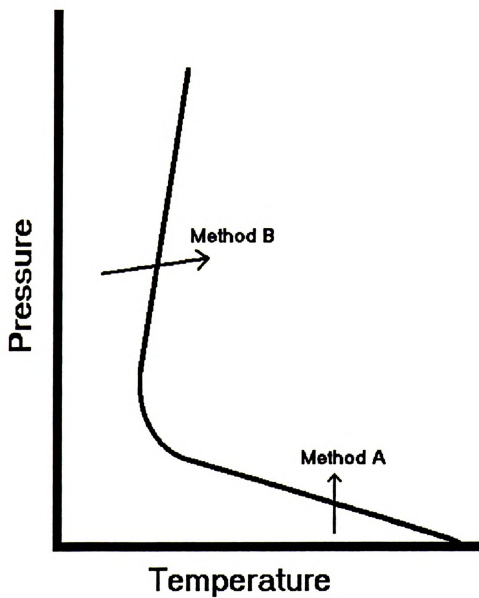


Figure 4.2 Methods for finding first melting points along SLV or SSLV phase boundary.

level and then the temperature is raised about 1.0 K/hour until the first melting is observed. At this rate of heating, thermal lag between the bath temperature and the temperature within the cell was less than 0.1 K. For this method, both the pressure and the temperature are changing with time. Accuracies for these measurements are ± 0.1 bar and ± 0.2 K. Method B corresponds to the method used by McHugh (1981) to determine similar P-T traces.

Sampling

One of the important parameters in phase equilibrium of multi-component systems is the composition of the phases. For this reason the view cell was designed to allow sampling of fluid phases (liquid, gas, or supercritical fluid). The first step in obtaining equilibrium composition data is to bring the system to the desired equilibrium state. For the binary systems, the pressure was fixed and the temperature was raised high enough to melt all solid. The temperature was adjusted until the first solid began to precipitate. For the ternary system, the temperature was the fixed variable while the pressure was gradually lowered until solid began precipitating. Pressures and temperatures were chosen to minimize the amount of solids in the cell, and thus avoid plugging the sampling ports, the HPLC valve and the lines leading to the HPLC valve and the plug valves. All samples in this work were taken along three phase boundaries (SLV). For the ternary system, this means data points are on a three phase surface instead of along a four phase line. To maximize

the information from these experiments, the cell was loaded with various initial naphthalene/biphenyl ratios different from the eutectic ratio and the sampling repeated at the same temperatures for each initial ratio. These isotherms should allow the phase boundary surfaces of this system to be at least partially defined by the intersection of the isotherms.

Figure 4.3 is a schematic of the equipment used for sampling. As shown in Figure 3.1, the view cell has two ports through which samples of the cell contents may be drawn. These two ports are connected to two ports of a Valco model C10W 10-port HPLC sampling valve (from Valco Instrument Co. Inc.) (e). The other HPLC valve ports connect to two sample loops, two plug valves (f1 and f2) and a flush line. Valves f1 and f2 are Whitey SS-4PDF4 rising plug valves with one end sealed on each with a stainless steel pipe plug. This allows the valves to be used as high pressure syringes with approximately 1 cc capacity. Figure 4.4 shows the two positions of the sampling valve. In position 1, the sample line is connected to the vapor sample loop while the liquid sample loop is in line with the cell and plug valve f2. In this position, the vapor sample loop is flushed when the sample line is flushed. In position 1, it is also possible to draw a sample into the liquid sample loop with plug valve f2. In position 2, the sample line is connected to the liquid sample line while the vapor sample loop is in line with the cell and plug valve f1. In this position, the liquid sample loop is flushed when the sample line is flushed. In position

Figure 4.3 Sampling system. Components are labeled as follows: a - burette, b - water overflow reservoir, c - volumetric flask, d - three-way valve, e - 10-port HPLC sampling valve, f1 and f2 - plug valves (used as small volume high pressure syringe pumps), g - Knurl-Lok HPLC fitting, h - sample loop pressurizing branch, i - hand pressure generator, j - CO₂ supply tank, V₃, 4, 8, and 9 - valves.

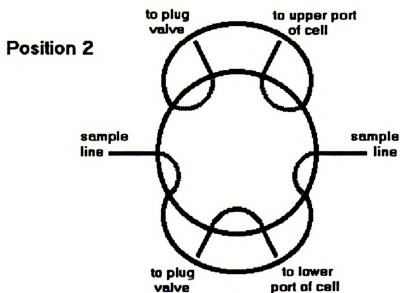
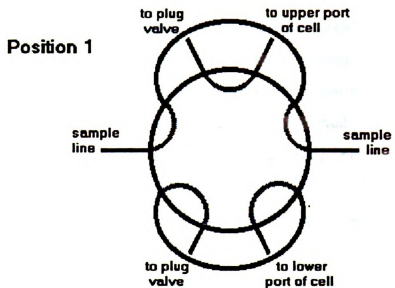


Figure 4.4

Sampling positions for the 10-port HPLC valve. Position 1 allows sampling of the vapor phase. Position 2 allows sampling of the liquid phase.

2, it is also possible to draw a sample into the vapor sample loop with plug valve f1.

Initially, an attempt was made to take a sample with each switch of valve position, thus sampling the phases alternately. This proved unfeasible, because when a sample loop at atmospheric pressure is switched in line with the cell, the pressure drop from the cell to the sample loop allows solids to precipitate and block the sample loop or the line from the cell to the loop before an equilibrium sample can fill the loop. To avoid this problem, a second method was devised.

The sample line and sample loop are first flushed with toluene to remove all residual solutes then dried with flowing CO_2 to remove residual toluene. The line and loop are then pressurized to the same pressure as the cell with CO_2 and the valve is switched to put the sample loop in line with the cell. Pressurizing the sample loop prevents a pressure gradient between the loop and the cell and the consequent premature solid precipitation. The sample line is again flushed with toluene to remove solutes which enter the line from the second sample loop (which was connected to the cell before switching). The sample line and this second loop are dried with CO_2 and left at atmospheric pressure. A sample is drawn into the first sample loop. The sample is drawn slowly to prevent solid precipitation and to avoid severely perturbing the equilibrium in the cell and thus getting a non-equilibrium sample. Some perturbation of the cell is

unavoidable during this process because the cell volume is effectively increased by the volume of the sample taken. Since the volume of the sample is small relative to the volume of the cell however, no change in pressure was noticed until the cell pressure exceeded about 200 bar. Above that pressure, sampling caused pressure drops of 0.1 to 1.0 bar in the CO₂+naphthalene system. This is expected since this region is near the upper critical end point of the binary system where molar volumes change rapidly with pressure.

Once the sample is in the loop, the sample valve is returned to the original position. The sample line is opened and the volume of gas released is measured. Since the line is at atmospheric pressure before this switch, the volume of the gas released when the sample line is opened is equal to the volume of gas in the sample loop alone expanded to ambient conditions. The sample line is then flushed with toluene to recover the solid portion of the sample. Specifics of the sampling procedure are outlined in the next section to allow duplication of the method.

The procedure for sampling the liquid phase is as follows:

1) Flush the line and loop

- A. The HPLC valve (e) is set to position 1.
- B. Valves v8 and v9 are opened.
- C. A syringe filled with toluene is connected to the Knurl-Lok finger tightened HPLC union (g).
- D. The sample loop is cleaned. Approximately 30 cc's of toluene is flushed through the line and sample

loop and into a beaker. This volume was chosen after analyzing samples of the exiting solvent on a gas chromatograph to find the flush volume which assured no residual solute could be detected in the solvent.

- E. The beaker is removed to dispose of the waste solvent.
- F. The syringe is removed and the CO₂ tank (j) connected to the Knurl-Lok fitting.
- G. The CO₂ is used to blow the line and loop dry of toluene and fill them with CO₂ at ambient conditions. Flushing for 30 to 45 seconds proved sufficient to produce a solvent free stream of gas from the sample line.

2) Pressurize the loop

- A. Valve v8 is closed.
- B. The CO₂ is disconnected and the loop pressurizing branch (h) is connected to the Knurl-Lok fitting.
- C. If valve v4 is open, it is closed. (Valve v3 is already closed at this point.)
- D. Valve v5 (see Figure 3.3) is closed to isolate the cell.
- E. The pressure reading on the Heise gauge (f on Figure 3.3) is noted.
- F. Valve v3 is opened.
- G. Valve v2 (Figure 3.3) is opened slightly and enough CO₂ is bled in from the reservoir (c - Figure 3.3)

to raise the pressure back to that noted in step E.
Once this pressure is reached, valve v2 is closed.

- H. Valve v3 is closed (to isolate the sample loop).
- I. The HPLC valve is switched to position 2.
- J. Plug valve f2 is closed $\frac{1}{2}$ turn.
- K. Valve v5 is opened.

3) Flush line

- A. Valve v8 is opened to allow all the pressure in the line to be relieved. If any pressure remains (because of precipitated solid blocking the line), valve v4 is opened to relieve it.
- B. A syringe filled with toluene is connected to the Knurl-Lok union.
- C. Approximately 30 cc's of toluene is flushed through the line and sample loop and into a beaker. If the line is plugged (because of precipitated solid blocking the line), the hand pressure generator (HIP Model 62-6-10) (i) is connected to the Knurl-Lok union and used to force toluene through the line to dissolve the solid.
- D. The beaker is removed and the waste solvent disposed of.
- E. The syringe is removed and the CO₂ tank is connected to the Knurl-Lok fitting.
- F. The CO₂ is used to blow the line and loop dry of toluene and fill them with CO₂ at ambient conditions. (See step 1G).

G. Valves v8 and v9 are closed.

4) Obtain sample and measure included gas

A. The three-way valve (d) is opened to the atmosphere, the burette and the flask to keep the pressure in the flask and the burette ambient when step 4B is performed.

B. A 25 ml volumetric flask (c) with 2.5 cc of toluene containing an internal standard is attached to the outlet from the sampling line.

C. The three-way valve is turned to connect the volumetric flask to the burette (a) only.

D. The liquid level in the burette is recorded.

E. The magnetic stirrer is turned off.

F. To draw a liquid sample, plug valve f2 is slowly opened 1 turn to draw about 0.25 cc through the sample loop. (The liquid sample loop internal volume is approximately 0.05 cc.)

G. The HPLC valve is turned to position 1.

H. The magnetic stirrer is turned on

I. Valve v8 is opened.

J. The hand pressure generator (i) is connected to the Knurl-Lok union and turned until some resistance is felt.

K. Valve v9 is opened.

L. The hand pressure generator is turned until the first drop of toluene can be seen at the tip of the outlet line entering the flask.

- M. The overflow bottle (b) is lowered until the water level matches that of the burette.
- N. The liquid level in the burette is recorded.
- O. The total gas volume is determined from the displaced volume of water minus the sample line volume.
- P. The pressure generator is disconnected and a syringe filled with toluene is used to flush 22.5 cc of toluene through the line and sample loop to fill the volumetric flask to 25 cc.
- Q. The flask is removed and a small magnetic spin bar is added before it is capped and placed on a magnetic stirring plate.
- R. The ambient temperature is read from an ASTM thermometer (calibrated against an NBS traceable standard) and recorded.
- S. The ambient pressure is read from a barometer (Cole-Parmer aneroid barometer stock# N-03316-70) and recorded.
- T. The line and loop are flushed with another 5 cc of toluene.
- U. The syringe is removed and the CO₂ tank is connected to the Knurl-Lok fitting.
- V. The CO₂ is used to blow the line and loop dry of toluene and fill them with CO₂ at ambient conditions.

Samples of the vapor phase are taken in the same way as the liquid with the following exceptions:

- 1) The HPLC valve is set to position 2 for step #2A.
- 2) In step #2I the HPLC valve is switched from position 2 to position 1.
- 3) In step #2J plug valve f1 is closed about $1\frac{1}{2}$ turns.
- 4) A 10 ml volumetric flask with 1 cc of internal standard solution is used for step #4B.
- 5) In step #4f valve f1 is turned about $1\frac{1}{2}$ turns to draw about 0.3 cc through the sample loop. (The vapor sample loop volume is approximately 0.05 cc.)
- 6) In step #4G the HPLC valve is switched from position 1 to position 2.
- 7) It is usually not necessary to use the hand pressure generator so steps #4J and #4L can be skipped and only the initial burette liquid level is subtracted to get the total gas volume in step #4O.
- 8) Only 9 cc of toluene are used to fill the flask with a total of 10 cc of liquid in step #4P.

Multiple samples were taken from both the liquid and vapor phases at each P-T point to be analyzed for composition. The phase sampled was alternated (i.e. two liquid then two vapor or one liquid then one vapor) to avoid biasing the result by the order of the sample.

The cell pressure and temperature must be monitored throughout the sampling to ensure that constant conditions are maintained. Cell pressure does drop when the sample loop is

pressurized to cell pressure, because the loop is connected to the same line supplying the cell. The volume of the supply line acts as a ballast to minimize the pressure drop, but it is necessary to add a small amount of CO₂ after each sample to maintain constant conditions. The entire process for taking one sample requires at least 30 minutes per sample which proved sufficient to re-establish equilibrium in the well stirred cell.

Composition Analysis

Phase compositions were determined by finding the number of moles of each component in each sample and using these values to determine mole fractions. The moles of CO₂ were calculated from the ideal gas law using the ambient pressure and temperature and the change in gas volume in the burette. Concentrations (and hence moles) of the heavy solutes in the toluene were measured on a Perkin-Elmer 8500 gas chromatograph with an FID detector and automatic integrator. Details of the chromatographic procedure are contained in Appendix A.

Materials

Chemicals used in this study are listed in Table 4.1. All chemicals were used without further purification. The purity of the naphthalene, phenanthrene and biphenyl were verified by measuring the melting point range of each at atmospheric pressure.

No significant difference in either melting point range or gas chromatograms was noted between the naphthalene from

Table 4.1 Purity of Materials		
Chemical	Supplier	Stated Purity
Acenaphthene	Aldrich	99 %
Anthracene	Aldrich	99.9 %
Biphenyl	Aldrich	99 %
Carbon Dioxide	Linde	Bone dry grade
Naphthalene	Aldrich	99+ %
Naphthalene	Alfa Products	99.8 %
Phenanthrene	Aldrich	98+ %

Aldrich and that from Alfa Products, so no distinction was made in the experiments or the analysis.

CHAPTER 5

EXPERIMENTAL RESULTS

Melting point experiments

Results of the melting point experiments are given in Table 5.1. The P-T traces of the SLV lines for the CO₂+naphthalene and CO₂+biphenyl systems have been previously measured to their upper critical end points by other researchers (McHugh and Yogan 1984, Zhang and Lu 1989) so no attempt was made to redetermine end points of these systems. The naphthalene+CO₂ system was measured to validate the experimental method. Measurements for the carbon dioxide+naphthalene+phenanthrene system conducted in the roughly triangular region shown in Figure 5.1 found no melting point for the system beyond that found at 64.12 bar and 310.55 bar. This is evidence that an invariant point for the SSLV line lies within this area. In the CO₂+naphthalene+biphenyl system, at pressures slightly above the last (i.e. highest pressure, lowest temperature) melting point, a second phase was observed running down the walls of the cell before the solid sample began to melt. This is evidence that the SSLV equilibrium line of this system does not terminate in a SS(L=V) equilibrium point. Two possibilities exist which would be consistent with these experimental observations. The first possibility is that the SSLV line may bend downwards in temperature just beyond the last point measured in this study and continue to a SSSLV point near the triple point of CO₂.

**Table 5.1 Experimental Pressure-Temperature Data Along the SLV and SSLV
Equilibrium Lines for 6 CO₂+Hydrocarbon Systems**

Naphthalene+CO ₂		Phenanthrene+CO ₂		Naphthalene+Phenanthrene+CO ₂	
Pressure Temperature		Pressure Temperature		Pressure Temperature	
Bar	K	Bar	K	Bar	K
28.96	347.25	1.03	371.65	8.96	321.55
33.09	346.35	48.26	364.15	16.89	319.15
55.85	341.95	61.36	361.25	29.65	316.95
66.19	340.15	70.33	359.85	36.87	315.75
69.60	340.80	76.53	359.65	56.54	311.65
75.15	338.75	79.98	358.05	64.12	310.55
85.49	336.95	84.46	356.85	77.22	308.55
102.04	334.80	90.32	355.95	88.25	307.15
128.20	333.50	106.18	355.65	92.04	306.65
134.45	331.65	106.32	355.75		
142.00	332.40				
159.30	332.10				
170.30	331.75				
199.26	332.65				
210.90	332.40				
222.00	332.70				
249.60	332.90				

Naphthalene+Anthracene+CO ₂		Naphthalene+Acenaphthene+CO ₂		Naphthalene+Biphenyl+CO ₂	
Pressure Temperature		Pressure Temperature		Pressure Temperature	
Bar	K	Bar	K	Bar	K
20.68	345.65	7.58	322.75	14.48	307.45
32.41	343.15	17.24	320.45	17.24	306.55
43.78	340.25	31.03	318.15	26.89	303.55
55.85	337.75	44.82	315.85	38.61	300.05
75.84	334.05	58.61	313.65	44.82	298.65
82.05	331.95	73.43	311.35	50.68	297.65
				59.98	296.25

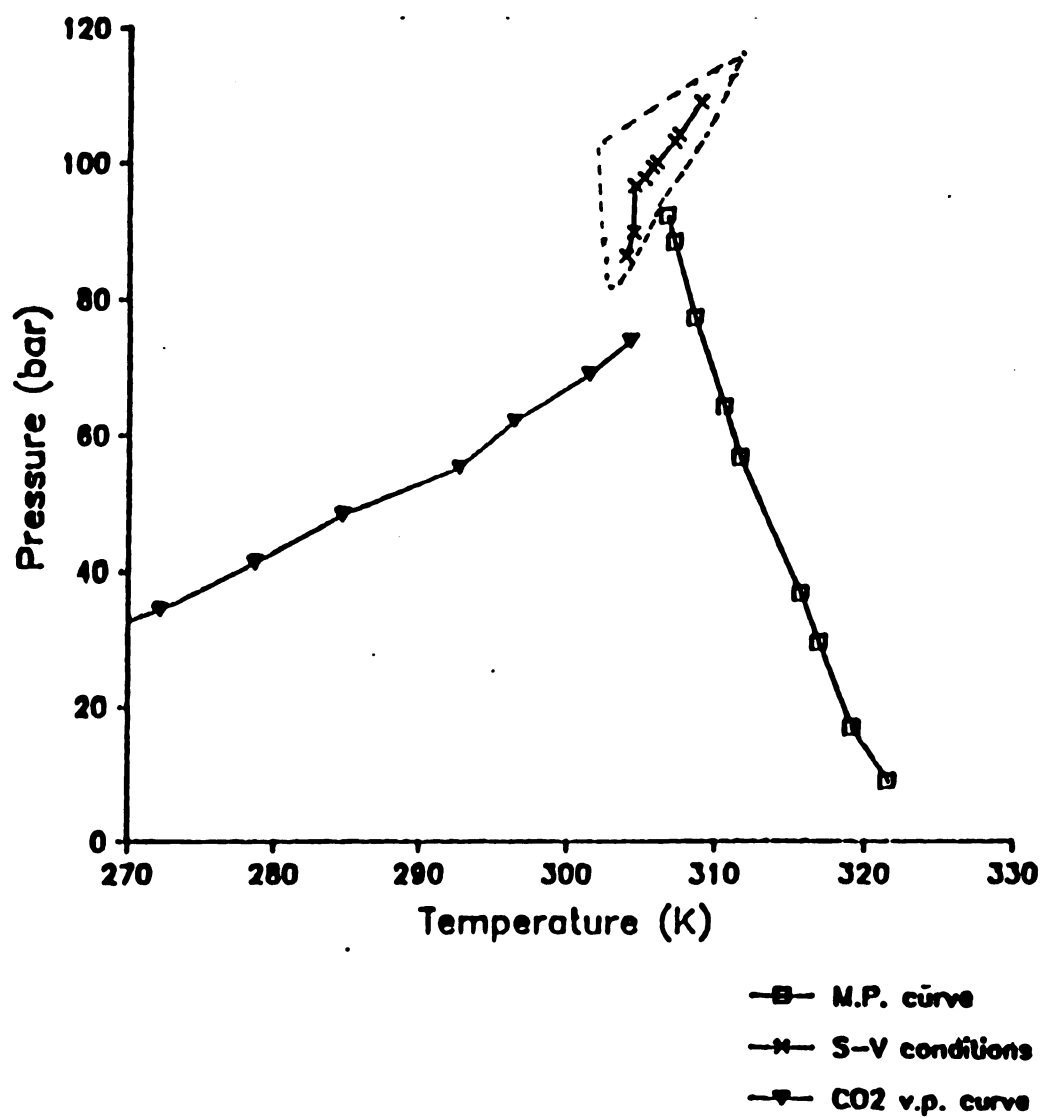


Figure 5.1 S-V region beyond the end point of the CO_2 +naphthalene+phenanthrene SSLV line.

This would be analogous to a type A or B binary system (see Figure 1.1). The second possibility is that the SSLV line may terminate in a SLLV point where the first liquid is organic rich and the second is a CO₂ rich liquid phase. This would be analogous to a type C, D or E binary system.

In this work, ternary eutectic melting point depressions were determined over a range from the solid-solid eutectic to near an apparent UCEP for the CO₂+naphthalene+phenanthrene system. This critical endpoint seems to occur hundreds of bar below the UCEP's for the CO₂+naphthalene and CO₂+phenanthrene systems. The CO₂+naphthalene+biphenyl melting point depression line was measured to near the CO₂ vapor pressure curve where more complicated phase behavior interfered with measurement.

Composition measurements

Compositions of the vapor and liquid phases were measured for the CO₂+naphthalene system along the three phase (SLV) line and for the CO₂+naphthalene+biphenyl system along three phase (SLV) isotherms. Results are given in Tables 5.2 and 5.3. For these measurements, mixtures of naphthalene and biphenyl at several overall compositions different from the expected eutectic compositions were prepared and loaded into the cell. Sampling for both the binary and ternary systems was carried out as described in Chapter 4. The raw data are tabulated in Appendix H. Average values were taken as the correct values with the values of obviously poor samples excluded.

Table 5.2 P-T-v-x-y Data for the CO₂+Naphthalene System

P (bar)	T (K)	X _{Naph.}	Y _{Naph.}	v _{liq.} (cc/mol)x10 ⁵	v _{vap.} (cc/mol)x10 ⁵
69.6	340.8	0.594	0.0030	157.5707	232.4015
128.2	333.5	0.514	0.0141	115.2424	90.0894
142.0	332.4	0.516	0.0231	125.4453	73.8286
159.3	332.1	0.459	0.0483	120.3322	70.9324
210.9	332.4	0.305	0.0728	180.7793	31.4755*
210.9	332.4		0.0868		68.9186
222.0	332.7		0.1280		170.7587
249.6	332.9	0.256	0.1770	79.7659	70.8801

* This low vapor molar volume value suggests this may have been an incomplete sample.

53

Table 5.3 P-T-v-x-y Data for the CO₂+Naphthalene+Biphenyl System

P(bar)	T (K)	X _{Naph.}	X _{Biph.}	Y _{Naph.}	Y _{Biph.}	v _{liq.} (cc/molx10 ⁵)	v _{vap.} (cc/mol)x10 ⁵)
52.4	325.95	0.558	0.213	0.00135	0.00037	121.8110	458.7717
28.3	315.35	0.238	0.584	0.00621	0.00895	130.8923	710.3258
81.4	315.35	0.371	0.114			97.9299	
53.8	305.80	0.228	0.463	0.00055	0.00065	128.6583	396.3258
73.8	305.80	0.162	0.404	0.00421**	0.00541**	96.1336	68.0685**
63.5	305.80	0.345	0.322	0.00662	0.00586	107.7962	269.3526
74.5	305.80	0.252	0.208	0.00702**	0.00338**	98.4690	92.4466**

** These data are probably from a second liquid phase.

The results of the binary measurements are compared in Figure 5.2 to liquid phase measurements reported by Cheong et al. (Cheong et al. 1986). The two sets of measurements in the liquid phase agree within the range of experimental error.

The results of the ternary measurements are compared in Figure 5.3 to those of Zhang et al. (Zhang et al. 1988) for the same system. The two sets of measurements do not appear compatible. Composition isotherms plotted through Zhang's data indicate much greater melting point depressions than those observed in this work. Since insufficient information is present in Zhang et al.'s paper to determine the exact conditions of the sample line during sampling, it is only possible to speculate about the reason for this disagreement. It should be noted that the values reported from this work are averages of multiple samples taken from alternating phases over periods ranging from several hours to days, depending on the time available for conducting the experiments in any given day or week. This method should be more reliable than the apparently single sample method employed by Zhang et al. (1988).

In determining phase compositions, it was necessary to calculate the number of moles of each component in each sample. With this information and the calibration of the sample loop volumes, it was possible to calculate values for molar volumes of the samples. Details of the loop volume calibration are detailed in Appendix G. The calculated values are listed in Tables 5.2 and 5.3. The scatter of the volume

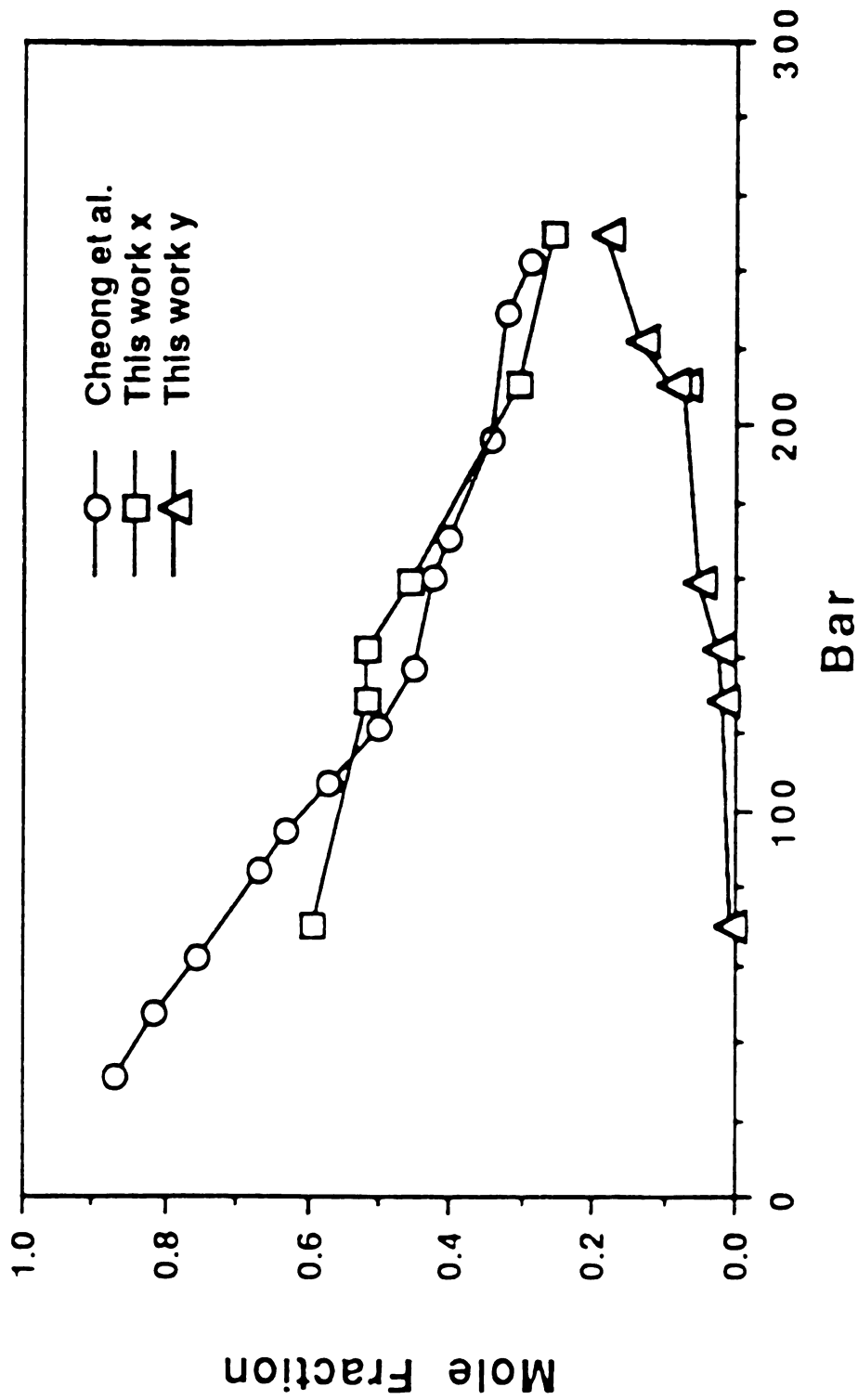


Figure 5.2 Comparison of liquid composition measurements along SLV line for the CO_2 +naphthalene system.

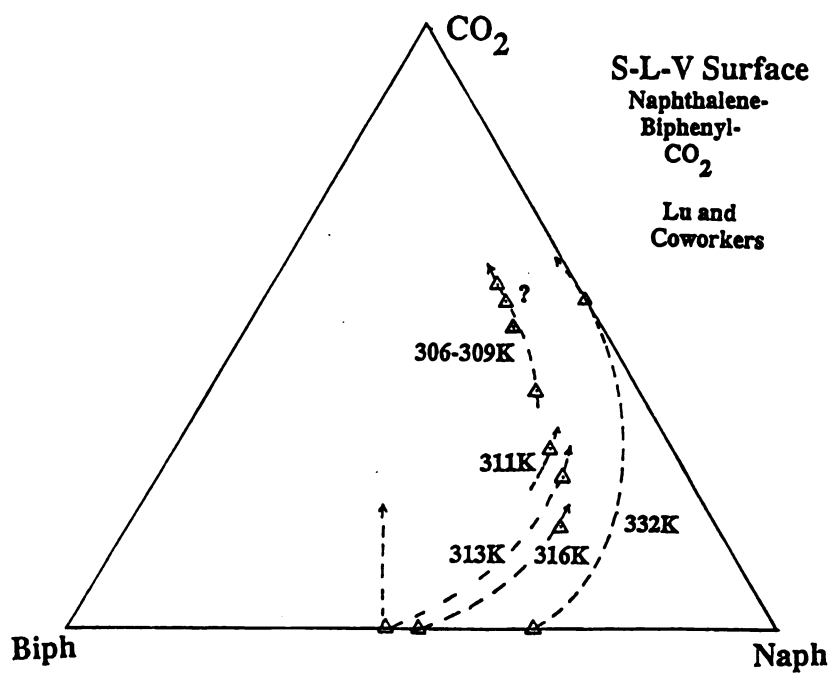
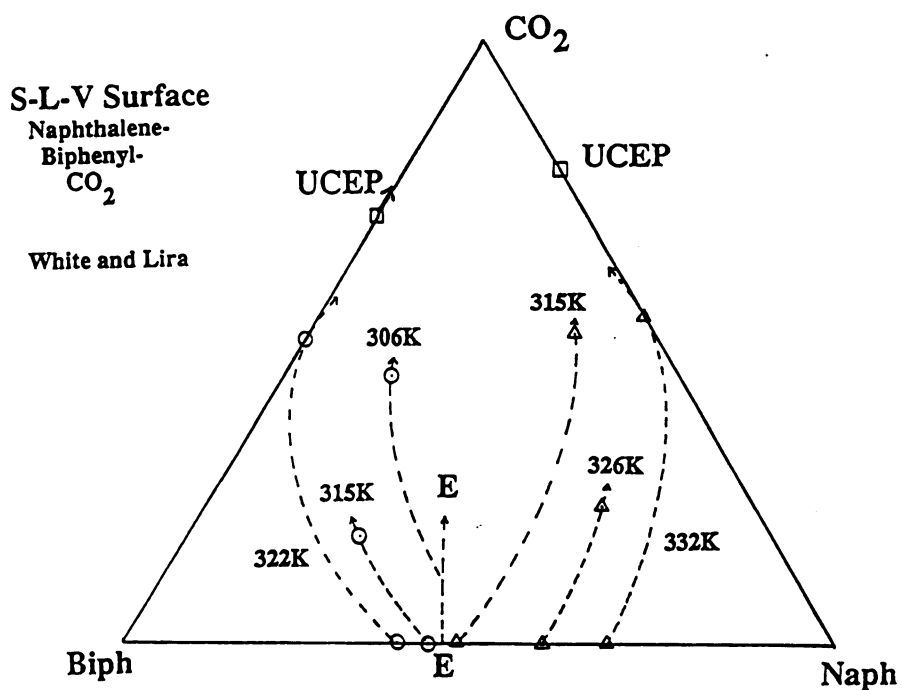


Figure 5.3 Comparison of data from this work and that of Lu and co-workers.

data in Table 5.2 at higher pressures is a consequence of the difficulty of sampling at higher pressures. From the degree of the scatter, it is estimated that the volumes calculated are accurate to within about 20%. This represents a lower degree of accuracy than can be obtained by some other methods, but, since all the information necessary to calculate the molar volumes is collected in the course of obtaining the composition data, and since it only requires a few additional elementary calculations, it would be imprudent to neglect the opportunity to glean this additional information.

As the pressure increases, the molar volume of the vapor phase in the CO_2 +naphthalene+biphenyl system becomes lower than that of the liquid phase. This does not, however indicate a phase inversion. Although the molar density of the vapor phase becomes greater than the molar density of the liquid, the mass density of the vapor remains greater than that of the liquid.

Two of the data points at 305.8 K (at 73.8 and 74.5 bar) have relatively low upper phase molar volumes. This is evidence that these samples come from a second liquid phase. Since the upper sampling port is out of the line of sight for the cell window, it is possible that such a phase transition may have occurred without being observed. This points out the importance of being able to observe the phase being sampled and the value of determining the molar volumes of the phases, even if the values are only moderately accurate.

CHAPTER 6

PREDICTIVE MODELING

Experiments to determine solubilities and other phase behavior in high pressure systems are difficult and expensive to perform. Accurate models and correlation schemes for high pressure systems would provide a highly attractive alternative, or at least supplement, to these experiments. They would greatly reduce the number of experiments necessary to reliably characterize a system by allowing more accurate interpolation and extrapolation from limited data. Experiments could be performed more efficiently if the phase behavior could be predicted with sufficient accuracy. Models can be used to indicate regions where phase transitions might occur and the range of expected concentrations in each phase. To date most models and correlations still have difficulty accurately representing some important thermodynamic properties of systems involving liquid, near critical, and supercritical fluid phases (including solute-SCF behavior). The problems lie primarily in two areas. First, dense fluid phases are still incompletely understood. In dense fluids, not only do the intermolecular forces of the nearest neighbor shells become more important, but forces from more remote shells exert significant influence on each molecule. Molecular interactions become more complicated than the primarily binary interactions of diffuse gases. Because of these difficulties, equations of state and correlations which

work well in the gas phase frequently fail when applied to dense fluids. The most widely used cubic equations of state (EOS's) do not always predict dense fluid volumes and compressible with high accuracy. The implications of this will be discussed shortly. Second, the close proximity of individual molecules to each other in dense fluids allows differences between like and unlike molecule interactions greater impact. Mixing rules and correlations to describe the impact of differences in molecular shape, size, polarity, and polarizability are mostly empirical. Despite these difficulties, some thermodynamic models can generate fairly accurate qualitative or somewhat quantitative predictions of high pressure phase behavior. (King et al. 1983, Paulaitis et al. 1983, Hong et al. 1983, Adachi et al. 1986, Ziger and Eckert 1983, Lemert and Johnston 1989) These fall into two categories: using an equation of state for all fluid phases, or using an equation of state for the vapor phase and an activity coefficient model for the liquid phase. The equation of state methods require minimal pure component data but do not work well in mixtures without binary interaction parameters. They tend to represent vapor phase thermodynamic properties better than liquid phase properties.

The second approach requires more pure component data and requires values for the liquid phase fugacity of the pure components. This means finding methods to calculate a hypothetical liquid fugacity above the pure component boiling

points and critical points for the supercritical fluid and below the triple point for the organic solids.

The first approach was adopted for this work. The Peng-Robinson and translated Peng-Robinson equations of state were tested and compared for their ability to predict multi-component phase behavior.

Phase Equilibrium

The fundamental thermodynamic requirement for multi-phase equilibrium is that the chemical potential of each component in each phase be equal, i.e.

$$\mu_i^\alpha = \mu_i^\beta = \mu_i^\gamma \quad (6.1)$$

where μ_i is the chemical potential of component i , and α , β , and γ are the phases. For a non-reacting system with solid, liquid, and vapor phases, this equality of chemical potentials is achieved when the following condition is satisfied:

$$f_i^S(P, T) = f_i^L(P, T, x_i) = f_i^V(P, T, y_i) \quad i = 1, 2, 3, \dots, n \quad (6.2)$$

where f_i is the fugacity of component i , the S, L, and V superscripts denote the solid, liquid and vapor phases, P is system pressure, T is system temperature, and x_i and y_i are the mole fractions of component i in the liquid and vapor phases respectively.

Solid Fugacities

Since the solids used in this study do not form solid solutions, all mole fractions are unity in the solid phases. The fugacity of a pure solid is calculated from the equation

$$f_i^S = \phi_i^S P \quad (6.3)$$

where the fugacity coefficient ϕ_i^S of the solid is found from

$$\begin{aligned} RT \ln \phi_i^S &= \int_0^P \left(V - \frac{RT}{P} \right) dP \\ &= \int_0^{p^{sat}} \left(V - \frac{RT}{P} \right) dP + \int_{p^{sat}}^P \left(V - \frac{RT}{P} \right) dP \quad (6.4) \\ &= RT \ln \phi_i^{sat} + \int_{p^{sat}}^P \left(V - \frac{RT}{P} \right) dP \end{aligned}$$

Most solids have very low saturation (sublimation) pressures, so their vapors may be treated as ideal gases and the first term of equation 6.4 becomes 0. Except at very, very high pressures, solids are effectively incompressible; a pressure of one kilobar only compresses iron by about 0.02%, copper by about 0.2% and NaCl by about 0.5% (Sherman and Stadtmuller, 1987). Since the pressures being examined in this work are even more modest, the volume in the second term of equation 6.4 may be assumed to be a constant with respect to pressure. With these assumptions, equation 6.4 becomes:

$$RT \ln \phi_i^S = V[P - P^{Sat}(T)] - RT \ln \frac{P}{P^{Sat}(T)} \quad (6.5)$$

which yields:

$$f_i^S = P_i^{Sat}(T) \exp\left(\frac{V_i^S [P - P_i^{Sat}(T)]}{RT}\right) \quad (6.6)$$

for the fugacity of the solids. V_i^S is actually a function of temperature, but for small temperature ranges, it may be treated as a constant. If the values of the solid vapor pressure as a function of temperature and the solid molar volume are known accurately, the value of the solid fugacity can be determined with high accuracy.

Liquid Fugacities

Liquid phase fugacities may be calculated by either the fugacity coefficient method or the activity coefficient method. In the fugacity coefficient method,

$$f_i^L = x_i \phi_i^L P \quad (6.7)$$

where ϕ_i^L is the fugacity coefficient of component i in the liquid phase. ϕ_i^L is defined by the equation:

$$RT \ln \phi_i^L = \int_{\infty}^{V_i^L} \left[\left(\frac{\partial P}{\partial n_i} \right)_{T, V, n_j, n_i} - \frac{RT}{V} \right] dV - \ln Z \quad (6.8)$$

where R is the gas constant, T is absolute temperature, V is total volume, n_i and n_j are the number of moles of components i and j respectively, and Z is the compressibility factor. Either actual data or an equation of state such as the Soave-Redlich-Kwong or Peng-Robinson equations may be used to solve the integral and determine the component fugacities. Reliable P - T - V - x data, if available, would allow accurate calculation of the liquid fugacities. Such data are usually very scarce or non-existent. For this reason, it is usually necessary to use an equation of state in the integration. The accuracy of fugacities calculated using an equation of state is heavily dependent on the ability of the equation to correctly predict the P - T - V values of the system modeled.

An activity coefficient model may be used to calculate the component activity coefficients in the liquid phase. In the activity coefficient method fugacities are found from:

$$f_i^L = x_i \gamma_i^L(P^*, T, x_i) f_i^{*L}(T) \exp \left[\frac{v_i^L(P - P^*)}{RT} \right] \quad (6.9)$$

where γ_i^L is the activity coefficient of component i in the liquid and P^* is the reference pressure where γ_i^L and f_i^{*L} are calculated. The partial molar volume of pure component i in the liquid, v_i^L , is assumed independent of pressure. Where pure component i cannot exist as a liquid at the stated temperature, a correlation for the volume and fugacity of a hypothetical superheated or subcooled pure liquid is used.

Such an approach has been used by Mackay and Paulaitis (1979), Hess et al. (1986), and Lemert and Johnston (1989), among others. Mackay and Paulaitis (1979) used an equation of state to calculate the pure component liquid fugacities at the reference pressure P^* and a temperature dependent Henry's constant in the activity coefficient to fit the data. Hess et al. (1986) developed a method for binary systems. Liquid phase fugacities were calculated using regular solution theory. The reference liquid phase fugacity for the light component was found from the correlation of Chao and Seader (1961). Lemert and Johnston (1989) used a method based in part on approaches developed by McHugh and Krukoniis (1986) and Hess et al. (1986) which treat the subcooled liquid volume and, to a lesser degree, the solubility parameters in the regular solution theory model as adjustable parameters to fit data. Lemert (1988) noted that the results of his model are significantly affected by the values of the solubility parameters used in the regular solution theory.

Vapor or Supercritical Phase Fugacities

Gases at high pressure and supercritical fluids can be modeled as expanded liquids and treated with the same equations as liquids (such as activity coefficient models) (McHugh and Krukoniis 1986). To cover the entire pressure range including lower pressures and densities with a single equation, however, an equation of state approach with fugacity coefficients would be thermodynamically consistent and the least complex. Using an equation of state, the vapor and

supercritical phase fugacities would be calculated from the equations:

$$f_i^V = y_i \phi_i^V P \quad (6.10)$$

and

$$RT \ln \phi_i^V = \int_V^{\infty} \left[\left(\frac{\partial P}{\partial n_i} \right)_{T, V, n_j, n_i} - \frac{RT}{V} \right] dV - \ln Z^V \quad (6.11)$$

Kurnik et al. (1981, Kurnik and Reid 1982) used the Peng-Robinson equation with one adjustable binary interaction parameter to model solid-supercritical fluid solubility behavior. They made the interaction parameter a function of temperature to fit their data. Deiters and Schneider (1976), and Chai (1981, Paulaitis et al. 1983) have used a second adjustable parameter in the Redlich-Kwong-Soave and Peng-Robinson equations of state to correlate data on phase behavior of heavy solids with supercritical fluids. Johnston and Eckert (1981, Johnston et al. 1982) used an augmented van der Waals equation of state to predict solid solubilities in SCF solvents with reasonable success. In this work, the phase behavior was modeled with the Peng-Robinson and translated Peng-Robinson equations of state with a single adjustable interaction parameter.

As in the liquid phase, the accuracy of the calculated fugacities depends on the accuracy of the volume, pressure, and temperature values generated by the equation of state.

Peng-Robinson Equation of State

The Peng-Robinson equation of state

$$P = \frac{RT}{v - b} - \frac{a(T, \omega)}{v(v + b) + b(v - b)} \quad (6.12)$$

where v is the molar volume, may be used in equations 6.8 and 6.11 to determine liquid and vapor phase component fugacities in a mixture. If the mixing rules

$$a = \sum_{i=1}^m \sum_{j=1}^m x_i x_j a_{ij} \quad (6.13)$$

$$a_{ij} = (1 - k_{ij}) \sqrt{a_i a_j} \quad (6.14)$$

$$b = \sum_{i=1}^m x_i b_i \quad (6.15)$$

are used, component fugacity coefficients can be calculated by

$$\ln \phi_i = \frac{b_i}{b} (Z - 1) - \ln(Z - B^*) + \frac{A^*}{B^* \sqrt{8}} \left(\frac{b_i}{b} - \delta_i \right) \ln \frac{Z + B^* (1 + \sqrt{8})}{Z + B^* (1 - \sqrt{8})} \quad (6.16)$$

where

$$\frac{b_i}{b} = \frac{T_{c,i}/P_{c,i}}{\sum_j x_j T_{c,j}/P_{c,j}} \quad (6.17)$$

$$\delta_i = \frac{2a_i^{1/2}}{a} \sum_j x_j a_j^{1/2} (1 - k_{ij}) \quad (6.18)$$

$$A^* = \frac{aP}{R^2 T^2} \quad (6.19)$$

$$B^* = \frac{bP}{RT} \quad (6.20)$$

and k_{ij} is the binary interaction parameter for components i and j . This equation of state has been found to work well in predicting P-T-x-y values in vapor/liquid equilibria for many systems. Liquid volumes predicted by this equation, however, are still usually in error by several percent although they are usually superior to those calculated by the Redlich-Kwong-Soave equation of state which is of comparable complexity.

Translated Peng-Robinson Equation of State

Peneloux and Rauzy showed that if the volumetric and phase behavior of a fluid mixture are calculated by an equation of state, certain translations may be made along the volume axis without affecting the predicted phase equilibria of the fluid phases. The molar volume calculated by the untranslated equation of state is denoted as v and the more accurate translated volume is denoted as \tilde{v} . This notation is opposite that used by Peneloux and Rauzy but is more consistent with the notation in the previous section of this dissertation. A translation parameter c is defined such that

$$\bar{v} = v - \sum_{i=1}^m c_i x_i = v - c \quad (6.21)$$

with

$$\bar{v}_i = v_i - c_i \quad (6.22)$$

and

$$v_i = \left(\frac{\partial v}{\partial n_i} \right)_{T, P, n_{j \neq i}} \quad (i=1, \dots, m) \quad (6.23)$$

where all the c_i 's have constant values specific to each component. When these volumes are substituted into the exact thermodynamic relation for fugacity coefficients,

$$\ln \bar{\phi}_i = \int_0^P \left(\frac{\bar{v}_i}{RT} - \frac{1}{P} \right) dP \quad (6.24)$$

the more accurate translated fugacity coefficient $\bar{\phi}_i$ may be found from the relation:

$$\ln \bar{\phi}_i = \ln \phi_i - \frac{c_i P}{RT} \quad (6.25)$$

If the translated equation yields more accurate values for the volumes, then it would be expected to also give more accurate values for the fugacities as well. This equation does use one more parameter than the original Peng-Robinson equation, but the value of this parameter requires only pure component liquid volume data. No additional mixture data are required.

Calculations and Comparison of Results

The Peng-Robinson and translated Peng-Robinson equations of state have been compared and tested for their ability to predict the thermodynamic properties and phase behavior of the carbon dioxide+hydrocarbon binaries and ternaries measured experimentally in this work. Details of the computational schemes and the computer programs are contained in Appendices C through F. Determination of parameter values is discussed in Appendix G. Two types of calculations were attempted: 1) P-T-x-y values were calculated along the SLV lines for the CO₂+naphthalene, CO₂+biphenyl, and CO₂+phenanthrene binary systems and along the SSLV lines for the CO₂+naphthalene+biphenyl and CO₂+naphthalene+phenanthrene ternary systems and 2) P-x-y values along isothermal SLV lines in ternary systems. For the first calculations, values of all other variables were solved for iteratively at fixed pressures along the SLV or SSLV lines. For the second set of calculations, temperature, pressure, and the component forming the solid phase were specified and all remaining variables were solved for iteratively. Both types of calculations were carried out first using the Peng-Robinson EOS for the fluid phases and then using the translated Peng-Robinson EOS for those phases.

The P-T traces calculated for the binary and ternary systems are shown in Figures 6.1 through 6.5. The triple points for the pure solids (where the binary P-T traces should begin) and eutectic temperatures for the solid/solid binaries

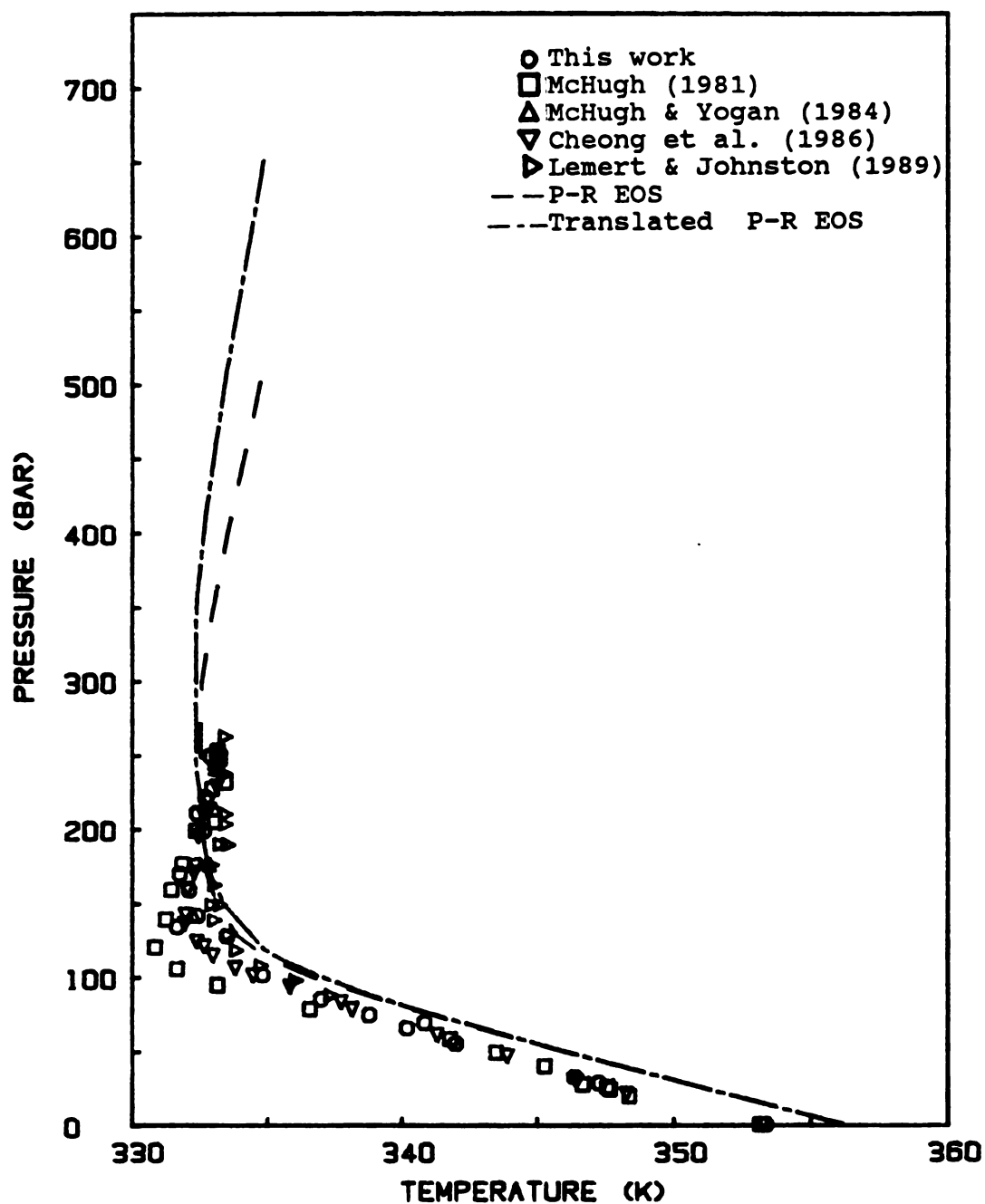


Figure 6.1 Predicted and measured SLV P-T traces for the CO_2 +naphthalene system.

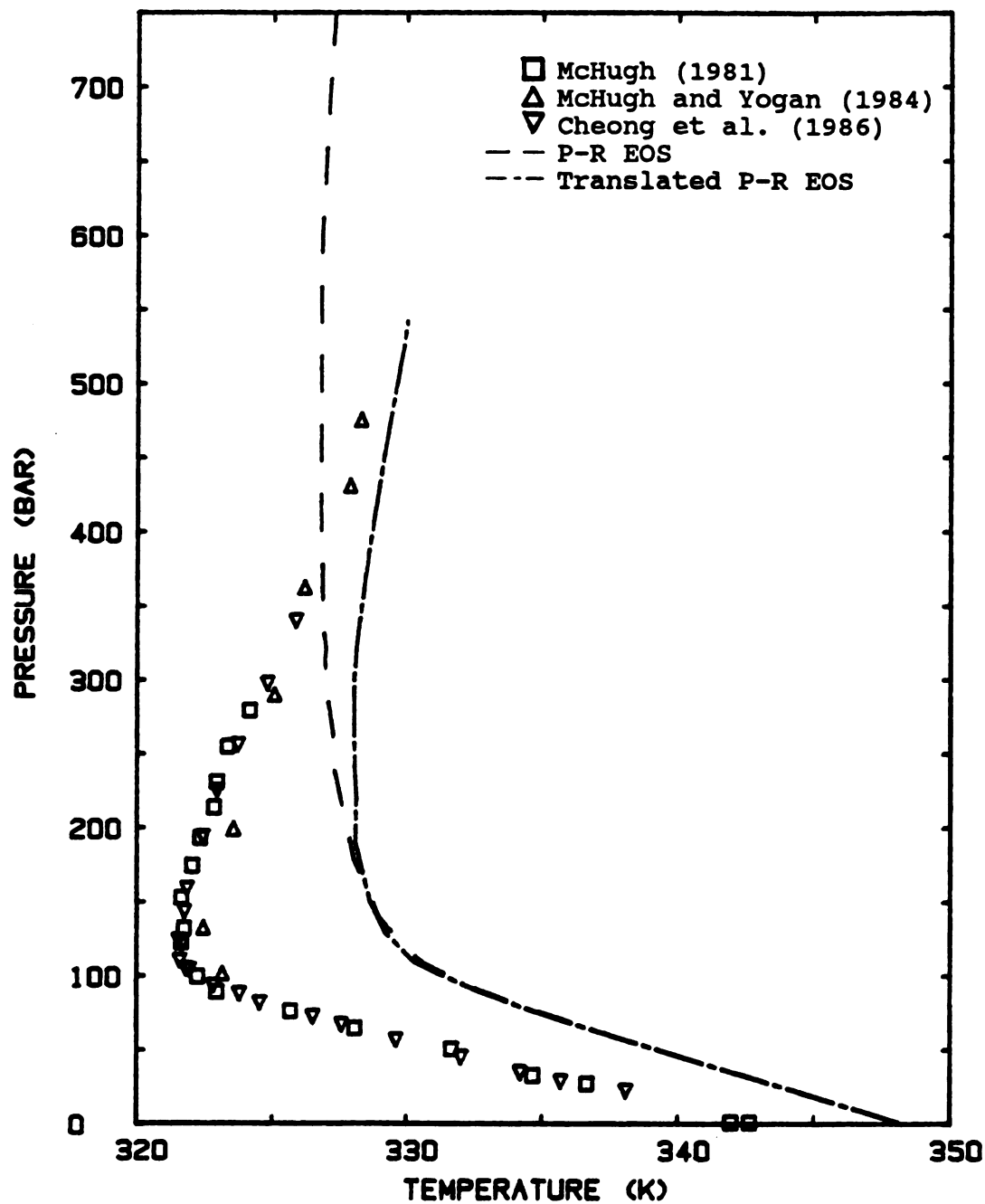


Figure 6.2 Predicted and measured SLV P-T traces for the CO_2 +biphenyl system.

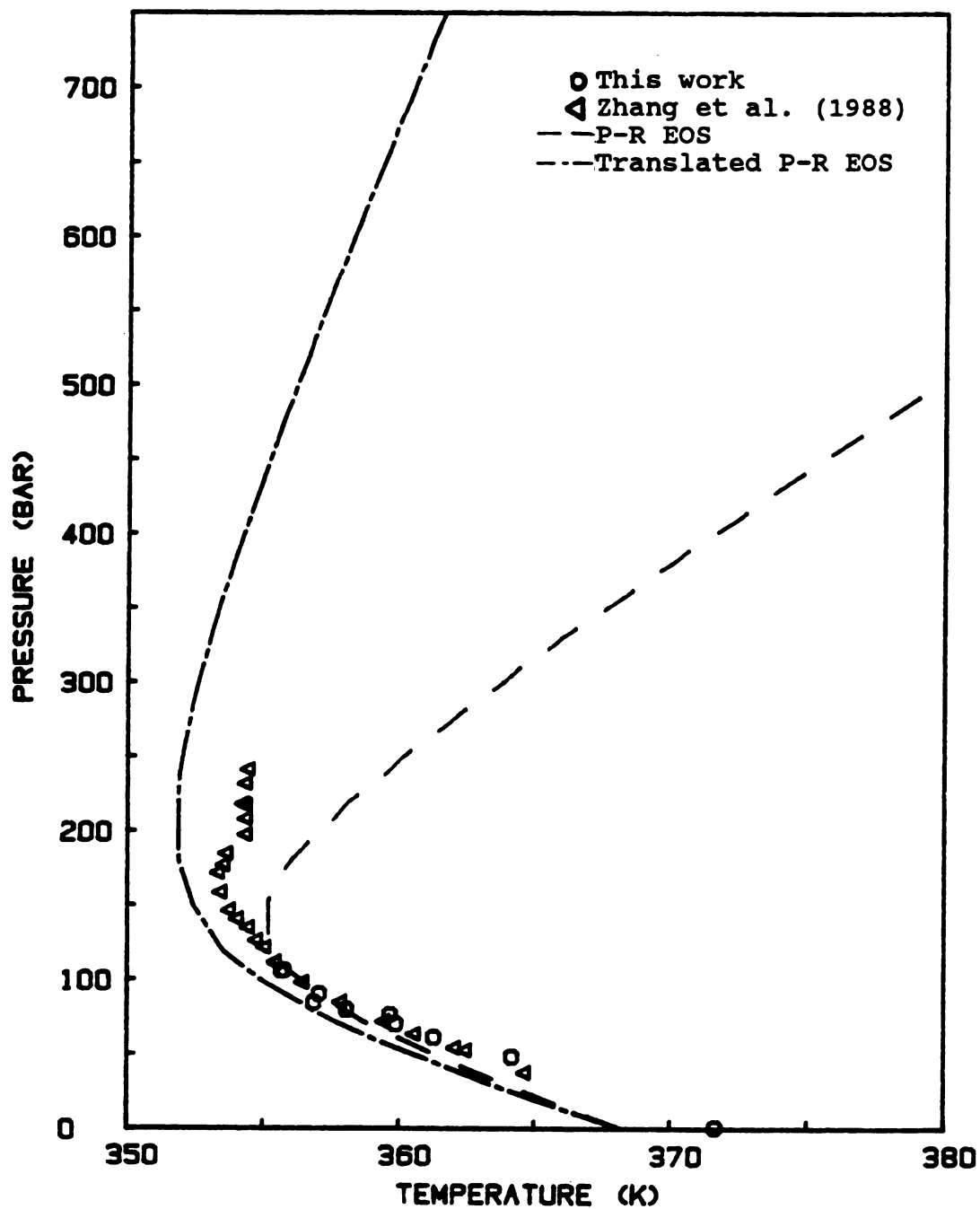


Figure 6.3 Predicted and measured SLV P-T traces for the CO_2 +phenanthrene system.

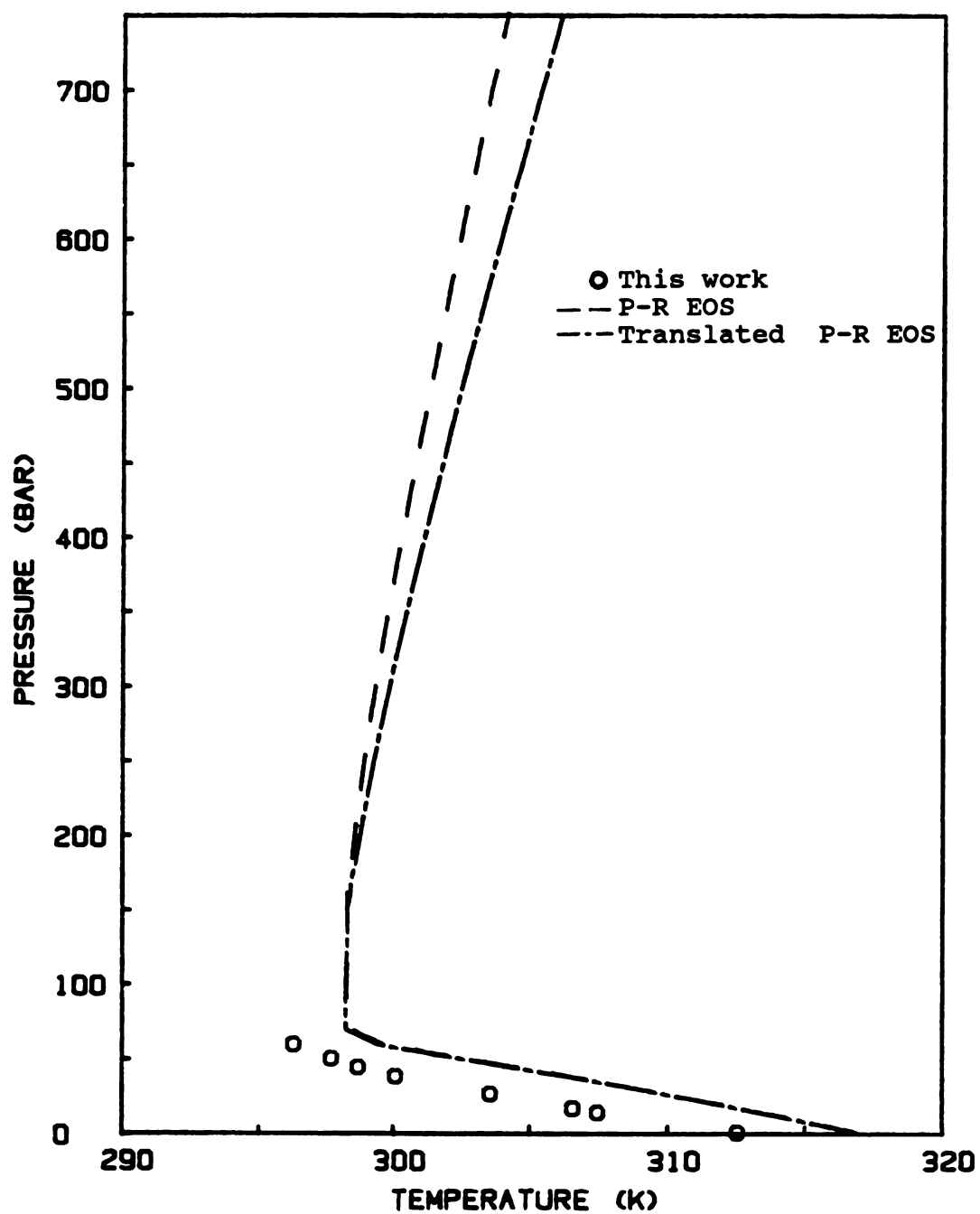


Figure 6.4 Predicted and measured SSLV P-T traces for the CO_2 +naphthalene+biphenyl system.

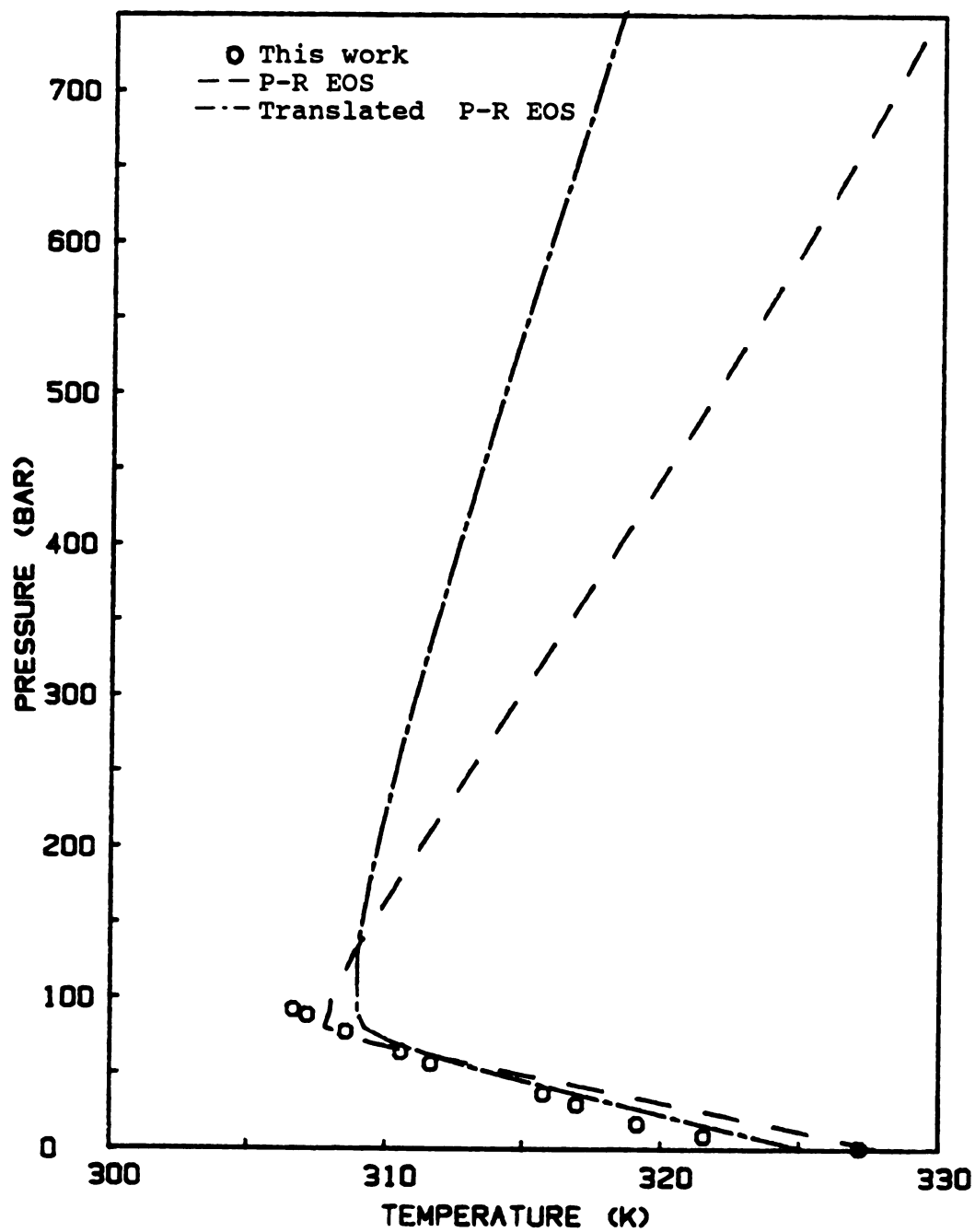


Figure 6.5 Predicted and measured SSLV P-T traces for the CO_2 +naphthalene+phenanthrene system.

(where ternary P-T traces should begin) are listed in Tables 6.1 and 6.2 for comparison.

Table 6.1
Pure Component Triple Points

<u>Component</u>	<u>Temperature (K)</u>	<u>Pressure (bar)</u>
Biphenyl	342.37	8.4262×10^{-4}
Naphthalene	353.43	9.9938×10^{-3}
Phenanthrene	372.38	2.9043×10^{-4}

Source: DIPPR data base

Table 6.2
Binary Eutectic Temperatures

<u>Binary</u>	<u>Temperature (K)</u>
Biphenyl and Naphthalene	312.55
Biphenyl and Naphthalene	312.85
Naphthalene and Phenanthrene	327.15
Naphthalene and Phenanthrene	321.25

Sources: Lee and Warner 1935
Gruberski 1961
Klochko-Zhovnir 1949
Rastogi and Varma 1956

The selection of parameter values is discussed in Appendix G. In determining the best values for the interaction parameters, the definition of what constitutes the "best" fit of the data is subjective. For this work, the fit of the predicted P-T curve to the experimental curve was used as the criterion for selecting parameters. Using compositions or volume data yields different parameters.

The original Peng-Robinson equation of state predicts the P-T traces of the binary and ternary systems qualitatively, but using the volume translated Peng-Robinson equation can improve the P-T trace predictions. Where the absolute value

of the pure component volume translation is relatively small, i.e. naphthalene, the models yield slightly different results. As the magnitude of c increases, the difference between the models becomes more pronounced. The effect of c is manifest in the P-T trace by the way the curves bend back. When c is positive, i.e. for naphthalene and phenanthrene, the curves bend back less. When c is negative, i.e. biphenyl, the trace bends back more.

Both models over-predicted the pressures of the upper critical end points of the CO_2 +naphthalene and CO_2 +biphenyl systems and invariant points for the CO_2 +naphthalene+biphenyl and CO_2 +naphthalene+phenanthrene systems. Based on the liquid phase mole fractions reported and predicted for the CO_2 +phenanthrene system, it appears that this binary system has not yet been measured up to its upper critical end point. For naphthalene and phenanthrene, computational instabilities and round-off errors caused the programs to terminate as the critical end points were approached, but before they were reached. Both equations predicted the upper critical end point of the CO_2 +naphthalene system to lie above the observed UCEP. The translated Peng-Robinson equation predicted an upper critical end point for the CO_2 +biphenyl system about 50 bar above the 475 bar reported by McHugh and Yogan (1984).

Predictions for both of the ternary systems indicate fairly sharp changes in the slope at approximately the pressures where the apparent invariant points were observed experimentally. Predictions above these points probably

represent metastable or unstable phases. The computer programs written for this work did not include any tests for such conditions.

The P-x-y traces calculated for the CO₂+hydrocarbon binaries are plotted in Figures 6.6 through 6.8. The values measured in this work and by Lu et al. are shown for comparison. For naphthalene, the models predict similar values at the lower pressures but diverge as the UCEP is approached. The untranslated Peng-Robinson equation yields an UCEP closer to the experimental value. For biphenyl, the translated equation is slightly better, than the untranslated equation, especially at the highest pressures. For phenanthrene, the translated equation yields significantly superior results to the untranslated equation.

The compositions predicted by the two equations of state along the SSLV line and along the 310, 320, 330 and 340 K SLV isotherms are plotted in Figures 6.9a and 6.9b. Data of Table 5.3 are also plotted in these figures for comparison. Except at very high pressures, the plots are indistinguishable. Both plots show better predictions in the right half of the diagram where the solid phase is naphthalene than in the left half where the solid phase is biphenyl. It should be noted that both equations yield a predicted triple point for biphenyl which is about 6 °C too high (compared to a 3 °C error for naphthalene). Consequently, the predicted composition of the naphthalene+biphenyl eutectic is shifted toward a higher biphenyl composition. This also results in a shift of the

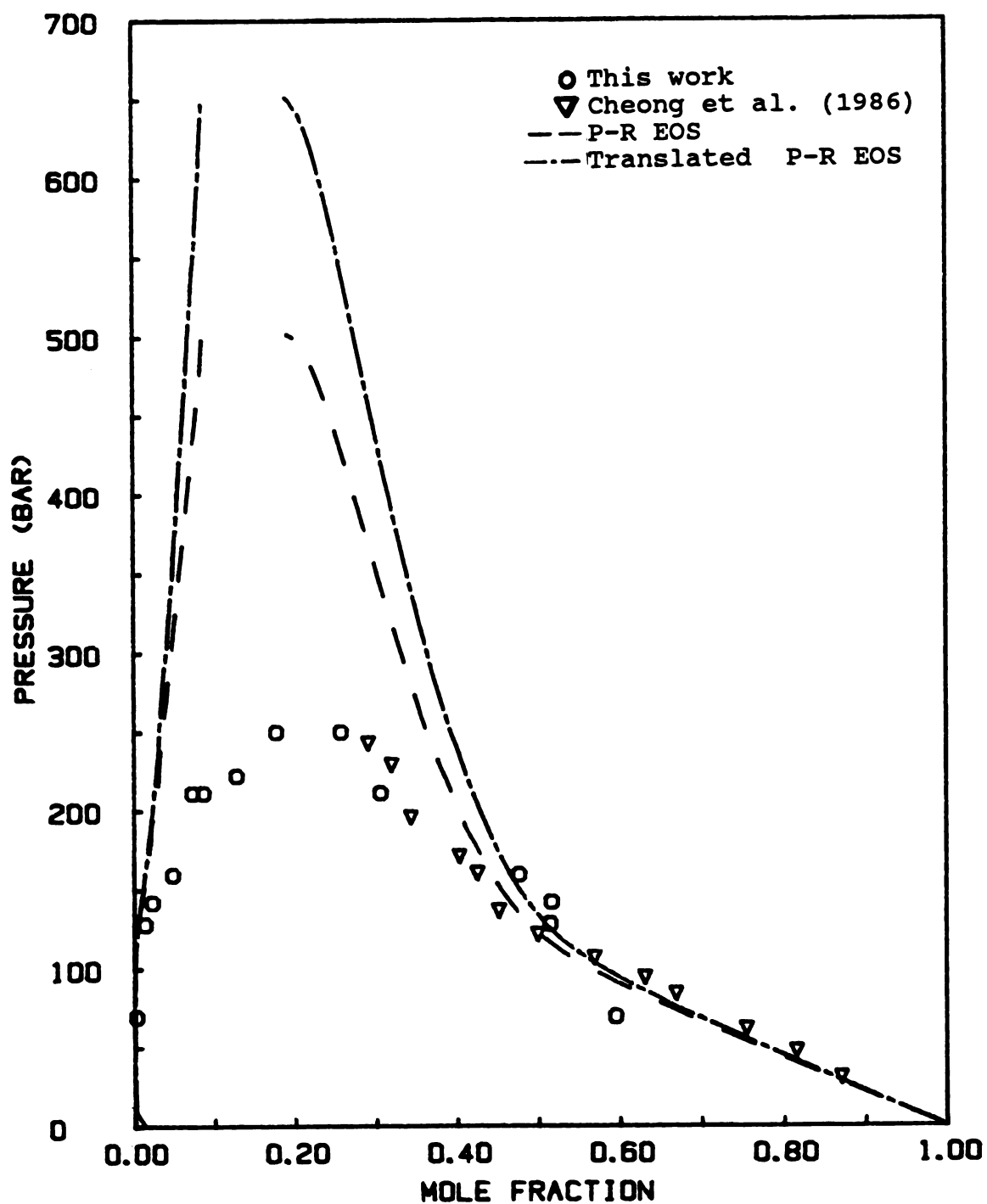


Figure 6.6 Predicted and measured P-x-y plot along the SLV line for the CO₂+naphthalene system.

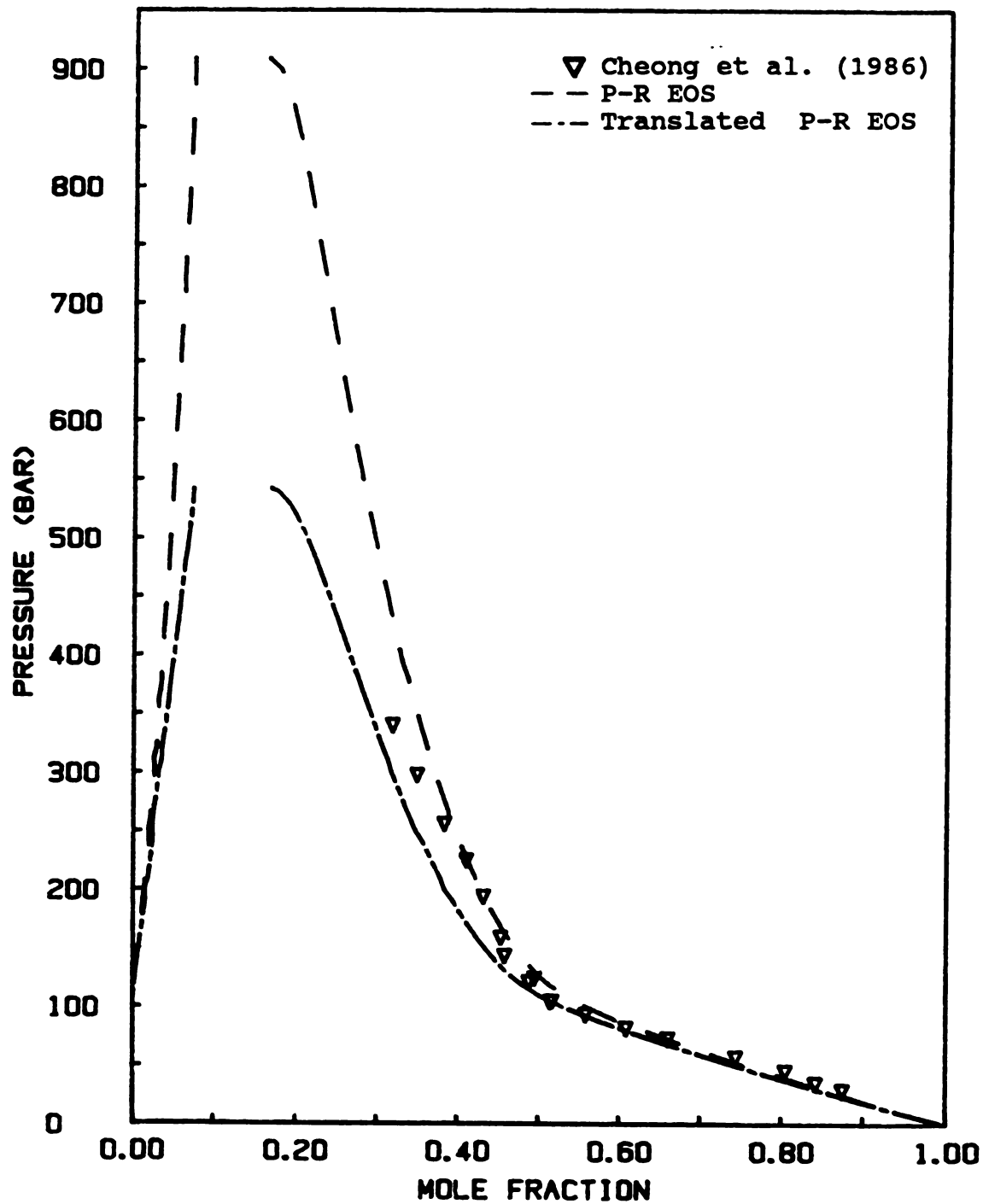


Figure 6.7 Predicted and measured P-x-y plot along the SLV line for the CO₂+biphenyl system.

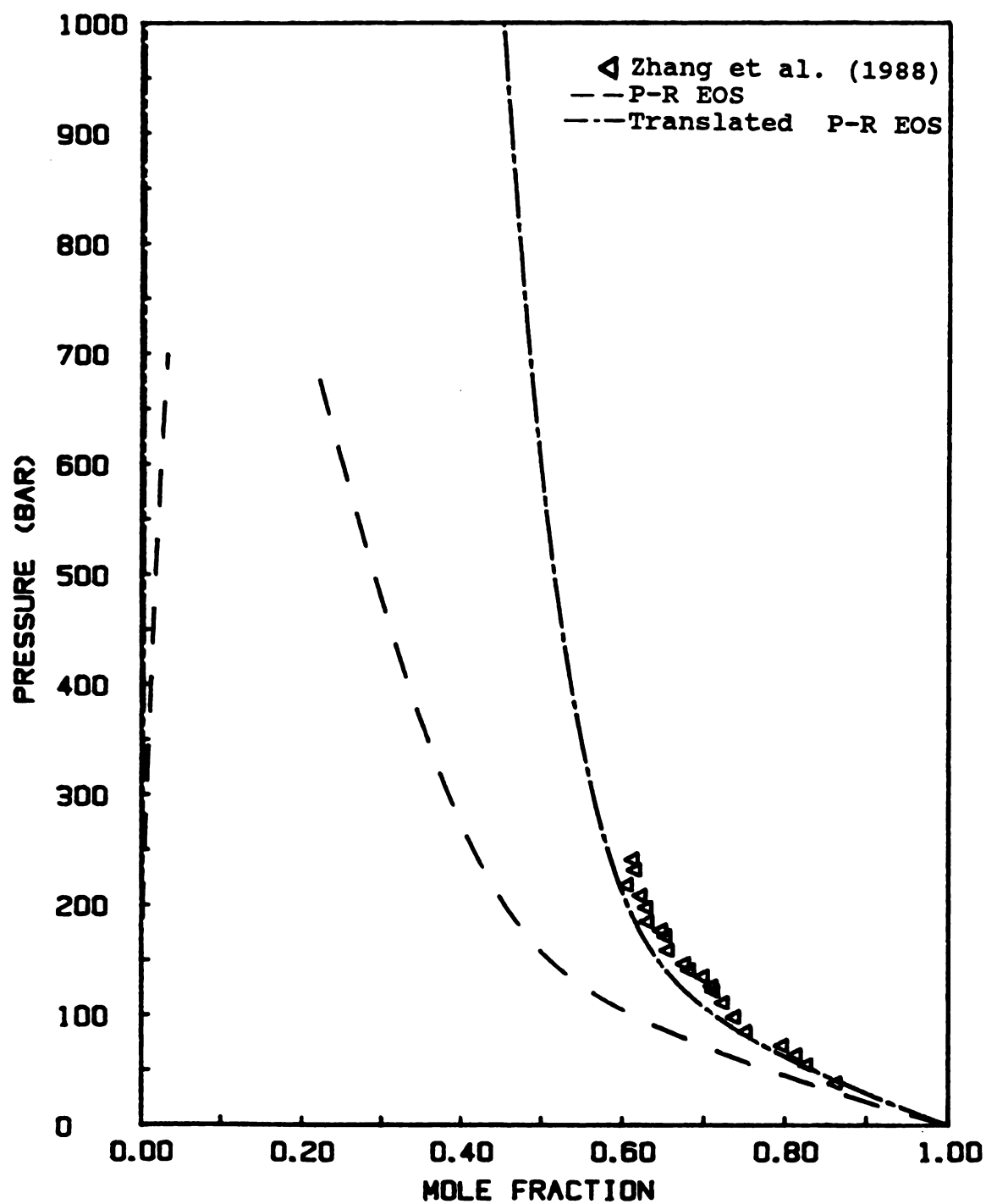


Figure 6.8 Predicted and measured P-x-y plot along the SLV line for the CO₂+phenanthrene system.

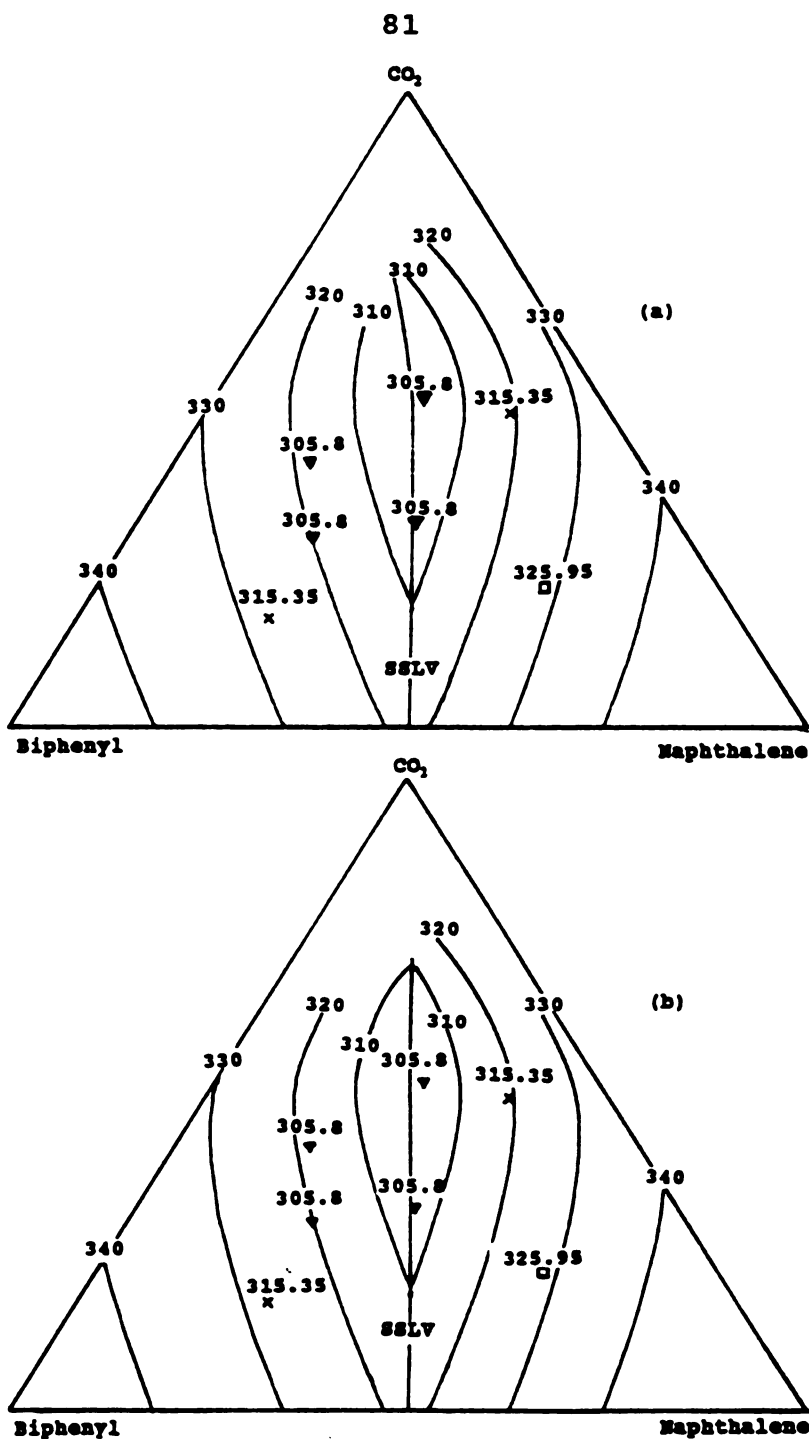


Figure 6.9 Comparison of equation of state phase equilibrium predictions to experimental data. SLV isotherms and SSLV lines were predicted using k_{ij} values indicated in the text with (a) the Peng-Robinson equation of state, and (b) the translated Peng-Robinson equation of state. Temperatures of the isotherms and data are in Kelvin.

isotherms toward the naphthalene-rich side of the diagram toward the experimental data on that side and away from the observed compositions of the biphenyl-rich side. Since the translated Peng-Robinson equation shows marked improvement over the original Peng-Robinson equation for representing the CO_2 +phenanthrene system, it is expected that predictions from the two equations for the CO_2 +naphthalene+phenanthrene system would show greater difference in their predictions with the translated equation yielding the more accurate results.

CHAPTER 7

CONCLUSIONS AND RECOMMENDATIONS

Conclusions

A new experimental apparatus has been constructed which can be used to study the phase equilibria of solids with liquids and dense gases at high pressures. A method was also devised to sample two equilibrium fluid phases at high pressures. P-T-v-x-y data were measured along the upper branch SLV line for the CO₂+naphthalene system and the values of these data were compared to the P-T and P-T-x data obtained by other researchers to validate the methods used in this study. These measurements were also the first measurements of the vapor phase compositions (y) and molar volumes (v) of this system along the SLV line.

P-T data were measured along the upper branch SLV line for the CO₂+phenanthrene system. P-T data were also measured along the SSLV lines starting at the solid-solid eutectics of the CO₂+naphthalene+biphenyl, CO₂+naphthalene+phenanthrene, CO₂+naphthalene+acenaphthene, and CO₂+naphthalene+anthracene systems. Except for the CO₂+phenanthrene system, for which P-T data were reported (Zhang et al., 1988) about the same time the results reported here were first presented at the 1988 AIChE national conference (White and Lira, 1989), none of these systems had been previously measured. These measurements were made up to apparent invariant points for the CO₂+naphthalene+biphenyl and CO₂+naphthalene+phenanthrene

systems. The nature of the invariant points differs between the two systems. In the CO_2 +naphthalene+biphenyl system, the SSLV line ends in a point where a second liquid phase is formed. This probably occurs when the SSLV line intersects a SLLV or SSSL line. In the CO_2 +naphthalene+phenanthrene system, the SSLV line seems to end in a point where the liquid and vapor phases become identical (i.e. a critical point). Vapor and liquid composition data were also measured for seven points along SLV isotherms of the CO_2 +naphthalene+biphenyl system. These measurements were not consistent with those reported by Zhang et al., but it is believed that the results reported here are more accurate.

Based on observations made during this work, to achieve phase equilibrium within a reasonable period of time, both the liquid and the vapor phases must be agitated. Although diffusion in dense gases and supercritical fluids tends to be much quicker than in liquids, unless these fluids are mixed, concentration and thermal gradients will take substantial time to dissipate. Thirty minutes of aggitation was adequate to achieve a well mixed, isothermal system.

Also, based on observations during this work, sampling of dense fluid phases where solid solubilities are a function of pressure must be done carefully in order to get representative samples. Pressure gradients between the equilibrium cell and the sample collection chamber (in this work, sample loops on an HPLC valve) may cause precipitation of solids, thus altering the composition of a sample. Solids may also block

lines connecting the cell and the sample volume, preventing a complete sample from being taken.

As demonstrated by the difference between the CO_2 +naphthalene+biphenyl and CO_2 +naphthalene+phenanthrene systems, binary data alone do not necessarily indicate some important aspects of the phase behavior of multi-component systems involving dense gases and supercritical fluids. Although the constituent binaries of these two ternary systems are very similar, the SSLV lines terminate in different types of invariant points. The magnitude of melting point depressions, and the location and nature of invariant points may differ significantly between multi-component systems even when the constituent binaries are similar.

The Peng-Robinson and translated Peng-Robinson equations were compared for their ability to accurately predict melting point depressions and phase compositions along the upper branch SLV lines for the CO_2 +naphthalene, CO_2 +biphenyl, and CO_2 +phenanthrene binary systems and melting point depressions along the SSLV lines for the CO_2 +naphthalene+biphenyl and CO_2 +naphthalene+phenanthrene ternary systems. This is the first time the translated Peng-Robinson equation has been applied to such equilibria. The SLV isotherms predicted by the translated and untranslated equations of state were also compared for their ability to reproduce the SLV isotherm data of the CO_2 +naphthalene+biphenyl system measured in this study. The translated equation is at least as good as the original Peng-Robinson equation of state for all systems examined in

this work. The improvement of the translated equation over the original is most dramatic when the pressure is high or the volume translation "c" for a pure component has a large absolute value. Both models still fail to predict some P-T-v-x-y values at the highest pressures. This is probably due to insufficient accounting for molecular interactions between unlike molecules, including differences in size and shape. At the highest pressures, the molecules become more densely packed, thus increasing the importance of these differences.

The molar volume values obtained by the methods of this work are accurate to only about $\pm 20\%$. Although this does not represent an improvement over other available methods for determining phase volumes, the information is easy to extract from the data taken in the course of finding the phase compositions and does offer a quick means to obtain additional useful information of fair accuracy about the systems being studied.

Recommendations

Based on the results of this work, three modifications of the experimental apparatus and several types of experiments are suggested. The apparatus modifications should make both melting point determinations and sampling easier. The experiments would facilitate a better understanding of the complex behavior of solute-supercritical fluid systems.

The current view cell has blind spots where the phase behavior cannot be observed and is sometimes difficult to

light adequately. The first apparatus modification entails building a high pressure view cell with two windows opposite each other instead of at right angles as in the current cell. The significant density and light scattering ability of the liquid phase makes it difficult to get adequate lighting into the current view cell to observe phase changes such as the precipitation of solids or formation of additional liquid phases. To get maximum improvement in lighting, the distance between the windows should be kept as small as possible. One limiting factor would be allowing sufficient space to insert a mechanism similar to the one used in the current view cell to agitate both phases. Since magnetic stir bars of sufficient size and strength to couple well with a magnetic stirrer are usually at least 1 inch long, this probably represents the smallest practical distance between the windows.

The current apparatus requires a fairly involved procedure to extract samples from the phases alternately. The second apparatus modification would be to use two 6-port HPLC valves for sampling instead of one 10-port valve. This would simplify sampling by eliminating the intermediate steps of flushing the lines and non-active sample loop during sampling to avoid contaminating the active sample loop. It would also allow the phases to be sampled more nearly simultaneously instead of alternately. Since the temperature within the bath may be too hot to allow putting a hand into the bath to turn the sample valves, long handles must be attached to the valves

to permit them to be switched from outside the bath. The sample ports should therefore be located such that the HPLC valves are not together on the same side of the cell.

Because a water bath is used, the experiments are limited to the range of temperatures for which water is a liquid at atmospheric pressure. The third change in the experimental apparatus would be to replace the water in the temperature control bath with a heat transfer fluid which can reach higher and lower temperatures than water without freezing and boiling. The fluid should be chosen such that it does not attack o-ring materials or corrode metals. It also ought to be one which can be thoroughly cleaned from the cell surface when the cell is removed for reloading since even small amounts of contaminants can alter the phase behavior of the cell contents.

The first extra measurements ought to be designed to extend the P-T trace of the CO₂+phenanthrene line to the upper critical end point. These experiments would probably have to be done in a capillary due to the high pressures necessary. This would permit better comparison of potential models to the data.

The second set of measurements should be designed to more completely characterize compositions along the three phase SLV isotherms of the CO₂+naphthalene+biphenyl system. This will require preparing samples of many different compositions and adjusting them isothermally to the pressure where solids just begin to form before sampling.

The third set of measurements should be designed to determine the nature of the invariant points reached in this work for both the CO_2 +naphthalene+biphenyl and the CO_2 +naphthalene+phenanthrene systems.

A fourth set of recommended experiments would involve studying the CO_2 +biphenyl+acenaphthene system. Since the eutectic temperature of the biphenyl+acenaphthene binary is lower than that of the biphenyl+naphthalene binary, the ternary eutectic with CO_2 should also be lower. The SSLV line of this system would almost certainly intersect a SLL line with a CO_2 rich liquid forming the second liquid.

It would also be illuminating to examine the accuracy of the translated Peng-Robinson equation when applied to multi-phase systems with supercritical solvents other than CO_2 . Ethane and ethylene are supercritical at relatively mild temperature and pressure conditions. Since some data already exist for multi-phase systems including these components (see Table 2.1), it is suggested these be examined next. Such studies are necessary to determine whether volume translation offers any improvements for systems with solvents for which the original Peng-Robinson equation provides better or worse predictions than it does for CO_2 systems.

To expand the understanding of supercritical fluids and facilitate evaluations of phase equilibrium prediction schemes such as the one just mentioned, additional P-T-v-x-y measurements should be made along multi-phase lines of systems with ethane and ethylene. Several classes of compounds ought

to be included in these studies, such as: long chain and branched alkanes, heavy alcohols, aromatics, ketones, and esters. Each of these types of compounds would provide information about the effects of different functional groups on the phase behavior of solid-SCF systems. The compounds should be chosen such that their triple points are well above the critical temperature of the supercritical solvent.

APPENDICES

APPENDIX A

GC CALIBRATION

The GC is calibrated twice --- once for determining the amount of naphthalene relative to biphenyl and the second time to determine both naphthalene and biphenyl concentrations relative to acenaphthene. Calibration standards are prepared by weighing out each component for the sample solution in the volumetric flask used as a sample container and filling the flask to the volume line with toluene to dissolve the solids. All solids are weighed out to within ± 0.0003 grams on a Sartorius R300S balance. A clean stir bar is added to each sample and they are placed on a magnetic stirrer for at least an hour to assure that each solution will be homogeneous. The area of each component peak divided by the area of the peak for the I.S. (internal standard) is determined for at least five different concentrations over a two order of magnitude range. The concentration of naphthalene or biphenyl as a function of the area ratio and concentration of the I.S. is then determined by a least squares fit of the data to an equation of the form:

$$\text{component mass} = \left[\text{ml solution} \times \frac{\text{g I.S.}}{\text{ml solution}} \right] \times \text{slope} \times \overline{\text{AR}} \quad (\text{A.1})$$

The compositions of the samples are analyzed on a Perkin-Elmer 8500 gas chromatograph using an Alltech 10 m x 0.53 mm Bonded FSOT RSL-50 column with a 6 inch length of uncoated 0.53 mm megabore tubing as a pre-column condensing section. The GC settings were as follows:

SECTION 1 GC CONTROL*

	1	2	3
Oven Temp (°C)	40	100	115
Iso Time (Min)	4.0	7.5	3.0
Ramp Rate (°C/Min)	7.5	30.0	

HWD 1 Range	Off	FID 2 Sens	High
HWD 1 Polarity	B-A		

INJ 1 Temp	Off	INJ 2 Temp	300 °C
DET 1 Temp	200 °C	DET 2 Temp	310 °C

Flow 1	10 ml/Min	Pressure 3	5.0 psig
Flow 2	10 ml/Min	Carrier Gas 2	He
Carrier Gas 1	He		

DET Zero	On	Equilib Time	0.0 Min
Initial DET	2	Total Run Time	23.0 Min

SECTION 2 TIMED EVENTS**

<u>Time</u>	<u>Event</u>	
-1.00	Relay 1	On
0.20	Relay 0	On

SECTION 3 DATA HANDLING**

<u>Data Acquisition</u>		<u>Report</u>	
Start Time	10.00 Min	Calc Type	%
End Time	23.00 Min	Area/Ht Calc	Area
		Print Tol	0.0000
Width	5	Output	
Skim Sens	1	Screen	Yes
Baseline Corr	B-B	Printer	No
		Ext Dev	Yes
DET 1 Area Sens	50		
DET 2 Area Sens	121		
DET 1 Base Sens	4		
DET 2 Base Sens	6		

* The Perkin-Elmer 8500 gas chromatograph was configured with dual packed columns and a hot-wire detector in position 1 and the single column (megabore or capillary column) connected to an FID detector in position 2. All analyses for this work were done with the position 2 hardware (column and detector).

** The "Timed Events" and "Data Handling" parameters given are specific to the instrument used and the configuration of that instrument. They are given here to document the exact conditions of the analysis as well as to enable duplication of the method.

APPENDIX B

SAMPLE LOOP VOLUME DETERMINATIONS

The equipment configuration used to determine the volume of the two sample loops was identical to that used in the composition measurements except that the sample loops were connected directly to a high pressure tank of helium.

Sample loop volumes were calculated using the equations:

$$V = nv(P_{\text{loop}}, T) \quad (\text{a.B})$$

$$n = \frac{P_{\text{ambient}} V_{\text{final}}}{RT} \quad (\text{a.B})$$

with V_{final} the volume of the helium at atmospheric pressure.

The molar volumes of helium at elevated pressures were calculated from the virial coefficients calculated from the data of Wiebe, Gaddy and Heins in The Virial Coefficients of Pure Gases and Mixtures by Dymond and Smith (1980).

Table B.1 Data for Volume Determination of Sample Loop 1

<u>Temperature (K)</u>	<u>Loop Pressure (bar)</u>	<u>Final Volume (cc)</u>	<u>Moles Helium $\times 10^4$</u>	<u>v Helium cc/gmol</u>	<u>Loop Volume (cc)</u>
296.75	75.8421	3.65	1.485	336.861	.050026
296.75	75.8421	3.65	1.485	336.861	.050026
296.75	75.7731	3.65	1.485	337.158	.050070
296.75	57.2263	2.75	1.119	442.701	.049556
296.85	57.9158	2.85	1.160	437.712	.050762
296.85	58.2605	2.85	1.160	435.190	.050469
296.85	58.6052	2.85	1.160	432.697	.050180
296.75	86.1842	4.20	1.709	297.815	.050911
296.85	86.5289	4.25	1.729	296.769	.051319
296.85	86.8736	4.20	1.709	295.637	.050521
296.85	86.8736	4.25	1.729	295.637	.051123
296.85	117.2105	5.75	2.339	222.076	.051954
296.90	117.2105	5.75	2.339	222.112	.051953
296.90	117.2105	5.75	2.339	222.112	.051953
average calculated volume					.050773
standard deviation					.000766
% std. deviation					1.508690

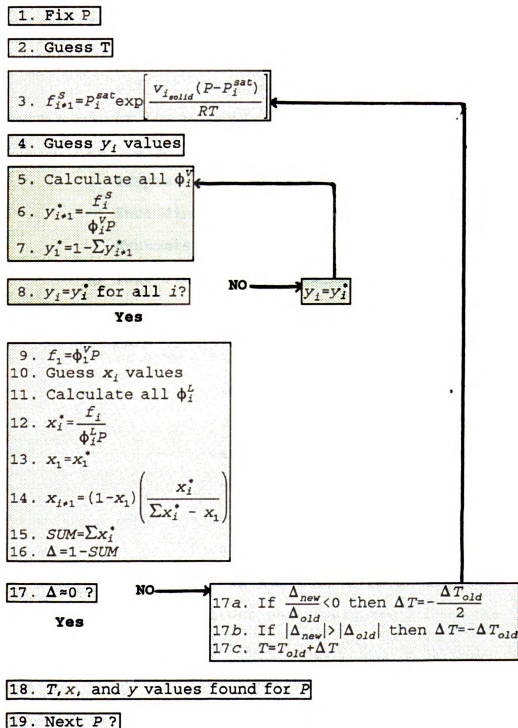
Table B.2 Data for Volume Determination of Sample Loop 2

<u>Temperature (K)</u>	<u>Loop Pressure (bar)</u>	<u>Final Volume (cc)</u>	<u>Moles Helium $\times 10^4$</u>	<u>v Helium cc/gmol</u>	<u>Loop Volume (cc)</u>
296.85	56.5368	5.70	2.321	448.106	.103994
296.85	57.2263	5.70	2.321	442.846	.102773
296.85	57.9158	5.70	2.321	437.712	.101582
296.90	58.2605	5.80	2.361	435.261	.102766
296.90	58.6052	5.80	2.361	432.768	.102178
296.90	83.4263	8.45	3.439	307.430	.105721
296.85	84.1158	8.50	3.460	304.954	.105508
296.85	84.8052	8.50	3.460	302.568	.104683
296.90	84.8052	8.50	3.459	302.617	.104682
296.90	119.2789	12.10	4.944	218.457	.108001
296.90	119.2789	12.10	4.944	218.457	.108001
296.85	119.6236	12.10	4.945	217.826	.107707
average calculated volume					.104800
standard deviation					.002169
% std. deviation					2.069595

NOTE: Ambient atmospheric pressure = 1.004 bar for both tables.

APPENDIX C

ITERATION SCHEME FOR SLV AND SSLV LINE DETERMINATIONS



Notes: 1) The programs in Appendix D are used to make these calculations.

2) x_1 and y_1 are the mole fractions of the solvent in the liquid and vapor phases respectively.

3) If cross parameters (k_{ij} for example) are used for the calculation of the ϕ_1^V and ϕ_1^L values (steps 5 and 11), they must be entered during the execution of the program.

4) The x iteration scheme (steps 10 through 17) is adapted from several sources in the literature including Henley and Seader (1981) and McHugh and Krukoni (1986).

5) This iteration scheme uses the following programs from Appendix D:

Main

Program - This is the first program listed in Appendix D. It follows the outline at the beginning of this appendix (C) and calls various subroutines to get initial and intermediate data.

INPUT - This subroutine reads initial variable values.

FIXXY - This subroutine returns values for mole fractions weighted by the initial guesses.

SFUG - This subroutine calculates the fugacities of solid phases.

- VEOS - This subroutine calculates vapor phase fugacity coefficients. There are two versions of this in Appendix D. The first uses the original Peng-Robinson EOS; the second uses the translated Peng-Robinson EOS.
- LEOS - This subroutine calculates liquid phase fugacity coefficients. There are two versions of this in Appendix D. The first uses the original Peng-Robinson EOS; the second uses the translated Peng-Robinson EOS.
- CUBIC - This subroutine solves a cubic polynomial for the three real or imaginary roots. It is required in the subroutines VEOS and LEOS.

APPENDIX D

COMPUTER CODE FOR CALCULATING SLV AND SSLV LINES

```

C *****
C * THIS PROGRAM CALCULATES THE COMPOSITION AND THE P,T TRACE OF *
C * THE THREE OR FOUR-PHASE LINE (SLV OR SSLV) FOR A BINARY OR *
C * TERNARY SYSTEM WITH ONE LIGHT (I.E. GAS AT AMBIENT CONDITIONS) *
C * COMPONENT AND ONE OR TWO HEAVY (I.E. SOLID AT AMBIENT *
C * CONDITIONS) COMPONENTS. *
C * COMPONENT 1 IS CHOSEN TO BE THE LIGHT COMPONENT. *
C *****
C
C *****
C * ADELTA1    ABSOLUTE VALUE OF DELTA1  (|DELTA1|) *
C * ADELTA2    ABSOLUTE VALUE OF DELTA2  (|DELTA2|) *
C * ANT(I,J)   ANTOINE COEFFICIENTS OF COMPONENT I *
C * C(I)       VOLUME TRANSLATION FOR COMPONENT I *
C * DELTA1     NEW VALUE OF (FUGV - FUGL) *
C * DELTA2     OLD VALUE OF (FUGV - FUGL) *
C * DELTAT     INCREMENTAL CHANGE TO T FOR THE NEXT ITERATION *
C * DELMIN     THE SMALLEST REASONABLE ABSOLUTE TEMPERATURE *
C *            INCREMENT *
C * DELX       THE CHANGE IN X(1) FROM THE LAST ITERATION LOOP *
C * DFG(I)     DOUBLE PRECISION FG(I) *
C * DHF(I)     MOLAR HEAT OF FUSION OF PURE COMPONENT I AT ITS *
C *            NORMAL MELTING POINT (CAL/G-MOLE) *
C * DI         MAXIMUM ALLOWABLE PRESSURE INCREMENT FOR THE NEXT *
C *            LOOP *
C * DINCR      PRESSURE INCREMENT FOR THE NEXT LOOP (UNITS OF BAR) *
C * DNEWX(I)   NEXT PREDICTED VALUE FOR X(I) BASED ON THE PHI *
C *            (FUGACITY COEFFICIENT) VALUES CALCULATED FROM THE *
C *            OLD X(I) VALUES *
C * DOLDX      VALUE OF X(1) FROM THE LAST ITERATION - USED TO *
C *            KEEP THE PROGRAM FROM CHASING AFTER A VALUE OF *
C *            X(1) IN A REGION WHERE IT WILL NEVER FIND A *
C *            SOLUTION (X(1) INCREASES MONOTONICALLY WITH *
C *            INCREASING PRESSURE.) *
C * DP         DOUBLE PRECISION P *
C * DP1        PRESSURE (IN BAR) FOR THE FIRST CALCULATION *
C * DPHI(I)    FUGACITY COEFFICIENT OF COMPONENT I *
C * DRATIO(I)  RATIO Y(I)/X(I) - USED TO CHECK FOR APPROACH TO *
C *            THE CRITICAL POINT - USUALLY THE UPPER CRITICAL *
C *            END POINT (UCEP) *
C * DPTOP      THE TOP PRESSURE FOR WHICH CALCULATIONS WILL BE *
C *            PERFORMED *
C * DSUMX      SUM OF THE X VALUES PREDICTED BASED ON THE *
C *            FUGACITIES CALCULATED IN THE SOLID AND VAPOR PHASES *
C *            - WHEN THE CORRECT TEMPERATURE HAS BEEN FOUND, *

```

```

C      *      THE X VALUES WILL SUM TO 1      *
C      * DSUMY      SUM OF THE Y VALUES OF THE SOLID COMPONENTS IN THE      *
C      *      VAPOR PHASE BASED ON THEIR SOLID PHASE FUGACITIES      *
C      * DX(I)      DOUBLE PRECISION X(I)      *
C      * DXOLD      VALUE OF DX(1) CALCULATED AT THE LAST PRESSURE -      *
C      *      DX(1) SHOULD KEEP INCREASING AS THE PRESSURE      *
C      *      INCREASES, SO ANY GUESS FOR X1 LOWER THAN THAT AT      *
C      *      THE LAST PRESSURE IS TOO LOW AND DX(1) IS RESET TO      *
C      *      DXOLD AS THE LOWER BOUND - USING THIS STRATEGY      *
C      *      HELPED KEEP THE SEARCH FOR THE LIQUID COMPOSITION      *
C      *      IN A FEASIBLE RANGE SO THE PROGRAM WOULD NOT CRASH      *
C      * DY(I)      DOUBLE PRECISION Y(I)      *
C      * DZ      DOUBLE PRECISION COMPRESSIBILITY FACTOR      *
C      * FG(I)      FUGACITY OF PURE COMPONENT I IN THE GAS OR SCF      *
C      *      PHASE      *
C      * FUGL      LIQUID PHASE PARTIAL MOLAR FUGACITY OF COMPONENT 1      *
C      * FUGV      VAPOR PHASE PARTIAL MOLAR FUGACITY OF COMPONENT 1      *
C      * I      COMPONENT NUMBER      *
C      * K(I,J)      INTERACTION PARAMETER FOR COMPONENTS I AND J      *
C      * OLD T      T VALUE USED IN THE PREVIOUS ITERATION - USED TO      *
C      *      KEEP TRACK OF WHICH WAY T IS BEING ADJUSTED AS THE      *
C      *      ITERATIONS PROCEED      *
C      * OMEGA(I)      PITZER ACENTRIC FACTOR OF COMPONENT I      *
C      * LV      MOLAR VOLUME OF LIQUID MIXTURE (CC/G-MOLE)      *
C      * NC      NUMBER OF COMPONENTS IN THE SYSTEM      *
C      * P      SYSTEM PRESSURE (UNITS OF BAR)      *
C      * P1      PRESSURE FOR THE FIRST LOOP (UNITS OF BAR)      *
C      * PC(I)      THE CRITICAL PRESSURE OF PURE COMPONENT I IN UNITS      *
C      *      OF BAR      *
C      * PPSIA      PRESSURE IN psia - CALCULATED BUT NOT USED IN THIS      *
C      *      VERSION OF THE PROGRAM      *
C      * PTOP      PRESSURE FOR THE LAST LOOP (UNITS OF BAR)      *
C      * PTOT      SYSTEM PRESSURE (UNITS OF ATM)      *
C      * T      SYSTEM TEMPERATURE IN UNITS OF KELVIN      *
C      * TC(I)      THE CRITICAL TEMPERATURE OF PURE COMPONENT I IN      *
C      *      UNITS OF KELVIN      *
C      * TDEGC      SYSTEM TEMPERATURE IN DEGREES CELSIUS      *
C      * TM(I)      NORMAL MELTING POINT OF PURE COMPONENT I (KELVIN)      *
C      * VC(I)      THE CRITICAL VOLUME OF PURE COMPONENT I (CC/G-MOLE)      *
C      * VL(I)      MOLAR VOLUME OF PURE LIQUID COMPONENT I (CC/G-MOLE)      *
C      * VS(I)      MOLAR VOLUME OF PURE SOLID COMPONENT I (CC/G-MOLE)      *
C      * VV      VOLUME OF VAPOR MIXTURE (CC/G-MOLE)      *
C      * X(I)      THE MOLE FRACTION OF COMPONENT I IN THE LIQUID      *
C      *      PHASE      *
C      * Y(I)      THE MOLE FRACTION OF COMPONENT I IN THE GAS OR      *
C      *      SCF PHASE      *
C      *****
C
C      *****
C      * NOTE: SOME OF THE ARGUMENT LISTS FOR SOME OF THE SUBROUTINES      *
C      *      CALLED IN THIS MAIN PROGRAM MAY CONTAIN VARIABLES WHICH      *
C      *      ARE NOT USED IN THIS PROGRAM.      *
C      *

```

```

C      *      THIS IS A RESULT OF MY ATTEMPTS TO MAKE THE PROGRAM AND *
C      *      SUBROUTINES FLEXIBLE ENOUGH TO ALLOW EASY CHANGE-OVER TO *
C      *      OTHER ALGORITHMS, EQUATIONS OF STATE, ETC. WITHOUT      *
C      *      REWRITING THE ENTIRE CODE.                                *
C      *
C      *      IF A VARIABLE LISTED IN THE CALLING ARGUMENT OF A        *
C      *      SUBROUTINE CALLED HERE IS NOT USED ELSEWHERE IN THE      *
C      *      PROGRAM, DO NOT GET CONCERNED, IT PROBABLY WAS NEEDED      *
C      *      WHEN THAT SUBROUTINE WAS CALLED IN A DIFFERENT PROGRAM      *
C      *      OR IS REQUIRED WHEN A DIFFERENT EQUATION OF STATE IS        *
C      *      USED.                                                       *
C      *****
C
      DIMENSION ANT(3,3),C(3),DHF(3),FG(3),K(3,3),OMEGA(3),PC(3)
      DIMENSION TC(3),TM(3),VC(3),VL(3),VS(3),X(3),Y(3)
      REAL LV
      DOUBLE PRECISION ADELTA1,ADELTA2,DELMIN,DELTA1,DELTA2,DELX,DFG(3)
      DOUBLE PRECISION DI,DINCR,DNEWX(3),DP,DP1,DPHI(3),DRATIO(3),DSUMY
      DOUBLE PRECISION DPTOP,DX(3),DXOLD,DY(3),DZ
      OPEN (UNIT = 5, STATUS = 'UNKNOWN')
      OPEN (UNIT = 6, STATUS = 'UNKNOWN')
      OPEN (UNIT = 17, STATUS = 'NEW', FILE = 'OUTPUT.DAT')
      CALL INPUT (ANT,C,DHF,K,NC,OMEGA,PC,PTOT,T,TC,TM,VC,VL,VS,X,Y)
      CALL FIXXY (NC,DX,DY,X,Y)
      DOLDX = 1.D0
      WRITE (6,70)
      READ (5,*) DP1
      WRITE (6,74)
      READ (5,*)DPTOP
      WRITE (6,78)
      READ (5,*)DINCR
      WRITE (17,86)
      WRITE (17,90)
      DI = DINCR
      DP = DP1
C  ***
C  * THE NEXT STATEMENT IS INTENDED TO GIVE A REASONABLE FIRST GUESS *
C  * FOR THE FUGACITY OF THE LIGHT COMPONENT FOR THE FIRST ITERATION. *
C  ***
      DFG(1) = DP1
      OLDT = T + 0.2D0*DINCR
      DELMIN = (.002)*DINCR
      300 DELTAT = (T - OLDT)
C  ***
C  * THE NEXT 4 LINES ARE TO PREVENT SUCH A SMALL INITIAL INCREMENT IN *
C  * THE TEMPERATURE GUESS THAT CONVERGENCE BECOMES A PROBLEM.          *
C  ***
      IF (ABS(DELTAT).LT.ABS(DELMIN)) THEN
        IF (DELTAT.GE.0.) DELTAT = DELMIN
        IF (DELTAT.LT.0.) DELTAT = - DELMIN
      ENDIF
      OLDT = T
      DELTA2 = -100.D0

```

```

      ADELTA2 = DABS(DELTA2)
400  CALL SFUG(ANT,DFG,NC,DP,T,VS)
      CALL VEOS(C,DFG,K,NC,OMEGA,DP,PC,DPHI,T,TC,VV,DY,DZ)
      DSUMY = 0.0DO
      DO 420 I = 2,NC
          DSUMY = DSUMY + DY(I)
420  CONTINUE
      DY(1) = 1.DO - DSUMY
      DFG(1) = DY(1)*DPHI(1)*DP
450  CALL LEOS(C,DFG,K,NC,OMEGA,DP,PC,DPHI,T,TC,LV,DX,DZ)
      DSUMX = 0.0DO
      DO 500 I = 1,NC
          DNEWX(I) = DFG(I)/DPHI(I)/DP
          DSUMX = DSUMX + DNEWX(I)
500  CONTINUE
      DELX = DABS(DNEWX(1)-DX(1))/DX(1)
      DX(1) = (DX(1)+DNEWX(1))/2
      IF (DX(1).EQ.DXOLD) THEN
          WRITE (6,50)
          50  FORMAT (X,'X(1) NOT CHANGING')
C *****
C * IF X(1) IS NOT CHANGING BUT THE CONVERGENCE CRITERIA HAVE NOT BEEN *
C * MET, THIS BRANCH WILL PREVENT AN ENDLESS LOOP. *
C *****
          STOP
          ENDIF
          IF (DX(1).LT.DXOLD) DX(1)=DXOLD
          DO 600 JJ=2,NC
              DX(JJ) = (1.DO - DX(1))*DNEWX(JJ)/(DSUMX-DX(1))
600  CONTINUE
          IF (DELX.GT.2.5D-4) GOTO 450
          DELTA1 = DELTA2
          DELTA2 = 1.DO - DSUMX
          ADELTA1 = DABS(DELTA1)
          ADELTA2 = DABS(DELTA2)
          IF (ADELTA2.GE.1.D-03) THEN
              IF (DELTA2/DELTA1.LT.0.DO) THEN
                  DELTAT = -DELTAT/2.DO
              ELSE IF(ADELTA2.GT.ADELTA1) THEN
                  DELTAT = -DELTAT/2.DO
              ENDIF
              T = T + DELTAT
              GOTO 400
          ENDIF
1000 PPSIA = DPTOT*14.696
      TDEGC = T - 273.15
      DOLDX = DX(1)
      WRITE (17,92) DP,T,DX(2),DX(3),DY(2),DY(3)
      WRITE (6,94) DP,T
      DO 1200 I=1,NC
          DRATIO(I) = DY(I)/DX(I)
1200  CONTINUE
      DO 1300 I = 2,NC

```



```

      IF (DRATIO(I).GT.5.0D-02) DI = 5.0
1300  CONTINUE
      DO 1310 I = 2,NC
      IF (DRATIO(I).GT.8.0D-02) DI = 2.5
1310  CONTINUE
      DO 1320 I = 2,NC
      IF (DRATIO(I).GT.1.1D-01) DI = 1.0
1320  CONTINUE
      DO 1330 I = 2,NC
      IF (DRATIO(I).GT.1.3D-01) DI = 0.5
1330  CONTINUE
      DO 1340 I = 2,NC
      IF (DRATIO(I).GT.2.0D-01) DI = 0.25
1340  CONTINUE
      DO 1350 I = 2,NC
      IF (DRATIO(I).GT.3.0D-01) DI = 0.1
1350  CONTINUE
      DO 1360 I = 2,NC
      IF (DRATIO(I).GT.3.5D-01) DI = 0.05
1360  CONTINUE
      IF (DI.LE.DINCR) DINCR = DI
      IF (DP.EQ.DPTOP) THEN
        GOTO 2000
      ELSE
        IF (DP.EQ.DP1) THEN
          DP = DINCR
1500      IF (DP.GT.DP1) GOTO 300
          DP = DP + DINCR
          GOTO 1500
        ELSE
          DP = DP + DINCR
          IF (DP.GT.DPTOP) DP = DPTOP
          GOTO 300
        ENDIF
      ENDIF

```

```

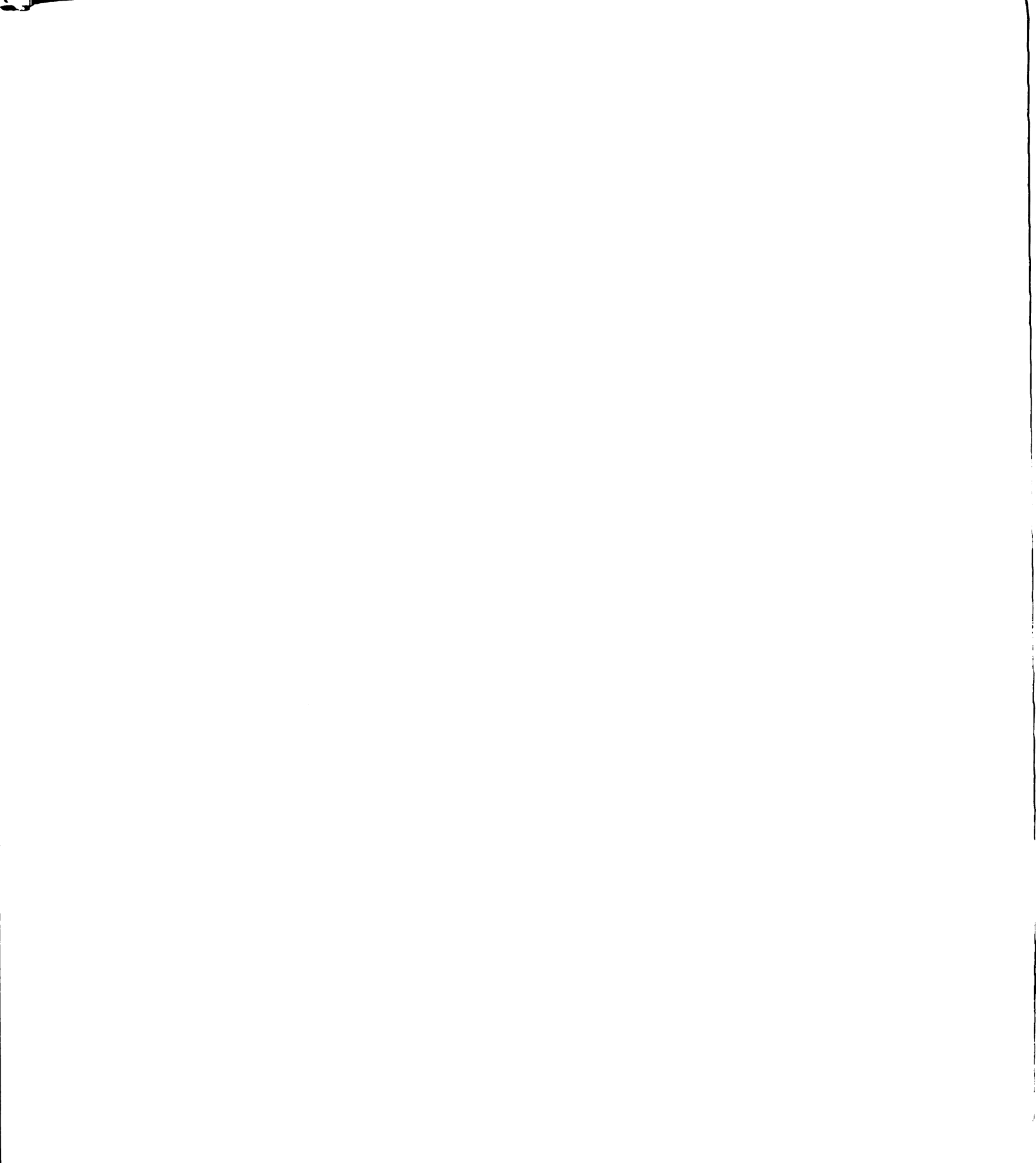
      ENDIF
2000 CONTINUE
      70 FORMAT (1X,'INPUT LOWEST PRESSURE IN BAR')
      74 FORMAT (1X,'INPUT HIGHEST PRESSURE IN BAR')
      78 FORMAT (1X,'INPUT THE SIZE OF THE PRESSURE INCREMENT IN BAR')
      82 FORMAT (1X,'INPUT K(',I1,',',I1,')')
      86 FORMAT (X,'PRESSURE MELTING POINT')
      90 FORMAT (X,' (BAR)          (K)          X2          X3          Y2
&          Y3')
      92 FORMAT (X,F8.3,2X,F13.5,4(2X,G9.4))
      93 FORMAT (X,3(G15.8,5X)/)
      94 FORMAT (1X,'THE MELTING POINT AT ',F8.3,' BAR IS ',G15.7)
      END

```

```

C *****
C * SUBROUTINE INPUT *
C *****
C * ANT(I,J) ANTOINE COEFFICIENTS FOR COMPONENT I FOR VAPOR *
C *          PRESSURE IN UNITS OF BAR *

```


```

      GOTO 100
    ENDIF
200  CONTINUE
    DO 400 I = 1,NC-1
      DO 300 J = I,NC
        IF (I.EQ.J) THEN
          K(I,J) = 0.
          GOTO 300
        ENDIF
        WRITE (6,86) I,J
        READ (5,*) K(I,J)
        K(J,I) = K(I,J)
300  CONTINUE
400  CONTINUE
    80  FORMAT (' ', 'ENTER THE NUMBER OF COMPONENTS (AS AN INTEGER)')
    81  FORMAT (1X, 'ENTER THE SYSTEM PRESSURE IN ATMOSPHERES')
    82  FORMAT (1X, 'ENTER AN INITIAL GUESS FOR THE SYSTEM TEMPERATURE')
    83  FORMAT (1X, 'ENTER THE NAME OF COMPONENT #', I1, '
      &      '/1X, 'CARBON DIOXIDE - CO2      ETHANE      - C2H6
      &      '/1X, 'ETHYLENE      - C2H4      NAPHTHALENE - NAPT
      &      '/1X, 'BIPHENYL      - BIPH      PHENANTHRENE - PHAN')
    86  FORMAT (' ', 'INPUT K(', I1, ', ', I1, ')')
    88  FORMAT (X,A4)
    90  FORMAT (I1)
    91  FORMAT (4G10.4)
    92  FORMAT (A4)
    93  FORMAT (4G10.4)
    94  FORMAT (3G10.4)
    96  FORMAT (A4/A4/A4/A4)
    RETURN
  END

```

```

C *****
C * SUBROUTINE FIXXY *
C *****
C * THIS SUBROUTINE RETURNS VALUES FOR MOLE FRACTIONS WEIGHTED BY *
C * THE INITIAL GUESSES *
C *****
C * I      DO LOOP INDEX *
C * NC     THE NUMBER OF COMPONENTS *
C * X(I)   THE MOLE FRACTION OF COMPONENT I IN THE LIQUID *
C * Y(I)   THE MOLE FRACTION OF COMPONENT I IN THE VAPOR *
C * XSUM   SUM OF THE X(I) VALUES *
C * YSUM   SUM OF THE Y(I) VALUES *
C *****
C SUBROUTINE FIXXY (NC,DX,DY,X,Y)
  DIMENSION X(3),Y(3)
  DOUBLE PRECISION DX(3),DY(3)
  XSUM = 0.0
  YSUM = 0.0
  DO 100 I = 1,NC
    XSUM = XSUM + X(I)
    YSUM = YSUM + Y(I)

```

```

100      CONTINUE
      IF (XSUM.EQ.0.0) THEN
        WRITE (6,77)
        STOP
      ENDIF
      IF (YSUM.EQ.0.0) THEN
        WRITE (6,77)
        STOP
      ENDIF
      DO 200 I = 1,NC
        X(I) = X(I)/XSUM
        DX(I) = DBLE(X(I))
        Y(I) = Y(I)/YSUM
        DY(I) = DBLE(Y(I))
200      CONTINUE
77      FORMAT (X,'ERROR ERROR ERROR ERROR ERROR ERROR ERROR ERROR
&          ',/X,'ERROR ERROR ERROR ERROR ERROR ERROR ERROR ERROR
&          ',/X,'ERROR ERROR ERROR ERROR ERROR ERROR ERROR ERROR
&          ',/X,'ERROR                                ERROR
&          ',/X,'ERROR  I AM AFRAID YOU ARE CLAIMING      ERROR
&          ',/X,'ERROR  ALL MOLE FRACTIONS ARE ZERO!      ERROR
&          ',/X,'ERROR                                ERROR
&          ',/X,'ERROR ERROR ERROR ERROR ERROR ERROR ERROR ERROR
&          ',/X,'ERROR ERROR ERROR ERROR ERROR ERROR ERROR ERROR
&          ',/X,'ERROR ERROR ERROR ERROR ERROR ERROR ERROR ERROR')
      RETURN
      END

```

```

C      *****
C      * SUBROUTINE SFUG *
C      *****
C      * THIS ASSUMES COMPONENT 1 TO BE GAS AND 2 AND 3 SOLIDS. *
C      *****
C      * VARIABLES *
C      *****
C      * ANT(I,J)  Jth ANTOINE COEFFICIENT FOR COMPONENT I *
C      * DANTA     A COEFFICIENT FOR THE ANTOINE EQUATION FOR THE SOLID *
C      * DANTB     B COEFFICIENT FOR THE ANTOINE EQUATION FOR THE SOLID *
C      * DANTC     C COEFFICIENT FOR THE ANTOINE EQUATION FOR THE SOLID *
C      * DEN       SYSTEM DENSITY IN MOLES/CC *
C      * DFG(I)    FUGACITY OF COMPONENT I *
C      * DP        SYSTEM PRESSURE IN BARS *
C      * DPSAT(I)  SATURATION PRESSURE (IN UNITS OF BAR) OF COMPONENT I *
C      *           AT SYSTEM TEMPERATURE *
C      * DPSATPA   SATURATION PRESSURE (IN UNITS OF Pa) OF SOLID AT *
C      *           SYSTEM TEMPERATURE *
C      * DR        GAS CONSTANT (IN CC-BAR/GMOLE-K) *
C      * DT        DOUBLE PRECISION T *
C      * DVSOL(I)  DOUBLE PRECISION VSOL(I) *
C      * NC        NUMBER OF COMPONENTS IN THE SYSTEM *
C      * T         SYSTEM TEMPERATURE IN KELVIN *
C      * VSOL(I)   VOLUME OF SOLID COMPONENT I IN CC/GMOLE *
C      *****

```

SUBROUTINE SFUG (ANT,DFG,NC,DP,T,VSOL)

REAL ANT(3,3),VSOL(3)

DOUBLE PRECISION DANTA,DANTB,DANTC,DFG(3),DPSAT(3),DPSATPA,DP

DOUBLE PRECISION DR,DT,DVSOL(3)

DR = DBLE(83.1439)

DT = DBLE(T)

DO 400 I = 2,NC

DANTA = DBLE(ANT(I,1))

DANTB = DBLE(ANT(I,2))

DANTC = DBLE(ANT(I,3))

DPSATPA = 10.DO**(DANTA-DANTB/(DT+DANTC))

DPSAT(I) = DPSATPA/1.DO5

C *****

C * CALCULATE SOLID FUGACITY *

C *****

DVSOL(I) = DBLE(VSOL(I))

DFG(I) = DPSAT(I)*DEXP(DVSOL(I)*(DP-DPSAT(I))/DR/DT)

400 CONTINUE

RETURN

END

C *****

C * SUBROUTINE VEOS USING ORIGINAL PENG-ROBINSON EOS *

C *****

C * A0 ----- THE ZEROETH ORDER TERM OF THE NORMALIZED CUBIC *

C * EQUATION TO BE SOLVED *

C * A1 ----- THE FIRST ORDER TERM OF THE NORMALIZED CUBIC *

C * EQUATION TO BE SOLVED *

C * A2 ----- THE SECOND ORDER TERM OF THE NORMALIZED CUBIC *

C * EQUATION TO BE SOLVED *

C * ASTAR SINGLE PRECISION DASTAR *

C * BSTAR SINGLE PRECISION DBSTAR *

C * C1 IMAGINARY PART OF THE 1ST ROOT OF THE SOLVED CUBIC *

C * C2 IMAGINARY PART OF THE 1ST ROOT OF THE SOLVED CUBIC *

C * C3 IMAGINARY PART OF THE 1ST ROOT OF THE SOLVED CUBIC *

C * C(I) VOLUME TRANSLATION FOR COMPONENT I - NOT USED IN *

C * THIS SUBROUTINE *

C * DA(I) PENG-ROBINSON a FOR PURE COMPONENT I *

C * DAM a OF THE MIXTURE *

C * DASTAR INTERMEDIATE VARIABLE USED TO SET UP CUBIC EQUATION *

C * TO SOLVE FOR Z *

C * DB(I) PENG-ROBINSON b FOR PURE COMPONENT I *

C * DBM b OF THE MIXTURE *

C * DBSTAR INTERMEDIATE VARIABLE USED TO SET UP CUBIC EQUATION *

C * TO SOLVE FOR Z *

C * DBTERM RATIO DB(I)/DBM, USED IN CALCULATING FUGACITY *

C * COEFFICIENT OF COMPONENT I *

C * DEL USED IN CALCULATING FUGACITY COEFFICIENTS *

C * DELY(I) CHANGE IN VALUE OF DY(I) FROM LAST ITERATION *

C * DFG(I) FUGACITY OF COMPONENT I *

C * DFOMEG FUNCTION OF OMEGA USED IN CALCULATING DA(I) VALUES *

C * DK(I,J) DOUBLE PRECISION K(I,J) *

C * DNEWY(I) NEXT GUESS FOR DY(I) *

```

C  *  DOM(I)    DOUBLE PRECISION OM(I)          *
C  *  DP        TOTAL SYSTEM PRESSURE (BAR)      *
C  *  DR        DOUBLE PRECISION R              *
C  *  DRLT      FIRST LOGARITHMIC TERM USED IN CALCULATING *
C  *            FUGACITY COEFFICIENTS            *
C  *  DRLT2     SECOND LOGARITHMIC TERM USED IN CALCULATING *
C  *            FUGACITY COEFFICIENTS            *
C  *  DT        DOUBLE PRECISION T              *
C  *  DTC(I)    DOUBLE PRECISION TC(I)          *
C  *  DTR       DOUBLE PRECISION TR             *
C  *  DY(I)     VAPOR PHASE MOLE FRACTION OF COMPONENT I *
C  *  DZ        DOUBLE PRECISION Z              *
C  *  I         COMPONENT SUBSCRIPT             *
C  *  ICNT      ITERATION LOOP COUNTER          *
C  *  J         COMPONENT SUBSCRIPT             *
C  *  K(I,J)    INTERACTION PARAMETER FOR THE I,J COMPONENT PAIR *
C  *  NC        TOTAL NUMBER OF COMPONENTS      *
C  *  OM(I)     PITZER ACENTRIC FACTOR          *
C  *  PC(I)     CRITICAL PRESSURE OF COMPONENT I *
C  *  PHI(I)    FUGACITY COEFFICIENT OF COMPONENT I IN THE MIXTURE *
C  *  R         GAS CONSTANT (CC-BAR/MOL-K)     *
C  *  R1        REAL PART OF THE 1ST ROOT OF THE SOLVED CUBIC *
C  *  R2        REAL PART OF THE 2ND ROOT OF THE SOLVED CUBIC *
C  *  R3        REAL PART OF THE 3RD ROOT OF THE SOLVED CUBIC *
C  *  T         SYSTEM TEMPERATURE (KELVIN)      *
C  *  TC(I)     CRITICAL TEMPERATURE OF COMPONENT I (KELVIN) *
C  *  TR        REDUCED TEMPERATURE             *
C  *  V         VAPOR PHASE MOLAR VOLUME (CC/MOL) OF MIXTURE AT *
C  *            SYSTEM P AND T                   *
C  *  Z         VAPOR PHASE COMPRESSIBILITY OF MIXTURE *
C  *****

```

SUBROUTINE VEOS (C,DFG,K,NC,OM,DP,PC,DPHI,T,TC,V,DY,DZ)

REAL C(3),K(3,3),OM(3),PC(3),TC(3)

DOUBLE PRECISION DA(3),DAM,DASTAR,DB(3),DBM,DBSTAR,DBTERM,DEL

DOUBLE PRECISION DELY(3),DFG(3),DFOMEG,DK(3,3),DNEWY(3),DOM(3)

DOUBLE PRECISION DP,DPC(3),DPHI(3),DR,DRLNPHI,DRLT,DRLT2,DT

DOUBLE PRECISION DTC(3),DTR,DY(3),DZ

R = 83.1439

DR = DBLE(R)

DT = DBLE(T)

DO 20 J = 1,NC

DOM(J) = DBLE(OM(J))

DPC(J) = DBLE(PC(J))

DTC(J) = DBLE(TC(J))

DTR=DT/DTC(J)

DFOMEG = 3.7464D-1 + 1.54226D0*DOM(J) - 2.6992D-1*DOM(J)**2.D0

DA(J) = 4.5724D-1*(DR*DTC(J)*(1.D0 + DFOMEG*(1.D0 -

& DSQRT(DTR))))**2.D0/DPC(J)

DB(J) = 7.78D-2*DR*DTC(J)/DPC(J)

CONTINUE

20

```

C *****
C * BEGINNING OF LOOP FOR COMPOSITION *
C *****

```

```

24      DAM=0
      DBM=0
      DO 30 I = 1,NC
        DBM = DBM + DY(I)*DB(I)
        DO 25 J = 1,NC
          DK(I,J) = DBLE(K(I,J))
          DAM=DAM+DY(I)*DY(J)*DSQRT(DA(I)*DA(J))*(1.D0-DK(I,J))
25      CONTINUE
30      CONTINUE
C *****
C * SOLVE CUBIC EOS *
C *****
      DASTAR = DAM*DP/(DR*DT)**2
      ASTAR = SNGL(DASTAR)
      DBSTAR = DBM*DP/DR/DT
      BSTAR = SNGL(DBSTAR)
      A2 = BSTAR-1.
      A1 = ASTAR-BSTAR*(2. + 3.*BSTAR)
      A0 = BSTAR*(BSTAR**2 + BSTAR - ASTAR)
      CALL CUBIC(A2,A1,A0,R1,R2,R3,C1,C2,C3,IFLAG)
C *****
C * IFLAG = 1 MEANS ONE REAL + TWO COMPLEX *
C *      - 2      ALL REAL, AT LEAST TWO SAME *
C *      - 3      THREE DISTINCT REAL ROOTS *
C *****
      IF (IFLAG.EQ.1)THEN
        Z = R1
      ELSE IF (IFLAG.EQ.2) THEN
        Z = R1
        IF (Z.LT.R2) Z=R2
      ELSE
        Z = R1
        IF (Z.LT.R2) Z=R2
        IF (Z.LT.R3) Z=R3
      ENDIF
      DZ = DBLE(Z)
      V = Z*DR*DT/DP
C *****
C * CALCULATE VAPOR PHASE FUGACITIES *
C *****
      DRLT = DLOG((2.D0*DZ + DBSTAR*(2.D0 + DSQRT(8.D0)))/(2.D0*DZ +
&          DBSTAR*(2.D0 - DSQRT(8.D0))))
      DRLT2 = DLOG(DZ - DBSTAR)
      DO 700 L = 1,NC
        DBTERM = DB(L)/DBM
        DEL = 0.D0
        DO 600 LL = 1,NC
          DEL = DEL + 2.D0*DY(LL)*DSQRT(DA(L)*DA(LL))*(1.D0 -
&          DK(L,LL))/DAM
600      CONTINUE
      DRLNPHI = DBTERM*(DZ - 1.D0) - DRLT2 + DASTAR*(DBTERM -
&          DEL)*DRLT/DBSTAR/DSQRT(8.D0)
      DPHI(L) = DEXP(DRLNPHI)

```

```

      DNEWY(L) = DFG(L)/DPHI(L)/DP
      DELY(L) = DABS((DNEWY(L)-DY(L))/(DNEWY(L)+DY(L)))
      DY(L) = (DNEWY(L)+3*DY(L))/4
700    CONTINUE
      DY(1) = 1.D0
      DO 750 I = 2,NC
        DY(1) = DY(1) - DY(I)
750    CONTINUE
      DO 800 L = 2,NC
        IF (DELY(L).GT.1D-04) GOTO 24
800    CONTINUE
      RETURN
      END

```

```

C *****
C * SUBROUTINE LEOS USING ORIGINAL PENG-ROBINSON EOS *
C *****
C * A0 ----- THE ZEROETH ORDER TERM OF THE NORMALIZED CUBIC *
C * EQUATION TO BE SOLVED *
C * A1 ----- THE FIRST ORDER TERM OF THE NORMALIZED CUBIC *
C * EQUATION TO BE SOLVED *
C * A2 ----- THE SECOND ORDER TERM OF THE NORMALIZED CUBIC *
C * EQUATION TO BE SOLVED *
C * ASTAR SINGLE PRECISION DASTAR *
C * BSTAR SINGLE PRECISION DBSTAR *
C * C1 IMAGINARY PART OF THE 1ST ROOT OF THE SOLVED CUBIC *
C * C2 IMAGINARY PART OF THE 1ST ROOT OF THE SOLVED CUBIC *
C * C3 IMAGINARY PART OF THE 1ST ROOT OF THE SOLVED CUBIC *
C * C(I) VOLUME TRANSLATION FOR COMPONENT I - NOT USED IN *
C * THIS SUBROUTINE *
C * DA(I) PENG-ROBINSON a FOR PURE COMPONENT I *
C * DAM a OF THE MIXTURE *
C * DASTAR INTERMEDIATE VARIABLE USED TO SET UP CUBIC EQUATION *
C * TO SOLVE FOR Z *
C * DB(I) PENG-ROBINSON b FOR PURE COMPONENT I *
C * DBM b OF THE MIXTURE *
C * DBSTAR INTERMEDIATE VARIABLE USED TO SET UP CUBIC EQUATION *
C * TO SOLVE FOR Z *
C * DBTERM RATIO DB(I)/DBM, USED IN CALCULATING FUGACITY *
C * COEFFICIENT OF COMPONENT I *
C * DEL USED IN CALCULATING FUGACITY COEFFICIENTS *
C * DFG(I) FUGACITY OF COMPONENT I *
C * DFOMEG FUNCTION OF OMEGA USED IN CALCULATING DA(I) VALUES *
C * DK(I,J) DOUBLE PRECISION K(I,J) *
C * DOM(I) DOUBLE PRECISION OM(I) *
C * DP TOTAL SYSTEM PRESSURE (BAR) *
C * DR DOUBLE PRECISION R *
C * DRLT FIRST LOGARITHMIC TERM USED IN CALCULATING *
C * FUGACITY COEFFICIENTS *
C * DRLT2 SECOND LOGARITHMIC TERM USED IN CALCULATING *
C * FUGACITY COEFFICIENTS *
C * DT DOUBLE PRECISION T *
C * DTC(I) DOUBLE PRECISION TC(I) *

```

```

C      * DTR          DOUBLE PRECISION TR          *
C      * DX(I)        LIQUID PHASE MOLE FRACTION OF COMPONENT I      *
C      * DZ           DOUBLE PRECISION Z           *
C      * I            COMPONENT SUBSCRIPT           *
C      * ICNT         ITERATION LOOP COUNTER        *
C      * J            COMPONENT SUBSCRIPT           *
C      * K(I,J)       INTERACTION PARAMETER FOR THE I,J COMPONENT PAIR *
C      * NC           TOTAL NUMBER OF COMPONENTS     *
C      * OM(I)        PITZER ACENTRIC FACTOR         *
C      * PC(I)        CRITICAL PRESSURE OF COMPONENT I      *
C      * PHI(I)       FUGACITY COEFFICIENT OF COMPONENT I IN THE MIXTURE *
C      * R            GAS CONSTANT (CC-BAR/MOL-K)       *
C      * R1           REAL PART OF THE 1ST ROOT OF THE SOLVED CUBIC    *
C      * R2           REAL PART OF THE 2ND ROOT OF THE SOLVED CUBIC    *
C      * R3           REAL PART OF THE 3RD ROOT OF THE SOLVED CUBIC    *
C      * T            SYSTEM TEMPERATURE (KELVIN)       *
C      * TC(I)        CRITICAL TEMPERATURE OF COMPONENT I (KELVIN)    *
C      * TR           REDUCED TEMPERATURE             *
C      * V            LIQUID PHASE MOLAR VOLUME (CC/MOL) OF MIXTURE AT *
C      *              SYSTEM P AND T                  *
C      * Z            LIQUID PHASE COMPRESSIBILITY OF MIXTURE          *
C *****
SUBROUTINE LEOS (C,DFG,K,NC,OM,DP,PC,DPHI,T,TC,V,DX,DZ)
  REAL C(3),K(3,3),OM(3),PC(3),TC(3)
  DOUBLE PRECISION DA(3),DAM,DASTAR,DB(3),DBM,DBSTAR,DBTERM,DEL
  DOUBLE PRECISION DFG(3),DFOMEG,DK(3,3),DOM(3),DP,DPC(3),DPHI(3)
  DOUBLE PRECISION DR,DRLNPHI,DRLT,DRLT2,DT,DTC(3),DTR,DX(3),DZ
  R = 83.1439
  DR = DBLE(R)
  DT = DBLE(T)
  DO 20 J = 1,NC
    DOM(J) = DBLE(OM(J))
    DPC(J) = DBLE(PC(J))
    DTC(J) = DBLE(TC(J))
    DTR=DT/DTC(J)
    DFOMEG = 3.7464D-1 + 1.54226D0*DOM(J) - 2.6992D-1*DOM(J)**2.D0
    DA(J) = 4.5724D-1*(DR*DTC(J)*(1.D0 + DFOMEG*(1.D0 -
&      DSQRT(DTR))))**2.D0/DPC(J)
    DB(J) = 7.78D-2*DR*DTC(J)/DPC(J)
  20  CONTINUE
C *****
C * BEGINNING OF LOOP FOR COMPOSITION *
C *****
  24  DAM=0
      DBM=0
      DO 30 I = 1,NC
        DBM = DBM + DX(I)*DB(I)
        DO 25 J = 1,NC
          DK(I,J) = DBLE(K(I,J))
          DAM=DAM+DX(I)*DX(J)*DSQRT(DA(I)*DA(J))*(1.D0-DK(I,J))
        25  CONTINUE
      30  CONTINUE
C *****

```

```

C * SOLVE CUBIC EOS *
C *****
      DASTAR = DAM*DP/(DR*DT)**2
      ASTAR = SNGL(DASTAR)
      DBSTAR = DBM*DP/DR/DT
      BSTAR = SNGL(DBSTAR)
      A2 = BSTAR-1.
      A1 = ASTAR-BSTAR*(2. + 3.*BSTAR)
      A0 = BSTAR*(BSTAR**2 + BSTAR - ASTAR)
      CALL CUBIC(A2,A1,A0,R1,R2,R3,C1,C2,C3,IFLAG)
C *****
C * IFLAG = 1 MEANS ONE REAL + TWO COMPLEX *
C *      - 2      ALL REAL, AT LEAST TWO SAME *
C *      - 3      THREE DISTINCT REAL ROOTS *
C *****
      IF (IFLAG.EQ.1) THEN
        Z = R1
      ELSE IF (IFLAG.EQ.2) THEN
        Z = R1
        IF (Z.GT.R2) Z=R2
      ELSE
        Z = R1
        IF (Z.GT.R2) Z=R2
        IF (Z.GT.R3) Z=R3
      ENDIF
      DZ = DBLE(Z)
      V = Z*DR*DT/DP
C *****
C * CALCULATE LIQUID PHASE FUGACITIES *
C *****
      DRLT = DLOG((2.DO*DZ + DBSTAR*(2.DO + DSQRT(8.DO)))/(2.DO*DZ +
&      DBSTAR*(2.DO - DSQRT(8.DO))))
      DRLT2 = DLOG(DZ - DBSTAR)
      DO 700 L = 1,NC
        DBTERM = DB(L)/DBM
        DEL = 0.DO
        DO 600 LL = 1,NC
          DEL = DEL + 2.DO*DX(LL)*DSQRT(DA(L)*DA(LL))*(1.DO -
&          DK(L,LL))/DAM
        CONTINUE
        DRLNPHI = DBTERM*(DZ - 1.DO) - DRLT2 + DASTAR*(DBTERM -
&          DEL)*DRLT/DBSTAR/DSQRT(8.DO)
        DPHI(L) = DEXP(DRLNPHI)
      CONTINUE
700    RETURN
      END

C *****
C * SUBROUTINE CUBIC *
C *****
C * THIS SUBROUTINE FINDS THE ROOTS OF A CUBIC EQUATION OF THE *
C * FORM       $X^3 + A2X^2 + A1X + A0 = 0$       ANALYTICALLY. *
C *****

```



```

C  * A0 ----- THE ZEROETH ORDER TERM OF THE NORMALIZED CUBIC      *
C  *                               EQUATION                          *
C  * A1 ----- THE FIRST ORDER TERM OF THE NORMALIZED CUBIC      *
C  *                               EQUATION                          *
C  * A2 ----- THE SECOND ORDER TERM OF THE NORMALIZED CUBIC      *
C  *                               EQUATION                          *
C  * C1 ----- THE COMPLEX ARGUMENT OF ROOT #1 OF THE EQUATION    *
C  * C2 ----- THE COMPLEX ARGUMENT OF ROOT #2 OF THE EQUATION    *
C  * C3 ----- THE COMPLEX ARGUMENT OF ROOT #3 OF THE EQUATION    *
C  * CCHECK --- THE SAME AS "CHECK" BUT CONVERTED TO COMPLEX      *
C  *                               NUMBER FORMAT                     *
C  * CHECK ---- Q**3 + R**2, USED TO CHECK FOR THE CASE OF THE     *
C  *                               SOLUTION AND IN FINDING THE ROOTS OF THE EQUATION, *
C  *                               DOUBLE PRECISION                 *
C  * DA0 ----- "A0" CONVERTED TO DOUBLE PRECISION                *
C  * DA1 ----- "A1" CONVERTED TO DOUBLE PRECISION                *
C  * DA2 ----- "A2" CONVERTED TO DOUBLE PRECISION                *
C  * ES1 ----- AN INTERMEDIATE CALCULATION TO USED IN THE        *
C  *                               CALCULATION OF "S1"              *
C  * ES2 ----- AN INTERMEDIATE CALCULATION TO USED IN THE        *
C  *                               CALCULATION OF "S2"              *
C  * IFLAG ---- A FLAG TO INDICATE THE CASE OF THE SOLUTION OF THE *
C  *                               EQUATION: -1 ONE REAL + TWO COMPLEX ROOTS, *
C  *                               -2 ALL REAL ROOTS, AT LEAST TWO THE SAME *
C  *                               -3 THREE DISTINCT REAL ROOTS      *
C  * P1 ----- AN INTERMEDIATE SUM USED IN THE CALCULATION OF      *
C  *                               "SS1"                             *
C  * P2 ----- AN INTERMEDIATE SUM USED IN THE CALCULATION OF      *
C  *                               "SS2"                             *
C  * Q ----- AN INTERMEDIATE SUM USED IN CALCULATING "CHECK"      *
C  * R ----- AN INTERMEDIATE SUM USED IN CALCULATING "CHECK"      *
C  * R1 ----- THE REAL ARGUMENT OF ROOT #1 OF THE EQUATION        *
C  * R2 ----- THE REAL ARGUMENT OF ROOT #2 OF THE EQUATION        *
C  * R3 ----- THE REAL ARGUMENT OF ROOT #3 OF THE EQUATION        *
C  * RECK ---- THE SAME AS "CHECK", BUT SINGLE PRECISION REAL      *
C  * S1 ----- AN INTERMEDIATE VALUE USED TO FIND THE ROOTS OF     *
C  *                               THE EQUATION, COMPLEX NUMBER      *
C  * S2 ----- AN INTERMEDIATE VALUE USED TO FIND THE ROOTS OF     *
C  *                               THE EQUATION, COMPLEX NUMBER      *
C  * SS1 ----- THE SAME AS S1 BUT DOUBLE PRECISION REAL           *
C  * SS2 ----- THE SAME AS S2 BUT DOUBLE PRECISION REAL           *
C  * Z1 ----- ROOT #1 OF THE EQUATION, COMPLEX NUMBER            *
C  * Z2 ----- ROOT #2 OF THE EQUATION, COMPLEX NUMBER            *
C  * Z3 ----- ROOT #3 OF THE EQUATION, COMPLEX NUMBER            *
C  *****
SUBROUTINE CUBIC(A2,A1,A0,R1,R2,R3,C1,C2,C3,IFLAG)
      DOUBLE PRECISION CHECK,DA0,DA1,DA2,P1,P2,Q,R,SS1,SS2
      COMPLEX ES1,ES2,S1,S2,Z1,Z2,Z3,CCHECK
      DA0 = DBLE(A0)
      DA1 = DBLE(A1)
      DA2 = DBLE(A2)
      Q = DA1/3.D00 - DA2*DA2/9.D00
      R = (DA1*DA2 - 3.D00*DA0)/6.D00 - (DA2/3.D00)**3

```

```

CHECK = Q**3 + R*R
IF (CHECK.GT.1.0E-10) THEN
  IFLAG = 1
  P1 = R + DSQRT(CHECK)
  P2 = R - DSQRT(CHECK)
  IF (P1.LT.0.0) THEN
    SS1 = -DEXP((DLOG(-1.D00*P1))/3.D00)
  ELSE
    SS1 = DEXP((DLOG(P1))/3.D00)
  ENDIF
  IF (P2.LT.0.0) THEN
    SS2 = -DEXP((DLOG(-1.D00*P2))/3.D00)
  ELSE
    SS2 = DEXP((DLOG(P2))/3.D00)
  ENDIF
  R1 = SS1 + SS2 - DA2/3.D00
  R2 = -(SS1 + SS2) - DA2/3.D00
  R3 = R2
  C1 = 0.0
  C2 = (SQRT(3.))*(SS1 - SS2)/2.D00
  C3 = -C2
ELSE IF (CHECK.LT.0.0) THEN
  IFLAG = 3
  RR = 1.*R
  RECK = 1.*CHECK
  CCHECK = CMPLX(RECK,0.0)
  ES1 = CLOG(RR + CSQRT(CCHECK))/3.
  ES2 = CLOG(RR - CSQRT(CCHECK))/3.
  S1 = CEXP(ES1)
  S2 = CEXP(ES2)
  Z1 = (S1 + S2) - A2/3
  Z2 = -(S1 + S2)/2 - A2/3 + (CMPLX(0.0,3**0.5))*(S1 - S2)/2
  Z3 = -(S1 + S2)/2 - A2/3 - (CMPLX(0.0,3**0.5))*(S1 - S2)/2
  R1 = REAL(Z1)
  R2 = REAL(Z2)
  R3 = REAL(Z3)
  C1 = 0.0
  C2 = C1
  C3 = C1
ELSE
  *****
  * IF THE ROOTS OF THE EQUATION ARE VERY, VERY SMALL AND VERY, *
  * VERY CLOSE TOGETHER, THIS SUBROUTINE MAY ERRONEOUSLY REPORT *
  * THAT THE EQUATION HAS ONLY ONE ROOT NEAR ZERO *
  *****
  IFLAG = 2
  IF (R.LT.0.0) THEN
    SS1 = -DEXP((DLOG(-1.D00*R))/3.D00)
  ELSE IF (R.EQ.0.0) THEN
    SS1 = 0.0
  ELSE
    SS1 = DEXP((DLOG(R))/3.D00)
  ENDIF

```

C
C
C
C
C

```

      SS2 = SS1
      R1 = SS1 + SS2 - DA2/3.D00
      R2 = -(SS1 + SS2)/2 - DA2/3.D00
      R3 = R2
      C1 = 0.0
      C2 = C1
      C3 = C2
    ENDIF
  RETURN
END

```

The following two subroutines were substituted for the corresponding original Peng-Robinson subroutines when the translated Peng-Robinson equation was used.

```

C *****
C * SUBROUTINE VEOS USING TRANSLATED PENG-ROBINSON EOS *
C *****
C * A0 ----- THE ZEROETH ORDER TERM OF THE NORMALIZED CUBIC *
C * EQUATION TO BE SOLVED *
C * A1 ----- THE FIRST ORDER TERM OF THE NORMALIZED CUBIC *
C * EQUATION TO BE SOLVED *
C * A2 ----- THE SECOND ORDER TERM OF THE NORMALIZED CUBIC *
C * EQUATION TO BE SOLVED *
C * ASTAR SINGLE PRECISION DASTAR *
C * BSTAR SINGLE PRECISION DBSTAR *
C * C1 IMAGINARY PART OF THE 1ST ROOT OF THE SOLVED CUBIC *
C * C2 IMAGINARY PART OF THE 1ST ROOT OF THE SOLVED CUBIC *
C * C3 IMAGINARY PART OF THE 1ST ROOT OF THE SOLVED CUBIC *
C * C(I) VOLUME TRANSLATION FOR COMPONENT I *
C * DA(I) PENG-ROBINSON a FOR PURE COMPONENT I *
C * DAM a OF THE MIXTURE *
C * DASTAR INTERMEDIATE VARIABLE USED TO SET UP CUBIC EQUATION *
C * TO SOLVE FOR Z *
C * DB(I) PENG-ROBINSON b FOR PURE COMPONENT I *
C * DBM b OF THE MIXTURE *
C * DBSTAR INTERMEDIATE VARIABLE USED TO SET UP CUBIC EQUATION *
C * TO SOLVE FOR Z *
C * DBTERM RATIO DB(I)/DBM, USED IN CALCULATING FUGACITY *
C * COEFFICIENT OF COMPONENT I *
C * DEL USED IN CALCULATING FUGACITY COEFFICIENTS *
C * DELY(I) CHANGE IN VALUE OF DY(I) FROM LAST ITERATION *
C * DFG(I) FUGACITY OF COMPONENT I *
C * DFOMEG FUNCTION OF OMEGA USED IN CALCULATING DA(I) VALUES *
C * DK(I,J) DOUBLE PRECISION K(I,J) *
C * DNEWY(I) NEXT GUESS FOR DY(I) *
C * DOM(I) DOUBLE PRECISION OM(I) *
C * DP TOTAL SYSTEM PRESSURE (BAR) *
C * DR DOUBLE PRECISION R *
C * DRLT FIRST LOGARITHMIC TERM USED IN CALCULATING *
C * FUGACITY COEFFICIENTS *

```

```

C      * DRLT2      SECOND LOGARITHMIC TERM USED IN CALCULATING      *
C      *           FUGACITY COEFFICIENTS                          *
C      * DT        DOUBLE PRECISION T                            *
C      * DTC(I)     DOUBLE PRECISION TC(I)                        *
C      * DTR        DOUBLE PRECISION TR                          *
C      * DY(I)      VAPOR PHASE MOLE FRACTION OF COMPONENT I      *
C      * DZ        DOUBLE PRECISION Z                            *
C      * I          COMPONENT SUBSCRIPT                          *
C      * ICNT       ITERATION LOOP COUNTER                       *
C      * J          COMPONENT SUBSCRIPT                          *
C      * K(I,J)     INTERACTION PARAMETER FOR THE I,J COMPONENT PAIR *
C      * NC         TOTAL NUMBER OF COMPONENTS                   *
C      * OM(I)      PITZER ACENTRIC FACTOR                       *
C      * PC(I)      CRITICAL PRESSURE OF COMPONENT I             *
C      * PHI(I)     FUGACITY COEFFICIENT OF COMPONENT I IN THE MIXTURE *
C      * R          GAS CONSTANT (CC-BAR/MOL-K)                  *
C      * R1         REAL PART OF THE 1ST ROOT OF THE SOLVED CUBIC *
C      * R2         REAL PART OF THE 2ND ROOT OF THE SOLVED CUBIC *
C      * R3         REAL PART OF THE 3RD ROOT OF THE SOLVED CUBIC *
C      * T          SYSTEM TEMPERATURE (KELVIN)                  *
C      * TC(I)      CRITICAL TEMPERATURE OF COMPONENT I (KELVIN) *
C      * TR         REDUCED TEMPERATURE                          *
C      * TZ        TRUE VAPOR PHASE COMPRESSIBILITY OF MIXTURE    *
C      * V          VAPOR PHASE MOLAR VOLUME (CC/MOL) OF MIXTURE AT *
C      *           SYSTEM P AND T                                *
C      * Z          VAPOR PHASE COMPRESSIBILITY OF MIXTURE      *
C *****
SUBROUTINE VEOS (C,DFG,K,NC,OM,DP,PC,DPHI,T,TC,V,DY,TZ)
  REAL C(3),K(3,3),OM(3),PC(3),TC(3)
  DOUBLE PRECISION DA(3),DAM,DASTAR,DB(3),DBM,DBSTAR,DBTERM,DC(3)
  DOUBLE PRECISION DCM,DEL,DELY(3),DFG(3),DFOMEG,DK(3,3),DNEWY(3)
  DOUBLE PRECISION DOM(3),DP,DPC(3),DPHI(3),DR,DRLNPHI,DRLT,DRLT2
  DOUBLE PRECISION DT,DTC(3),DTR,DY(3),DZ,TZ
  R = 83.1439
  DR = DBLE(R)
  DT = DBLE(T)
  DO 20 J = 1,NC
    DC(J) = DBLE(C(J))
    DOM(J) = DBLE(OM(J))
    DPC(J) = DBLE(PC(J))
    DTC(J) = DBLE(TC(J))
    DTR=DT/DTC(J)
    DFOMEG = 3.7464D-1 + 1.54226D0*DOM(J) - 2.6992D-1*DOM(J)**2
    DA(J) = 4.5724D-1*(DR*DTC(J))*(1.DO + DFOMEG*(1.DO -
      & DSQRT(DTR))))**2.DO/DPC(J)
    DB(J) = 7.78D-2*DR*DTC(J)/DPC(J)
  20 CONTINUE
C *****
C * BEGINNING OF LOOP FOR COMPOSITION *
C *****
  24 DAM = 0.0D0
    DBM = 0.0D0
    DCM = 0.0D0

```

```

DO 30 I = 1,NC
  DBM = DBM + DY(I)*DB(I)
  DCM = DCM + DY(I)*DC(I)
  DO 25 J = 1,NC
    DK(I,J) = DBLE(K(I,J))
    DAM=DAM+DY(I)*DY(J)*DSQRT(DA(I)*DA(J))*(1.D0-DK(I,J))
  25 CONTINUE
  30 CONTINUE
C *****
C * SOLVE CUBIC EOS *
C *****
  DASTAR = DAM*DP/(DR*DT)**2
  ASTAR = SNGL(DASTAR)
  DBSTAR = DBM*DP/DR/DT
  BSTAR = SNGL(DBSTAR)
  A2 = BSTAR-1.
  A1 = ASTAR-BSTAR*(2. + 3.*BSTAR)
  A0 = BSTAR*(BSTAR**2 + BSTAR - ASTAR)
  CALL CUBIC(A2,A1,A0,R1,R2,R3,C1,C2,C3,IFLAG)
C *****
C * IFLAG = 1 MEANS ONE REAL + TWO COMPLEX *
C *      - 2      ALL REAL, AT LEAST TWO SAME *
C *      - 3      THREE DISTINCT REAL ROOTS *
C *****
  IF (IFLAG.EQ.1)THEN
    Z = R1
  ELSE IF (IFLAG.EQ.2) THEN
    Z = R1
    IF (Z.LT.R2) Z=R2
  ELSE
    Z = R1
    IF (Z.LT.R2) Z=R2
    IF (Z.LT.R3) Z=R3
  ENDIF
  DZ = DBLE(Z)
  TZ = DZ - DCM*DP/DR/DT
  V = TZ*DR*DT/DP
C *****
C * CALCULATE VAPOR PHASE FUGACITIES *
C *****
  DRLT = DLOG((2.D0*DZ + DBSTAR*(2.D0 + DSQRT(8.D0)))/(2.D0*DZ +
& DBSTAR*(2.D0 - DSQRT(8.D0))))
  DRLT2 = DLOG(DZ - DBSTAR)
  DO 700 L = 1,NC
    DBTERM = DB(L)/DBM
    DEL = 0.D0
    DO 600 LL = 1,NC
      DEL = DEL + 2.D0*DY(LL)*DSQRT(DA(L)*DA(LL))*(1.D0 -
& DK(L,LL))/DAM
    600 CONTINUE
    DRLNPHI = DBTERM*(DZ - 1.D0) - DRLT2 + DASTAR*(DBTERM -
& DEL)*DRLT/DBSTAR/DSQRT(8.D0) - DC(L)*DP/DR/DT
    DPHI(L) = DEXP(DRLNPHI)

```

```

      DNEWY(L) = DFG(L)/DPHI(L)/DP
      DELY(L) = DABS((DNEWY(L)-DY(L))/(DNEWY(L)+DY(L)))
      DY(L) = (DNEWY(L)+3*DY(L))/4
700    CONTINUE
      DY(1) = 1.D0
      DO 750 I = 2,NC
        DY(1) = DY(1) - DY(I)
750    CONTINUE
      DO 800 L = 2,NC
        IF (DELY(L).GT.1D-04) GOTO 24
800    CONTINUE
      RETURN
      END

```

```

C *****
C * SUBROUTINE LEOS USING TRANSLATED PENG-ROBINSON EOS *
C *****
C * A0 ----- THE ZEROETH ORDER TERM OF THE NORMALIZED CUBIC *
C * EQUATION TO BE SOLVED *
C * A1 ----- THE FIRST ORDER TERM OF THE NORMALIZED CUBIC *
C * EQUATION TO BE SOLVED *
C * A2 ----- THE SECOND ORDER TERM OF THE NORMALIZED CUBIC *
C * EQUATION TO BE SOLVED *
C * ASTAR SINGLE PRECISION DASTAR *
C * BSTAR SINGLE PRECISION DBSTAR *
C * C1 IMAGINARY PART OF THE 1ST ROOT OF THE SOLVED CUBIC *
C * C2 IMAGINARY PART OF THE 1ST ROOT OF THE SOLVED CUBIC *
C * C3 IMAGINARY PART OF THE 1ST ROOT OF THE SOLVED CUBIC *
C * C(I) VOLUME TRANSLATION FOR COMPONENT I *
C * DA(I) PENG-ROBINSON a FOR PURE COMPONENT I *
C * DAM a OF THE MIXTURE *
C * DASTAR INTERMEDIATE VARIABLE USED TO SET UP CUBIC EQUATION *
C * TO SOLVE FOR Z *
C * DB(I) PENG-ROBINSON b FOR PURE COMPONENT I *
C * DBM b OF THE MIXTURE *
C * DBSTAR INTERMEDIATE VARIABLE USED TO SET UP CUBIC EQUATION *
C * TO SOLVE FOR Z *
C * DBTERM RATIO DB(I)/DBM, USED IN CALCULATING FUGACITY *
C * COEFFICIENT OF COMPONENT I *
C * DEL USED IN CALCULATING FUGACITY COEFFICIENTS *
C * DFG(I) FUGACITY OF COMPONENT I *
C * DFOMEG FUNCTION OF OMEGA USED IN CALCULATING DA(I) VALUES *
C * DK(I,J) DOUBLE PRECISION K(I,J) *
C * DNEWX(I) NEXT GUESS FOR DX(I) *
C * DOM(I) DOUBLE PRECISION OM(I) *
C * DP TOTAL SYSTEM PRESSURE (BAR) *
C * DR DOUBLE PRECISION R *
C * DRLT FIRST LOGARITHMIC TERM USED IN CALCULATING *
C * FUGACITY COEFFICIENTS *
C * DRLT2 SECOND LOGARITHMIC TERM USED IN CALCULATING *
C * FUGACITY COEFFICIENTS *
C * DT DOUBLE PRECISION T *
C * DTC(I) DOUBLE PRECISION TC(I) *

```

```

C      * DTR          DOUBLE PRECISION TR          *
C      * DX(I)        LIQUID PHASE MOLE FRACTION OF COMPONENT I      *
C      * DZ           DOUBLE PRECISION Z            *
C      * I            COMPONENT SUBSCRIPT            *
C      * ICNT         ITERATION LOOP COUNTER         *
C      * J            COMPONENT SUBSCRIPT            *
C      * K(I,J)        INTERACTION PARAMETER FOR THE I,J COMPONENT PAIR *
C      * NC           TOTAL NUMBER OF COMPONENTS      *
C      * NEWX(I)       NEXT GUESS FOR X(I)            *
C      * OM(I)         PITZER ACENTRIC FACTOR         *
C      * PC(I)         CRITICAL PRESSURE OF COMPONENT I      *
C      * PHI(I)        FUGACITY COEFFICIENT OF COMPONENT I IN THE MIXTURE *
C      * R            GAS CONSTANT (CC-BAR/MOL-K)      *
C      * R1           REAL PART OF THE 1ST ROOT OF THE SOLVED CUBIC    *
C      * R2           REAL PART OF THE 2ND ROOT OF THE SOLVED CUBIC    *
C      * R3           REAL PART OF THE 3RD ROOT OF THE SOLVED CUBIC    *
C      * T            SYSTEM TEMPERATURE (KELVIN)      *
C      * TZ           TRUE LIQUID PHASE COMPRESSIBILITY OF MIXTURE    *
C      * TC(I)        CRITICAL TEMPERATURE OF COMPONENT I (KELVIN)    *
C      * TR           REDUCED TEMPERATURE             *
C      * V            LIQUID PHASE MOLAR VOLUME (CC/MOL) OF MIXTURE AT *
C      *              SYSTEM P AND T                  *
C      * Z            PSEUDO LIQUID PHASE COMPRESSIBILITY OF MIXTURE    *
C      *****
SUBROUTINE LEOS (C,DFG,K,NC,OM,DP,PC,DPHI,T,TC,V,DX,TZ)
  REAL C(3),K(3,3),OM(3),PC(3),TC(3)
  DOUBLE PRECISION DA(3),DAM,DASTAR,DB(3),DBM,DBSTAR,DBTERM,DC(3)
  DOUBLE PRECISION DCM,DEL,DFG(3),DFOMEG,DK(3,3),DOM(3),DP,DPC(3)
  DOUBLE PRECISION DPHI(3),DR,DRLNPHI,DRLT,DRLT2,DT,DTC(3),DTR
  DOUBLE PRECISION DX(3),DZ,TZ
  R = 83.1439
  DR = DBLE(R)
  DT = DBLE(T)
  DO 20 J = 1,NC
    DC(J) = DBLE(C(J))
    DOM(J) = DBLE(OM(J))
    DPC(J) = DBLE(PC(J))
    DTC(J) = DBLE(TC(J))
    DTR=DT/DTC(J)
    DFOMEG = 3.7464D-1 + 1.54226D0*DOM(J) - 2.6992D-1*DOM(J)**2.
    DA(J) = 4.5724D-1*(DR*DTC(J)*(1.D0 + DFOMEG*(1.D0 -
&          DSQRT(DTR))))**2.D0/DPC(J)
    DB(J) = 7.78D-2*DR*DTC(J)/DPC(J)
  20  CONTINUE
C *****
C * BEGINNING OF LOOP FOR COMPOSITION *
C *****
  24  DAM = 0.0
      DBM = 0.0
      DCM = 0.0
      DO 30 I = 1,NC
        DBM = DBM + DX(I)*DB(I)
        DCM = DCM + DX(I)*DC(I)

```

```

                DO 25 J = 1,NC
                    DK(I,J) = DBLE(K(I,J))
                    DAM=DAM+DX(I)*DX(J)*DSQRT(DA(I)*DA(J))*(1.D0-DK(I,J))
25                CONTINUE
30                CONTINUE
C *****
C * SOLVE CUBIC EOS *
C *****
                DASTAR = DAM*DP/(DR*DT)**2
                ASTAR = SNGL(DASTAR)
                DBSTAR = DBM*DP/DR/DT
                BSTAR = SNGL(DBSTAR)
                A2 = BSTAR-1.
                A1 = ASTAR-BSTAR*(2. + 3.*BSTAR)
                A0 = BSTAR*(BSTAR**2 + BSTAR - ASTAR)
                CALL CUBIC(A2,A1,A0,R1,R2,R3,C1,C2,C3,IFLAG)
C *****
C * IFLAG = 1 MEANS ONE REAL + TWO COMPLEX *
C *      = 2      ALL REAL, AT LEAST TWO SAME *
C *      = 3      THREE DISTINCT REAL ROOTS *
C *****
                IF (IFLAG.EQ.1) THEN
                    Z = R1
                ELSE IF (IFLAG.EQ.2) THEN
                    Z = R1
                    IF (Z.GT.R2) Z=R2
                ELSE
                    Z = R1
                    IF (Z.GT.R2) Z=R2
                    IF (Z.GT.R3) Z=R3
                ENDIF
                DZ = DBLE(Z)
                TZ = DZ - DCM*DP/DR/DT
                V = TZ*DR*DT/DP
C *****
C * CALCULATE LIQUID PHASE FUGACITIES *
C *****
                DRLT = DLOG((2.D0*DZ + DBSTAR*(2.D0 + DSQRT(8.D0)))/(2.D0*DZ +
&                DBSTAR*(2.D0 - DSQRT(8.D0))))
                DRLT2 = DLOG(DZ - DBSTAR)
                DO 700 L = 1,NC
                    DBTERM = DB(L)/DBM
                    DEL = 0.D0
                    DO 600 LL = 1,NC
                        DEL = DEL + 2.D0*DX(LL)*DSQRT(DA(L)*DA(LL))*(1.D0 -
&                        DK(L,LL))/DAM
600                CONTINUE
                    DRLNPHI = DBTERM*(DZ - 1.D0) - DRLT2 + DASTAR*(DBTERM -
&                    DEL)*DRLT/DBSTAR/DSQRT(8.D0) - DC(L)*DP/DR/DT
                    DPHI(L) = DEXP(DRLNPHI)
700                CONTINUE
                RETURN
                END

```


The following page contains the data file PHASE5.DAT used with these programs. The data for each substance are organized according to the following grid:

ω	P_C	T_C	V_C	
δ	v^L	v^S	T_m	
ΔH^{fus}	x	y	c	
A	B	C		

Where: 1) ω is the acentric factor.

2) P_C , T_C , V_C are the pure component critical pressure, temperature, and volume in bar, Kelvin, and g/cc.

3) T_m is the pure component melting point in Kelvin.

4) δ is the solubility parameter in $(\text{cal/cc})^{\frac{1}{2}}$.

5) v^L and v^S are the molar volumes of the liquid and solid respectively in cc/mol.

6) ΔH^{fus} is the molar heat of fusion in cal/mol.

7) x and y are mole fractions in the liquid and vapor phases.

8) c is the volume translation for the translated EOS in cc/mol.

9) A, B, and C are the Antoine coefficients for the vapor pressure of the solid.

CO2				
	0.239	73.8	304.2	94.0
	6.0	55.0	28.75	216.6
	1900.0	0.005	0.999	-1.6892
	22.5898	3103.39	-0.16	
C2H6				
	0.099	48.8	305.4	148.0
	6.6	70.0	55.07	89.9
	682.943	0.005	0.999	0.0
	15.	1511.42	-17.16	
C2H4				
	0.089	50.4	282.4	130.4
	6.6	65.0	49.21	104.0
	900.9447	0.005	0.999	0.0
	15.5368	1347.01	-18.15	
C2H2				
	0.190	61.4	308.3	112.7
	5.329	42.18	??.	192.4
	599.9109	0.005	0.999	0.0
	16.3481	1637.14	-19.77	
NAPT				
	0.302	40.5	748.4	413.0
	10.07	123.0	111.93	353.5
	4487.7	0.995	0.001	4.1651
	12.808	3270.8	-19.89	
BIPH				
	0.372	38.5	789.0	502.0
	10.56	155.7677	132.8021	342.4
	4441.277	0.995	0.001	-9.2485
	15.6603	4993.366	22.922	
PHAN				
	0.4536	27.43	869.25	554.0
	9.777	167.667	152.8585	373.7
	4456.00	0.995	0.001	47.2597
	12.9935	3922.33	-31.597	

References for data sources indexed by locatation in the above table

C	CO2					1) R. C. Reid, J. M. Prausnitz, B. E. Poling The Properties of Gases & Liquids, 4ed. McGraw-Hill, New York (1986)
C	1	2	2	2		
C	10	10	2	1		
C	?	x	y	2*		2) S. Angus, B. Armstrong, K. M. Reuck International Thermodynamic Tables of the Fluid State - Vol. 3 Carbon Dioxide Pergamon Press, New York (1976)
C	F	F	F			
C	C2H6					3) D. Ambrose, I.J. Lawrenseon, C. H. Sprake J. Chem. Thermodynamics (1975) 7, 1173-76
C	1	1	1	1		
C	10	10	?	1		
C	?	x	y	0		4) A. F. M. Barton Handbook of Solubility Parameters and Other Cohesion Parameters CRC Press, Boca Raton, FL (1983)
C	F	F	F			
C	C2H4					5) M. Grayson, D. Eckroth, eds. Kirk-Othmer Encyclopedia of Chemical
C	1	1	1	1		
C	10	10	?	1		
C	?	x	y	0		
C	F	F	F			

C C2H2
 C 1 1 1 1
 C 11 ? ? ?
 C ? x y 0
 C F F F
 C NAPT
 C 1 1 1 1
 C ? ? ? 1
 C ? x y 12*
 C 3 3 3
 C BIPH
 C 1 1 1 1
 C 4 9 5 1
 C 7 x y 12*
 C 9 9 9
 C PHAN
 C 8 8 8 8
 C 4 8 8 1
 C 6 x y 8*
 C 8 8 8
 C
 C * BASED ON LIQUID
 C VOLUME DATA FROM
 C THIS SOURCE
 C
 C
 C
 C
 C
 C

- Technology
 John Wiley & Sons, New York (1979)
- 6) R. C. Weast & M. J. Astle, eds.
 CRC Handbook of Chemistry and Physics
 63rd ed. 1982-1983
 CRC Press, Boca Raton, FL
- 7) R. H. Perry & C. H. Chilton, eds.
 Chemical Engineers' Handbook 5th ed.
 McGraw-Hill, New York (1973)
- 8) API Monograph Series "Anthracene and
 Phenanthrene", API Publication 708
 Washington D.C. (January 1979)
- 9) J. Timmermans
 Physico-Chemical Constants of Pure
 Organic Compounds
 Elsevier, New York (1950)
- 10) J. M. Prausnitz
 Molecular Thermodynamics of Fluid
 Phase Equilibrium
 Prentice-Hall, Englewood Cliffs, NJ
 (1969)
- 11) E. J. Henley & J. D. Seader
 Equilibrium-Stage Separation
 Operations in Chemical Engineering
 John Wiley & Sons, New York (1981)
- 12) DIPPR data base entries for this
 component
- F) False values used to fill the space
 for this entry
- ?) Source of entry one of the above with
 some unit conversions to get the value
 entered in the table

APPENDIX E

ITERATION SCHEME FOR ISOTHERMAL SLV LINE DETERMINATIONS IN TERNARY SYSTEMS

- Notes: 1) The programs in Appendices D and F are used to make these calculations.
- 2) x_1 and y_1 are the mole fractions of the solvent in the liquid and vapor phases respectively.
- 3) y_S is the mole fraction in the vapor phase of the solute which is assumed to also form the single pure solid phase.
- 4) y_{NS} is the mole fraction in the vapor phase of the solute which is assumed not to form a solid phase.
- 5) Since only one of the solutes forms a solid phase in these calculations, the fugacity of the other solute is not immediately fixed by a solid phase fugacity, so fewer variable values are known at the beginning of the calculations. For this reason, the ratio $R_V = y_{NS}/y_S$ is sought by iteration.
- 6) A slightly different method (relative to that given in Appendix C) was used for updating the chosen values of all x_i . The main reason for this is that the method given in this appendix seemed to be less prone to crash if the initial guess for R_V is not very good.

- 7) If cross parameters (k_{ij} for example) are used for the calculation of the ϕ_i^V and ϕ_i^L values (steps 7 and 14), they must be entered during the execution of the program.
- 8) This iteration scheme uses the following programs from Appendices D and F:

Main

Program - This is the first program listed in Appendix F. It follows the outline at the beginning of this appendix (E) and calls various subroutines to get initial and intermediate data.

INPUT - This subroutine reads initial variable values. (Appendix D)

FIXXY - This subroutine returns values for mole fractions weighted by the initial guesses. (Appendix D)

SFUG - This subroutine calculates the fugacities of solid phases. (Appendix D)

VEOS2 - This subroutine calculates vapor phase fugacity coefficients. There are two versions of this in Appendix F. The first uses the original Peng-Robinson EOS; the second uses the translated Peng-Robinson EOS.

LEOS - This subroutine calculates liquid phase fugacity coefficients. There are two

versions of this in Appendix D. The first uses the original Peng-Robinson EOS; the second uses the translated Peng-Robinson EOS.

CUBIC - This subroutine solves a cubic polynomial for the three real or imaginary roots. It is required in the subroutines VEOS and LEOS. (Appendix D)

1. Fix T
2. Fix P
3. Guess ratio $R_v = y_{NS}/y_S$

$$4. f_{i+s}^{solid} = P_i^{sat} \exp \left[\frac{V_{i,solid} (P - P_i^{sat})}{RT} \right]$$

5. $y_1 = 1 - y_S(1 + R_v)$
6. $y_{NS} = y_S R_v$
7. Calculate all ϕ_i^v
8. $y_S^* = \frac{f_S}{\phi_S^v P}$
9. $\Delta y_S = \left| \frac{y_S^* - y_S}{y_S^* + y_S} \right|$
10. $y_S = y_S^*$

$$11. \Delta y_S \leq 10^{-4} ?$$

Yes

12. $f_1 = y_1 \phi_1^v P$
13. Guess x_i values
14. Calculate all ϕ_i^L
15. $x_i^* = \frac{f_i}{\phi_i^L P}$
16. $\Delta x = |(x_1^* - x_1) / x_1|$
17. $\Delta = 1 - \sum x_i^*$
18. $x_1 = (x_1^* + x_1) / 2$
19. $x_{i+1} = \frac{1 - x_1}{\sum x_i - x_1} x_{i+1}$

$$20. \Delta x > 2.5 \times 10^{-4} ?$$

NO

$$21. |\Delta_{new}| \geq 10^{-3} ?$$

NO

22. Output P, T, x , and y
23. Next P

NO

YES

Yes

$$21a. \text{ If } \Delta_{new} / \Delta_{old} < 0 \text{ then } \Delta R_v = -\Delta R_v / 2$$

$$21b. \text{ If } |\Delta_{new}| > |\Delta_{old}| \text{ then } \Delta R_v = -\Delta R_v / 2$$

$$21c. R_v = R_v + \Delta R_v$$

APPENDIX F

COMPUTER CODE FOR CALCULATING ISOTHERMAL SLV LINES IN TERNARY SYSTEMS

Subroutines called in the programs of this appendix but not included in the appendix are listed in Appendix D.

```

C *****
C * THIS PROGRAM CALCULATES THE COMPOSITION TRACE AT CONSTANT *
C * TEMPERATURE OF THE THREE-PHASE LINE (SLG) FOR A TERNARY SYSTEM *
C * WITH ONE LIGHT (I.E. GAS AT AMBIENT CONDITIONS) COMPONENT AND *
C * TWO HEAVY (I.E. SOLID AT AMBIENT CONDITIONS) COMPONENTS. *
C * COMPONENT 1 IS CHOSEN TO BE THE LIGHT COMPONENT. *
C * THE SUBSCRIPT OF THE HEAVY COMPONENT ASSUMED TO COMPRISE THE *
C * SOLID PHASE MUST BE SPECIFIED. *
C *****
C
C *****
C * ADELTA1    ABSOLUTE VALUE OF DELTA1  (|DELTA1|) *
C * ADELTA2    ABSOLUTE VALUE OF DELTA2  (|DELTA2|) *
C * ANT(I,J)   ANTOINE COEFFICIENTS OF COMPONENT I *
C * C(I)       VOLUME TRANSLATION FOR COMPONENT I *
C * DELTA1     NEW VALUE OF (FUGV - FUGL) *
C * DELTA2     OLD VALUE OF (FUGV - FUGL) *
C * DELTAT     INCREMENTAL CHANGE TO T FOR THE NEXT ITERATION *
C * DHF(I)     MOLAR HEAT OF FUSION OF PURE COMPONENT I AT ITS *
C *            NORMAL MELTING POINT (CAL/G-MOLE) *
C * FG(I)      FUGACITY OF PURE COMPONENT I IN THE GAS OR SCF *
C *            PHASE *
C * FUGL       LIQUID PHASE PARTIAL MOLAR FUGACITY OF COMPONENT 1 *
C * FUGV       VAPOR PHASE PARTIAL MOLAR FUGACITY OF COMPONENT 1 *
C * I          COMPONENT NUMBER *
C * INCR       PRESSURE INCREMENT FOR THE NEXT LOOP (UNITS OF BAR) *
C * K(I,J)     INTERACTION PARAMETER FOR COMPONENTS I AND J *
C * OMEGA(I)   PITZER ACENTRIC FACTOR OF COMPONENT I *
C * LV        MOLAR VOLUME OF LIQUID MIXTURE (CC/G-MOLE) *
C * NC        NUMBER OF COMPONENTS IN THE SYSTEM *
C * P          SYSTEM PRESSURE (UNITS OF BAR) *
C * P1         PRESSURE FOR THE FIRST LOOP (UNITS OF BAR) *
C * PC(I)      THE CRITICAL PRESSURE OF PURE COMPONENT I IN UNITS *
C *            OF BAR *
C * PHI(I)     FUGACITY COEFFICIENT OF COMPONENT I *
C * PTOP       PRESSURE FOR THE LAST LOOP (UNITS OF BAR) *
C * PTOT       SYSTEM PRESSURE (UNITS OF ATM) *
C * SOLFG(I)   GAS OR SCF PHASE FUGACITY OF COMPONENT I IN

```



```

C      *      SOLUTION
C      * T      SYSTEM TEMPERATURE IN UNITS OF KELVIN
C      * TC(I)   THE CRITICAL TEMPERATURE OF PURE COMPONENT I IN
C      *         UNITS OF KELVIN
C      * TDEGC   SYSTEM TEMPERATURE IN DEGREES CELSIUS
C      * TM(I)   NORMAL MELTING POINT OF PURE COMPONENT I (KELVIN)
C      * VC(I)   THE CRITICAL VOLUME OF PURE COMPONENT I (CC/G-MOLE)
C      * VL(I)   MOLAR VOLUME OF PURE LIQUID COMPONENT I (CC/G-MOLE)
C      * VS(I)   MOLAR VOLUME OF PURE SOLID COMPONENT I (CC/G-MOLE)
C      * VV      VOLUME OF VAPOR MIXTURE (CC/G-MOLE)
C      * X(I)    THE MOLE FRACTION OF COMPONENT I IN THE LIQUID
C      *         PHASE
C      * Y(I)    THE MOLE FRACTION OF COMPONENT I IN THE GAS OR
C      *         SCF PHASE
C      *****
C      DIMENSION ANT(3,3),C(3),DHF(3),FG(3),K(3,3),OMEGA(3),PC(3),PHI(3)
C      DIMENSION SOLFG(3),TC(3),TM(3),VC(3),VL(3),VS(3),X(3),Y(3),ZRA(3)
C      INTEGER NS,S
C      REAL INCR,LV,NEWX(3)
C      DOUBLE PRECISION ADELTA1,DELTA2,DELRV,DELTAR,DELTA1,DELTA2,DELX
C      DOUBLE PRECISION DFG(3),DI,DINCR,DNEWX(3),DP,DP1,DPHI(3),DRATIO(3)
C      DOUBLE PRECISION DPTOP,DX(3),DXOLD,DY(3),DYNEW,DZ,OLDRV,RV
C      DOUBLE PRECISION DELRVMIN
C      OPEN (UNIT = 5, STATUS = 'UNKNOWN')
C      OPEN (UNIT = 6, STATUS = 'UNKNOWN')
C      OPEN (UNIT = 17, STATUS = 'NEW', FILE = 'OUTPUT.DAT')
C      CALL INPUT (ANT,C,DHF,K,NC,OMEGA,PC,PTOT,T,TC,TM,VC,VL,VS,X,Y)
C      CALL FIXXY (NC,DX,DY,X,Y)
C      DOLDX = 1.D0
C      WRITE (6,66)
C      READ (5,*) T
C      WRITE (6,68)
C      READ (5,*) S
C      IF (S.EQ.2) NS = 3
C      IF (S.EQ.3) NS = 2
C      WRITE (6,70)
C      READ (5,*) DP1
C      WRITE (6,74)
C      READ (5,*) DPTOP
C      WRITE (6,78)
C      READ (5,*) DINCR
C      WRITE (17,86)
C      WRITE (17,90)
C      DI = DINCR
C      DP = DP1
C      *****
C      * THE NEXT STATEMENT IS INTENDED TO GIVE A REASONABLE FIRST GUESS
C      * FOR THE FUGACITY OF THE LIGHT COMPONENT FOR THE FIRST ITERATION.
C      *****
C      DFG(1) = DP1
C      WRITE (6,84)
C      READ (5,*) RV
C      OLDRV = RV*2.D0

```

```

      DELRV = RV*1.D-01
      DELRMIN = -1.D-07
300  DELTAR = (RV - OLDRV)
      OLDRV = RV
      DELRV = .3*DELTAR
      IF (ABS(DELRV).LT.DELRMIN) DELRV = DELRMIN
      DELTA2 = -100.D0
      ADELTA2 = DABS(DELTA2)
      LOOPS = 1.
400  CALL SFUG(ANT,DFG,NC,DP,T,VS)
410  DY(1) = 1.D0 - DY(S)*(1.D0 + RV)
      DY(NS) = DY(S)*RV
      CALL VEOS2(C,DFG,K,NC,OMEGA,DP,PC,DPHI,T,TC,VV,DY,DZ)
      DYNEW = DFG(S)/DPHI(S)/DP
      DELY = ABS((DYNEW - DY(S))/(DYNEW + DY(S)))
      DY(S) = DYNEW
      IF (DELY.GE.1.D-4) GOTO 410
      DFG(1) = DY(1)*DPHI(1)*DP
      DFG(NS) = DY(NS)*DPHI(NS)*DP
450  CALL LEOS(C,DFG,K,NC,OMEGA,DP,PC,DPHI,T,TC,LV,DX,DZ)
      DSUMX = 0.0D0
      DO 500 I = 1,NC
          DNEWX(I) = DFG(I)/DPHI(I)/DP
          DSUMX = DSUMX + DNEWX(I)
500  CONTINUE
      DELX = DABS(DNEWX(1)-DX(1))/DX(1)
      DX(1) = (DX(1)+DNEWX(1))/2
      IF (DX(1).EQ.DXOLD) THEN
          WRITE (6,50)
50   FORMAT (X,'X(1) NOT CHANGING')
          STOP
          ENDIF
      IF (DX(1).LT.DXOLD) DX(1)=DXOLD
      DO 600 JJ=2,NC
          DX(JJ) = (1.D0 - DX(1))*DNEWX(JJ)/(DSUMX-DX(1))
600  CONTINUE
      IF (DELX.GT.2.5D-4) GOTO 450
      DELTA1 = DELTA2
      DELTA2 = 1.D0 - DSUMX
      ADELTA1 = DABS(DELTA1)
      ADELTA2 = DABS(DELTA2)
      IF (ADELTA2.GE.1.D-03) THEN
          IF (DELTA2/DELTA1.LT.0.D0) THEN
              DELRV = -DELRV/2.D0
          ELSE IF(ADELTA2.GT.ADELTA1) THEN
              DELRV = -DELRV/2.D0
          ENDIF
      RV = RV + DELRV
      LOOPS = LOOPS + 1
      IF (LOOPS.GT.5000) THEN
          WRITE (6,92) DP,T,DX(1),DX(2),DY(1),DY(2)
          WRITE (6,93) DELTA2,ADELTA2,DELRV
          ENDIF

```

```

      GOTO 400
    ENDIF
1000 PPSIA = DPTOT*14.696
    TDEGC = T - 273.15
    DOLDX = DX(1)
    WRITE (17,92) DP,T,DX(2),DX(3),DY(2),DY(3)
    WRITE (6,94) DP,T,LOOPS
    DO 1200 I=1,NC
      DRATIO(I) = DY(I)/DX(I)
1200  CONTINUE
    DO 1300 I = 2,NC
      IF (DRATIO(I).GT.5.0D-02) DI = 5.0
1300  CONTINUE
    DO 1310 I = 2,NC
      IF (DRATIO(I).GT.8.0D-02) DI = 2.5
1310  CONTINUE
    DO 1320 I = 2,NC
      IF (DRATIO(I).GT.1.1D-01) DI = 1.0
1320  CONTINUE
    DO 1330 I = 2,NC
      IF (DRATIO(I).GT.1.3D-01) DI = 0.5
1330  CONTINUE
    DO 1340 I = 2,NC
      IF (DRATIO(I).GT.2.0D-01) DI = 0.25
1340  CONTINUE
    DO 1350 I = 2,NC
      IF (DRATIO(I).GT.3.0D-01) DI = 0.1
1350  CONTINUE
    DO 1360 I = 2,NC
      IF (DRATIO(I).GT.3.5D-01) DI = 0.05
1360  CONTINUE
    IF (DI.LE.DINCR) DINCR = DI
    IF (DP.EQ.DPTOP) THEN
      GOTO 2000
    ELSE
      IF (DP.EQ.DP1) THEN
        DP = DINCR
1500      IF (DP.GT.DP1) GOTO 300
        DP = DP + DINCR
        GOTO 1500
      ELSE
        DP = DP + DINCR
        IF (DP.GT.DPTOP) DP = DPTOP
        GOTO 300
      ENDIF
    ENDIF
2000 CONTINUE
    66 FORMAT (X,'INPUT TEMPERATURE IN KELVIN (REAL #)')
    68 FORMAT (X,'WHICH COMPONENT FORMS A SOLID PHASE?')
    70 FORMAT (1X,'INPUT LOWEST PRESSURE IN BAR')
    74 FORMAT (1X,'INPUT HIGHEST PRESSURE IN BAR')
    78 FORMAT (1X,'INPUT THE SIZE OF THE PRESSURE INCREMENT IN BAR')
    82 FORMAT (1X,'INPUT K(',I1,',',I1,')')

```

```

84 FORMAT (X,'INPUT INITIAL GUESS FOR Rv')
86 FORMAT (X,'PRESSURE MELTING POINT')
90 FORMAT (X,' (BAR) (K) X2 X3 Y2
& Y3')
92 FORMAT (X,F8.3,2X,F13.5,4(2X,G9.4))
93 FORMAT (X,3(G15.8,5X)/)
94 FORMAT (1X,'THE MELTING POINT AT ',F8.3,' BAR IS ',G15.7,3X,I5)
96 FORMAT (X,F5.1,F7.2,8(X,G9.3))
END

```

```

C *****
C * SUBROUTINE VEOS2 USING ORIGINAL PENG-ROBINSON EOS *
C *****
C * A0 ----- THE ZEROETH ORDER TERM OF THE NORMALIZED CUBIC *
C * EQUATION TO BE SOLVED *
C * A1 ----- THE FIRST ORDER TERM OF THE NORMALIZED CUBIC *
C * EQUATION TO BE SOLVED *
C * A2 ----- THE SECOND ORDER TERM OF THE NORMALIZED CUBIC *
C * EQUATION TO BE SOLVED *
C * ASTAR SINGLE PRECISION DASTAR *
C * BSTAR SINGLE PRECISION DBSTAR *
C * C1 IMAGINARY PART OF THE 1ST ROOT OF THE SOLVED CUBIC *
C * C2 IMAGINARY PART OF THE 1ST ROOT OF THE SOLVED CUBIC *
C * C3 IMAGINARY PART OF THE 1ST ROOT OF THE SOLVED CUBIC *
C * C(I) VOLUME TRANSLATION FOR COMPONENT I - NOT USED IN *
C * THIS SUBROUTINE *
C * DA(I) PENG-ROBINSON a FOR PURE COMPONENT I *
C * DAM a OF THE MIXTURE *
C * DASTAR INTERMEDIATE VARIABLE USED TO SET UP CUBIC EQUATION *
C * TO SOLVE FOR Z *
C * DB(I) PENG-ROBINSON b FOR PURE COMPONENT I *
C * DBM b OF THE MIXTURE *
C * DBSTAR INTERMEDIATE VARIABLE USED TO SET UP CUBIC EQUATION *
C * TO SOLVE FOR Z *
C * DBTERM RATIO DB(I)/DBM, USED IN CALCULATING FUGACITY *
C * COEFFICIENT OF COMPONENT I *
C * DEL USED IN CALCULATING FUGACITY COEFFICIENTS *
C * DELY(I) CHANGE IN VALUE OF DY(I) FROM LAST ITERATION *
C * DFG(I) FUGACITY OF COMPONENT I *
C * DFOMEG FUNCTION OF OMEGA USED IN CALCULATING DA(I) VALUES *
C * DK(I,J) DOUBLE PRECISION K(I,J) *
C * DNEWY(I) NEXT GUESS FOR DY(I) *
C * DOM(I) DOUBLE PRECISION OM(I) *
C * DP TOTAL SYSTEM PRESSURE (BAR) *
C * DR DOUBLE PRECISION R *
C * DRLT FIRST LOGARITHMIC TERM USED IN CALCULATING *
C * FUGACITY COEFFICIENTS *
C * DRLT2 SECOND LOGARITHMIC TERM USED IN CALCULATING *
C * FUGACITY COEFFICIENTS *
C * DT DOUBLE PRECISION T *
C * DTC(I) DOUBLE PRECISION TC(I) *
C * DTR DOUBLE PRECISION TR *
C * DY(I) VAPOR PHASE MOLE FRACTION OF COMPONENT I *

```

```

C      * DZ      DOUBLE PRECISION Z      *
C      * I       COMPONENT SUBSCRIPT      *
C      * ICNT    ITERATION LOOP COUNTER    *
C      * J       COMPONENT SUBSCRIPT      *
C      * K(I,J)  INTERACTION PARAMETER FOR THE I,J COMPONENT PAIR *
C      * NC      TOTAL NUMBER OF COMPONENTS      *
C      * OM(I)   PITZER ACENTRIC FACTOR      *
C      * PC(I)   CRITICAL PRESSURE OF COMPONENT I      *
C      * PHI(I)  FUGACITY COEFFICIENT OF COMPONENT I IN THE MIXTURE *
C      * R       GAS CONSTANT (CC-BAR/MOL-K)      *
C      * R1      REAL PART OF THE 1ST ROOT OF THE SOLVED CUBIC      *
C      * R2      REAL PART OF THE 2ND ROOT OF THE SOLVED CUBIC      *
C      * R3      REAL PART OF THE 3RD ROOT OF THE SOLVED CUBIC      *
C      * T       SYSTEM TEMPERATURE (KELVIN)      *
C      * TC(I)   CRITICAL TEMPERATURE OF COMPONENT I (KELVIN)      *
C      * TR      REDUCED TEMPERATURE      *
C      * V       VAPOR PHASE MOLAR VOLUME (CC/MOL) OF MIXTURE AT      *
C      *         SYSTEM P AND T      *
C      * Z       VAPOR PHASE COMPRESSIBILITY OF MIXTURE      *
C *****
SUBROUTINE VEOS2 (C,DFG,K,NC,OM,DP,PC,DPHI,T,TC,V,DY,DZ)
  REAL C(3),K(3,3),OM(3),PC(3),TC(3)
  DOUBLE PRECISION DA(3),DAM,DASTAR,DB(3),DBM,DBSTAR,DBTERM,DEL
  DOUBLE PRECISION DFG(3),DFOMEG,DK(3,3),DOM(3)
  DOUBLE PRECISION DP,DPC(3),DPHI(3),DR,DRLNPHI,DRLT,DRLT2,DT
  DOUBLE PRECISION DTC(3),DTR,DY(3),DZ
C      OPEN (UNIT = 8, STATUS = 'NEW', FILE = 'VEOS.DAT')
      R = 83.1439
      DR = DBLE(R)
      DT = DBLE(T)
      DO 20 J = 1,NC
        DOM(J) = DBLE(OM(J))
        DPC(J) = DBLE(PC(J))
        DTC(J) = DBLE(TC(J))
        DTR=DT/DTC(J)
        DFOMEG = 3.7464D-1 + 1.54226D0*DOM(J) - 2.6992D-1*DOM(J)**2.D0
        DA(J) = 4.5724D-1*(DR*DTC(J))*(1.D0 + DFOMEG*(1.D0 -
&          DSQRT(DTR)))*2.D0/DPC(J)
        DB(J) = 7.78D-2*DR*DTC(J)/DPC(J)
      20      CONTINUE
C *****
C * BEGINNING OF LOOP FOR COMPOSITION *
C *****
      24      DAM=0
      DBM=0
      DO 30 I = 1,NC
        DBM = DBM + DY(I)*DB(I)
        DO 25 J = 1,NC
          DK(I,J) = DBLE(K(I,J))
          DAM=DAM+DY(I)*DY(J)*DSQRT(DA(I)*DA(J))*(1.D0-DK(I,J))
        25      CONTINUE
      30      CONTINUE
C *****

```

```

C * SOLVE CUBIC EOS *
C *****
      DASTAR = DAM*DP/(DR*DT)**2
      ASTAR = SNGL(DASTAR)
      DBSTAR = DBM*DP/DR/DT
      BSTAR = SNGL(DBSTAR)
      A2 = BSTAR-1.
      A1 = ASTAR-BSTAR*(2. + 3.*BSTAR)
      A0 = BSTAR*(BSTAR**2 + BSTAR - ASTAR)
      CALL CUBIC(A2,A1,A0,R1,R2,R3,C1,C2,C3,IFLAG)
C *****
C * IFLAG - 1 MEANS ONE REAL + TWO COMPLEX      *
C *          - 2          ALL REAL, AT LEAST TWO SAME *
C *          - 3          THREE DISTINCT REAL ROOTS *
C *****
      IF (IFLAG.EQ.1) THEN
        Z = R1
      ELSE IF (IFLAG.EQ.2) THEN
        Z = R1
        IF (Z.LT.R2) Z=R2
      ELSE
        Z = R1
        IF (Z.LT.R2) Z=R2
        IF (Z.LT.R3) Z=R3
      ENDIF
      DZ = DBLE(Z)
      V = Z*DR*DT/DP
C *****
C * CALCULATE VAPOR PHASE FUGACITIES *
C *****
      DRLT = DLOG((2.DO*DZ + DBSTAR*(2.DO + DSQRT(8.DO)))/(2.DO*DZ +
&          DBSTAR*(2.DO - DSQRT(8.DO))))
      DRLT2 = DLOG(DZ - DBSTAR)
      DO 700 L = 1,NC
        DBTERM = DB(L)/DBM
        DEL = 0.DO
        DO 600 LL = 1,NC
          DEL = DEL + 2.DO*DY(LL)*DSQRT(DA(L)*DA(LL))*(1.DO -
&          DK(L,LL))/DAM
600      CONTINUE
      DRLNPHI = DBTERM*(DZ - 1.DO) - DRLT2 + DASTAR*(DBTERM -
&          DEL)*DRLT/DBSTAR/DSQRT(8.DO)
      DPHI(L) = DEXP(DRLNPHI)
700      CONTINUE
      RETURN
      END

```

The following subroutine was substituted for the corresponding original Peng-Robinson subroutine (above) when the translated Peng-Robinson equation was used.

```

C *****
C * SUBROUTINE VEOS2 USING TRANSLATED PENG-ROBINSON EOS *
C *****
C * A0 ----- THE ZEROETH ORDER TERM OF THE NORMALIZED CUBIC *
C * EQUATION TO BE SOLVED *
C * A1 ----- THE FIRST ORDER TERM OF THE NORMALIZED CUBIC *
C * EQUATION TO BE SOLVED *
C * A2 ----- THE SECOND ORDER TERM OF THE NORMALIZED CUBIC *
C * EQUATION TO BE SOLVED *
C * ASTAR SINGLE PRECISION DASTAR *
C * BSTAR SINGLE PRECISION DBSTAR *
C * C1 IMAGINARY PART OF THE 1ST ROOT OF THE SOLVED CUBIC *
C * C2 IMAGINARY PART OF THE 1ST ROOT OF THE SOLVED CUBIC *
C * C3 IMAGINARY PART OF THE 1ST ROOT OF THE SOLVED CUBIC *
C * C(I) VOLUME TRANSLATION FOR COMPONENT I *
C * DA(I) PENG-ROBINSON a FOR PURE COMPONENT I *
C * DAM a OF THE MIXTURE *
C * DASTAR INTERMEDIATE VARIABLE USED TO SET UP CUBIC EQUATION *
C * TO SOLVE FOR Z *
C * DB(I) PENG-ROBINSON b FOR PURE COMPONENT I *
C * DBM b OF THE MIXTURE *
C * DBSTAR INTERMEDIATE VARIABLE USED TO SET UP CUBIC EQUATION *
C * TO SOLVE FOR Z *
C * DBTERM RATIO DB(I)/DBM, USED IN CALCULATING FUGACITY *
C * COEFFICIENT OF COMPONENT I *
C * DCM c OF THE MIXTURE *
C * DEL USED IN CALCULATING FUGACITY COEFFICIENTS *
C * DELY(I) CHANGE IN VALUE OF DY(I) FROM LAST ITERATION *
C * DFG(I) FUGACITY OF COMPONENT I *
C * DFOMEG FUNCTION OF OMEGA USED IN CALCULATING DA(I) VALUES *
C * DK(I,J) DOUBLE PRECISION K(I,J) *
C * DNEWY(I) NEXT GUESS FOR DY(I) *
C * DOM(I) DOUBLE PRECISION OM(I) *
C * DP TOTAL SYSTEM PRESSURE (BAR) *
C * DR DOUBLE PRECISION R *
C * DRLT FIRST LOGARITHMIC TERM USED IN CALCULATING *
C * FUGACITY COEFFICIENTS *
C * DRLT2 SECOND LOGARITHMIC TERM USED IN CALCULATING *
C * FUGACITY COEFFICIENTS *
C * DT DOUBLE PRECISION T *
C * DTC(I) DOUBLE PRECISION TC(I) *
C * DTR DOUBLE PRECISION TR *
C * DY(I) VAPOR PHASE MOLE FRACTION OF COMPONENT I *
C * DZ DOUBLE PRECISION Z *
C * I COMPONENT SUBSCRIPT *

```

```

C      * ICNT      ITERATION LOOP COUNTER      *
C      * J         COMPONENT SUBSCRIPT          *
C      * K(I,J)    INTERACTION PARAMETER FOR THE I,J COMPONENT PAIR *
C      * NC        TOTAL NUMBER OF COMPONENTS   *
C      * OM(I)     PITZER ACENTRIC FACTOR        *
C      * PC(I)     CRITICAL PRESSURE OF COMPONENT I *
C      * PHI(I)    FUGACITY COEFFICIENT OF COMPONENT I IN THE MIXTURE *
C      * R         GAS CONSTANT (CC-BAR/MOL-K)   *
C      * R1        REAL PART OF THE 1ST ROOT OF THE SOLVED CUBIC *
C      * R2        REAL PART OF THE 2ND ROOT OF THE SOLVED CUBIC *
C      * R3        REAL PART OF THE 3RD ROOT OF THE SOLVED CUBIC *
C      * T         SYSTEM TEMPERATURE (KELVIN)    *
C      * TC(I)     CRITICAL TEMPERATURE OF COMPONENT I (KELVIN) *
C      * TR        REDUCED TEMPERATURE           *
C      * TZ        TRUE VAPOR PHASE COMPRESSIBILITY OF MIXTURE *
C      * V         VAPOR PHASE MOLAR VOLUME (CC/MOL) OF MIXTURE AT *
C      *           SYSTEM P AND T                *
C      * Z         VAPOR PHASE COMPRESSIBILITY OF MIXTURE *
C      *****

```

```

SUBROUTINE VEOS2 (C,DFG,K,NC,OM,DP,PC,DPHI,T,TC,V,DY,TZ)

```

```

    REAL C(3),K(3,3),OM(3),PC(3),TC(3),ZRA(3)
    DOUBLE PRECISION DA(3),DAM,DASTAR,DB(3),DBM,DBSTAR,DBTERM,DC(3)
    DOUBLE PRECISION DCM,DEL,DFG(3),DFOMEG,DK(3,3),DOM(3)
    DOUBLE PRECISION DP,DPC(3),DPHI(3),DR,DRLNPHI,DRLT,DRLT2,DT
    DOUBLE PRECISION DTC(3),DTR,DY(3),DZ,TZ

```

```

    R = 83.1439

```

```

    DR = DBLE(R)

```

```

    DT = DBLE(T)

```

```

    DO 20 J = 1,NC

```

```

        DC(J) = DBLE(C(J))

```

```

        DOM(J) = DBLE(OM(J))

```

```

        DPC(J) = DBLE(PC(J))

```

```

        DTC(J) = DBLE(TC(J))

```

```

        DTR=DT/DTC(J)

```

```

        DFOMEG = 3.7464D-1 + 1.54226D0*DOM(J) - 2.6992D-1*DOM(J)**2.D0

```

```

        DA(J) = 4.5724D-1*(DR*DTC(J)*(1.D0 + DFOMEG*(1.D0 -

```

```

        & DSQRT(DTR))))**2.D0/DPC(J)

```

```

        DB(J) = 7.78D-2*DR*DTC(J)/DPC(J)

```

```

    20    CONTINUE

```

```

C *****

```

```

C * BEGINNING OF LOOP FOR COMPOSITION *

```

```

C *****

```

```

    24    DAM = 0.0D0

```

```

        DBM = 0.0D0

```

```

        DCM = 0.0D0

```

```

        DO 30 I = 1,NC

```

```

            DBM = DBM + DY(I)*DB(I)

```

```

            DCM = DCM + DY(I)*DC(I)

```

```

            DO 25 J = 1,NC

```

```

                DK(I,J) = DBLE(K(I,J))

```

```

                DAM=DAM+DY(I)*DY(J)*DSQRT(DA(I)*DA(J))*(1.D0-DK(I,J))

```

```

    25    CONTINUE

```

```

    30    CONTINUE

```



```

C *****
C * SOLVE CUBIC EOS *
C *****
      DASTAR = DAM*DP/(DR*DT)**2
      ASTAR = SNGL(DASTAR)
      DBSTAR = DBM*DP/DR/DT
      BSTAR = SNGL(DBSTAR)
      A2 = BSTAR-1.
      A1 = ASTAR-BSTAR*(2. + 3.*BSTAR)
      A0 = BSTAR*(BSTAR**2 + BSTAR - ASTAR)
      CALL CUBIC(A2,A1,A0,R1,R2,R3,C1,C2,C3,IFLAG)
C *****
C * IFLAG = 1 MEANS ONE REAL + TWO COMPLEX      *
C *      - 2      ALL REAL, AT LEAST TWO SAME *
C *      - 3      THREE DISTINCT REAL ROOTS  *
C *****
      IF (IFLAG.EQ.1)THEN
        Z = R1
      ELSE IF (IFLAG.EQ.2) THEN
        Z = R1
        IF (Z.LT.R2) Z=R2
      ELSE
        Z = R1
        IF (Z.LT.R2) Z=R2
        IF (Z.LT.R3) Z=R3
      ENDIF
      DZ = DBLE(Z)
      TZ = DZ - DCM*DP/DR/DT
      V = TZ*DR*DT/DP
C *****
C * CALCULATE VAPOR PHASE FUGACITIES *
C *****
      DRLT = DLOG((2.DO*DZ + DBSTAR*(2.DO + DSQRT(8.DO)))/(2.DO*DZ +
&          DBSTAR*(2.DO - DSQRT(8.DO))))
      DRLT2 = DLOG(DZ - DBSTAR)
      DO 700 L = 1,NC
        DBTERM = DB(L)/DBM
        DEL = 0.DO
        DO 600 LL = 1,NC
          DEL = DEL + 2.DO*DY(LL)*DSQRT(DA(L)*DA(LL))*(1.DO -
&          DK(L,LL))/DAM
600      CONTINUE
      DRLNPHI = DBTERM*(DZ - 1.DO) - DRLT2 + DASTAR*(DBTERM -
&          DEL)*DRLT/DBSTAR/DSQRT(8.DO) - DC(L)*DP/DR/DT
      DPHI(L) = DEXP(DRLNPHI)
700      CONTINUE
      RETURN
      END

```

APPENDIX G

EQUATION OF STATE PARAMETER DETERMINATIONS

The values of most of the parameters used for the phase equilibria modeling were taken from existing references. The values of the parameters and the sources they were obtained from are tabulated in the data files of Appendix D. The critical pressure value reported for phenanthrene in a literature search was originally estimated by the method of Lydersen with an expected accuracy of $\pm 10\%$. In light of this degree of uncertainty, for the calculations in this work, the value used for the critical pressure of phenanthrene was optimized to minimize the sum of the squares of the errors for a fit to the liquid vapor pressure curve from the triple point to about 50 K below the critical temperature. The optimized P_c (critical pressure) was 27.43 bar compared to 29.0 bar from the Lydersen method estimate. This is within the stated range of accuracy for the correlation value. The acentric factor was calculated simultaneously for each guess of the P_c value and using the known values for the vapor pressure and critical temperature of phenanthrene. Values of the pure component c_i 's for the translated equation were obtained by translating at the triple points of the pure components. The k_{ij} parameters for the CO_2 +hydrocarbon binary systems were chosen to fit the predicted P-T traces to match the measured traces as closely as possible. Increasing the k_{ij} values caused the

predicted melting points to increase and caused the melting point curve to bend back more sharply at higher pressures. Decreasing the k_{ij} values caused the predicted melting points to decrease and caused the melting point curve to bend back less; at low enough values for the CO_2/solid interaction parameters, the melting point curves fail to have any minimum (i.e. the melting point temperature continue to decrease until the upper critical end point is reached). The solid/solid interaction parameters were chosen to improve the fit of the model to the ternary melting point depression data. The interaction parameters were optimized independently for the Peng-Robinson and translated Peng-Robinson equations of state. The values chosen were:

<u>Binary</u>	<u>k_{ij_PR}</u>	<u>k_{ij_TPR}</u>
$\text{CO}_2/\text{biphenyl}$	0.100	0.095
$\text{CO}_2/\text{naphthalene}$	0.109	0.116
$\text{CO}_2/\text{phenanthrene}$	0.110	0.175
biphenyl/naphthalene	-0.02	-0.020
naphthalene/phenanthrene	0.0	-0.008

Figures G.1 to G.6 demonstrate the effect of changing the value of k_{ij} has on the P-T traces and liquid mole fractions predicted by the Peng-Robinson equation of state. The data of Cheong et al. (1986) and Zhang and Lu (1988) and the corresponding predictions by the translated Peng-Robinson equation are also shown for comparison. Increasing k_{ij} causes the P-T trace to bend back more and increases the predicted mole fraction of the solid in the liquid. Varying k_{ij} in the translated equation has the same effect.

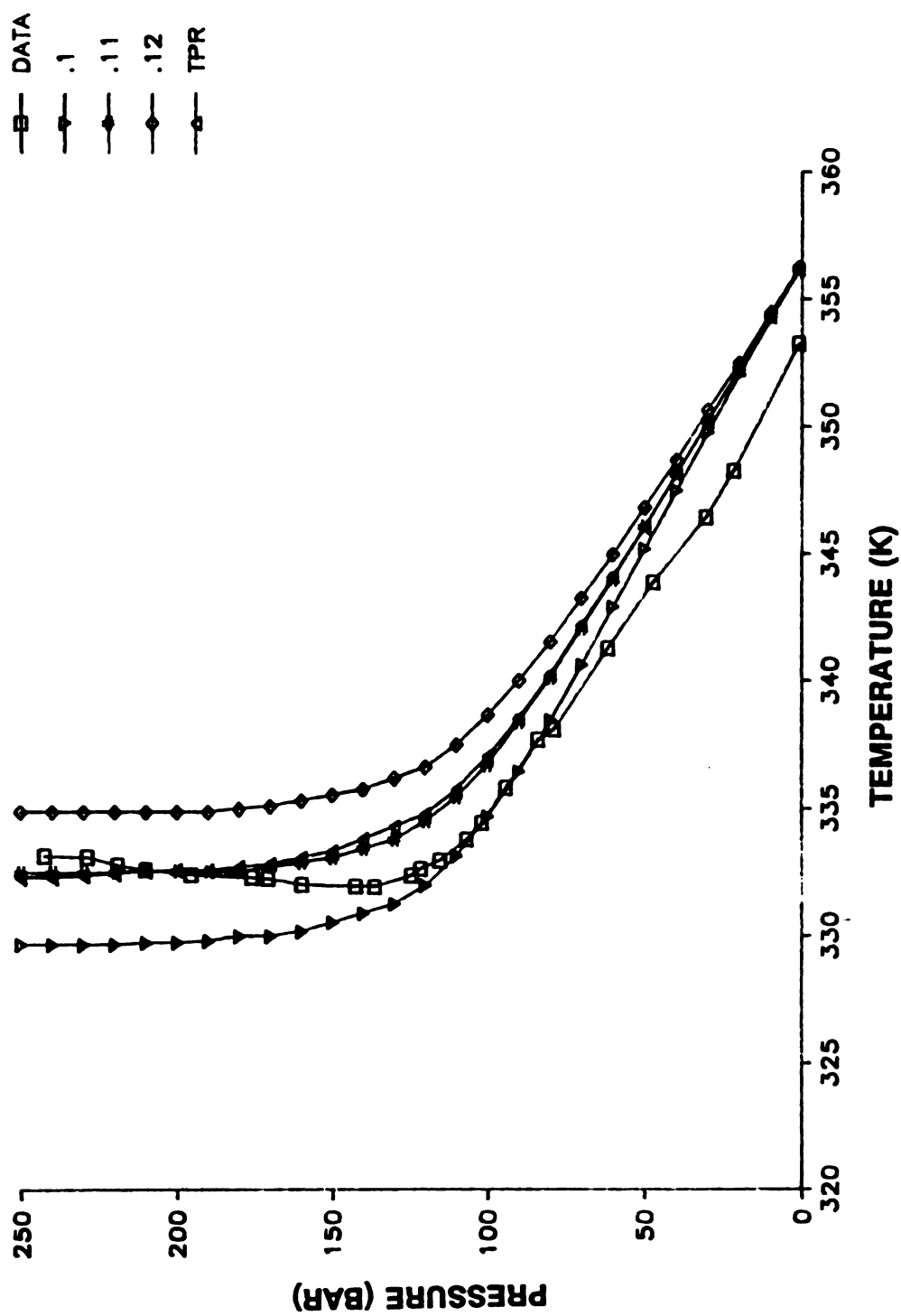


Figure G.1

Comparison of fits of the SLV P-T trace for different values of k_{ij} in the Peng-Robinson equation for the CO_2 +naphthalene system.

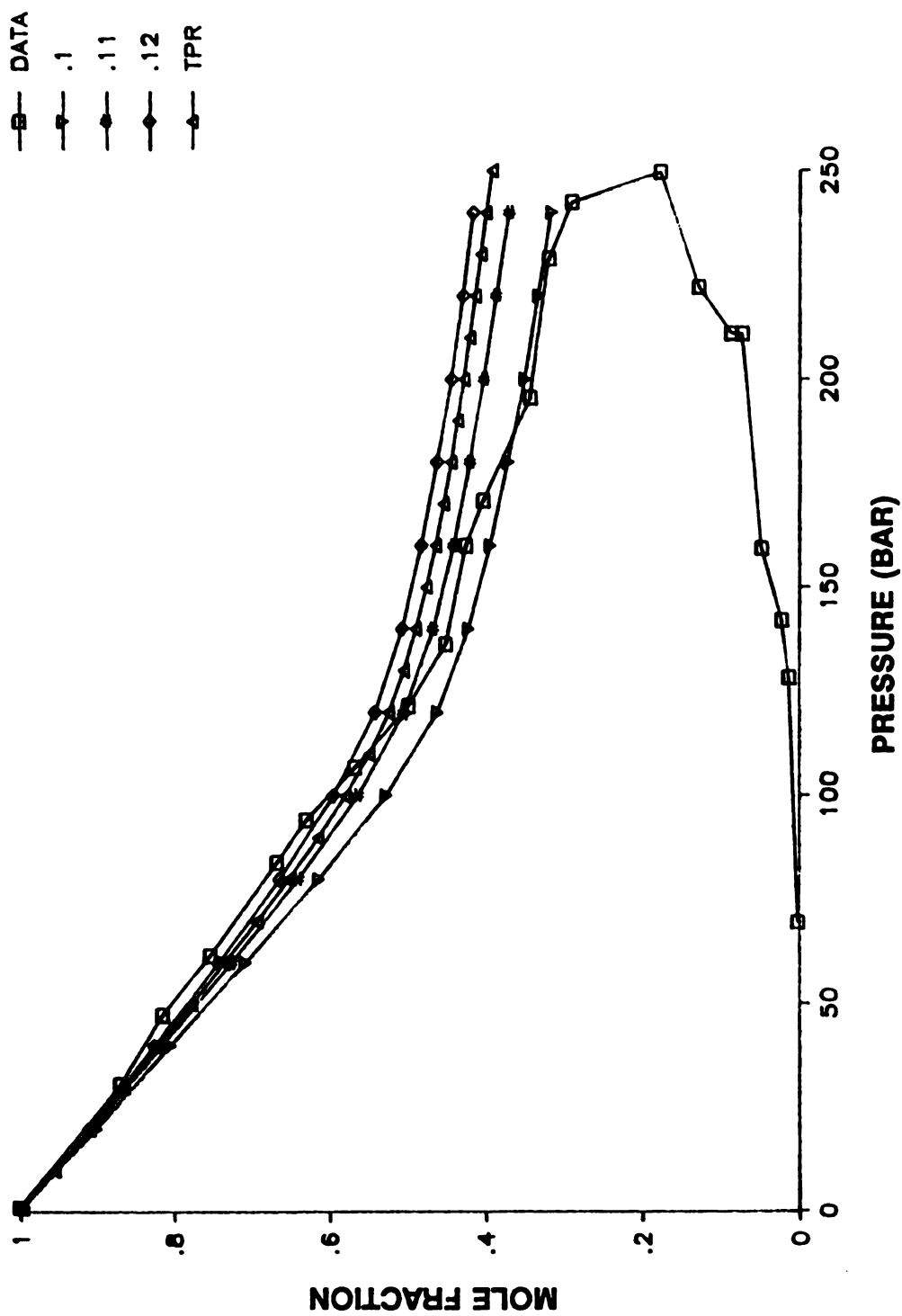


Figure G.2 Comparison of fits to the P-x-y plot along the SLV line for the CO₂+naphthalene system.

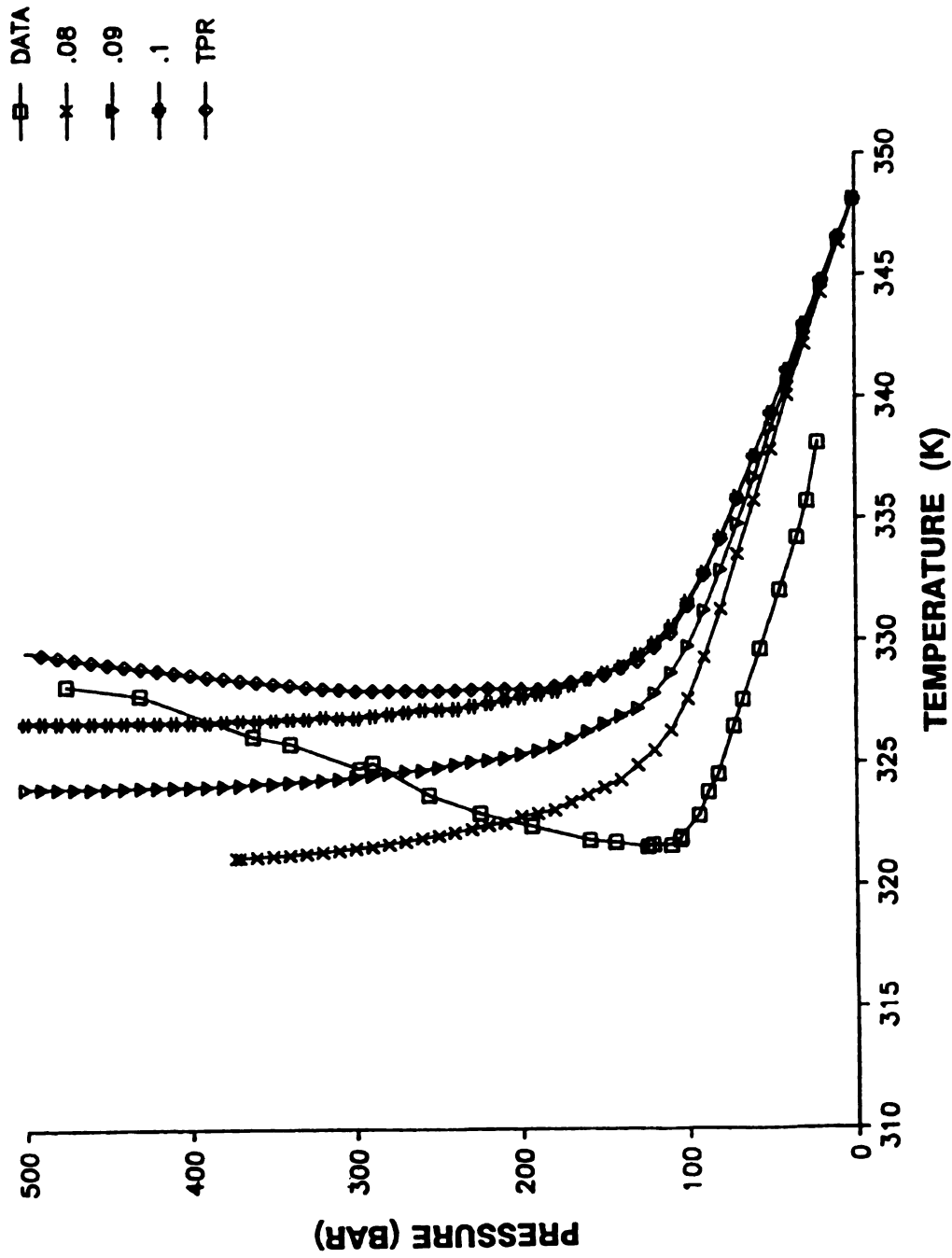


Figure G.3 Comparison of fits of the SLV P-T trace for different values of k_{ij} in the Peng-Robinson equation for the CO_2 +biphenyl system.

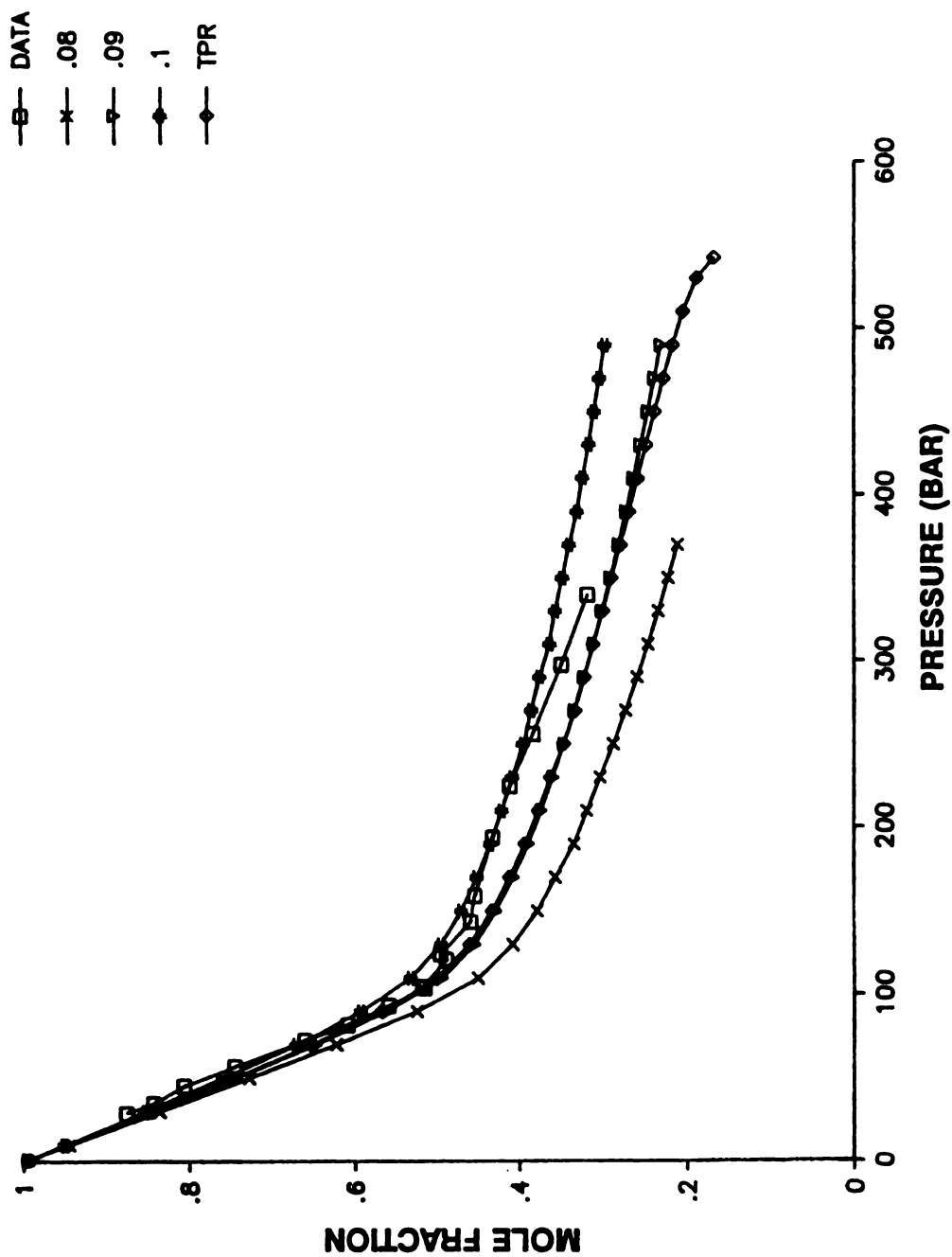


Figure G.4 Comparison of fits to the P-x-y plot along the SLV line for the CO₂+biphenyl₁ system.

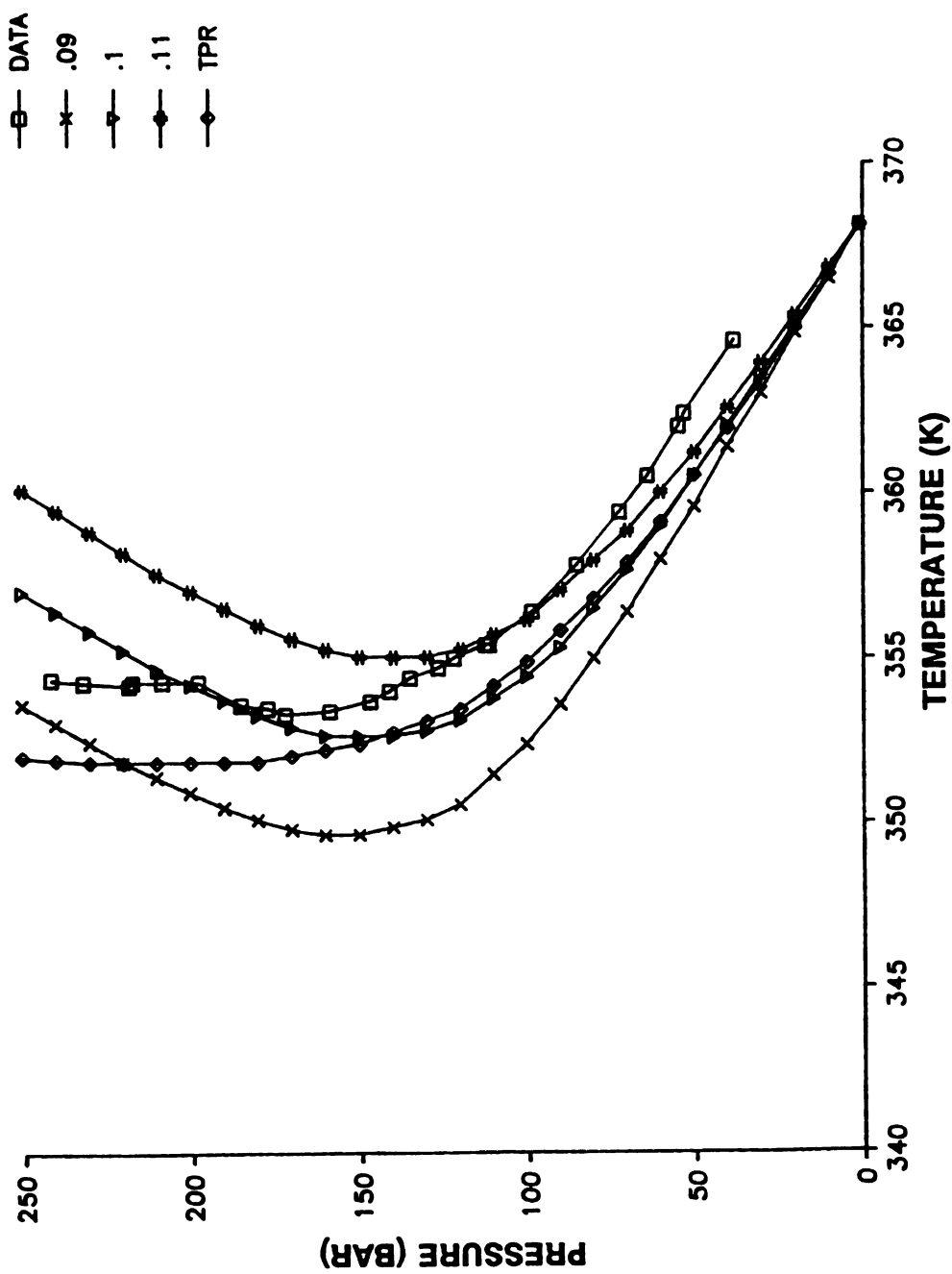


Figure G.5 Comparison of fits of the SLV P-T trace for different values of k_{ij} in the Peng-Robinson equation for the CO_2 +phenanthrene system.

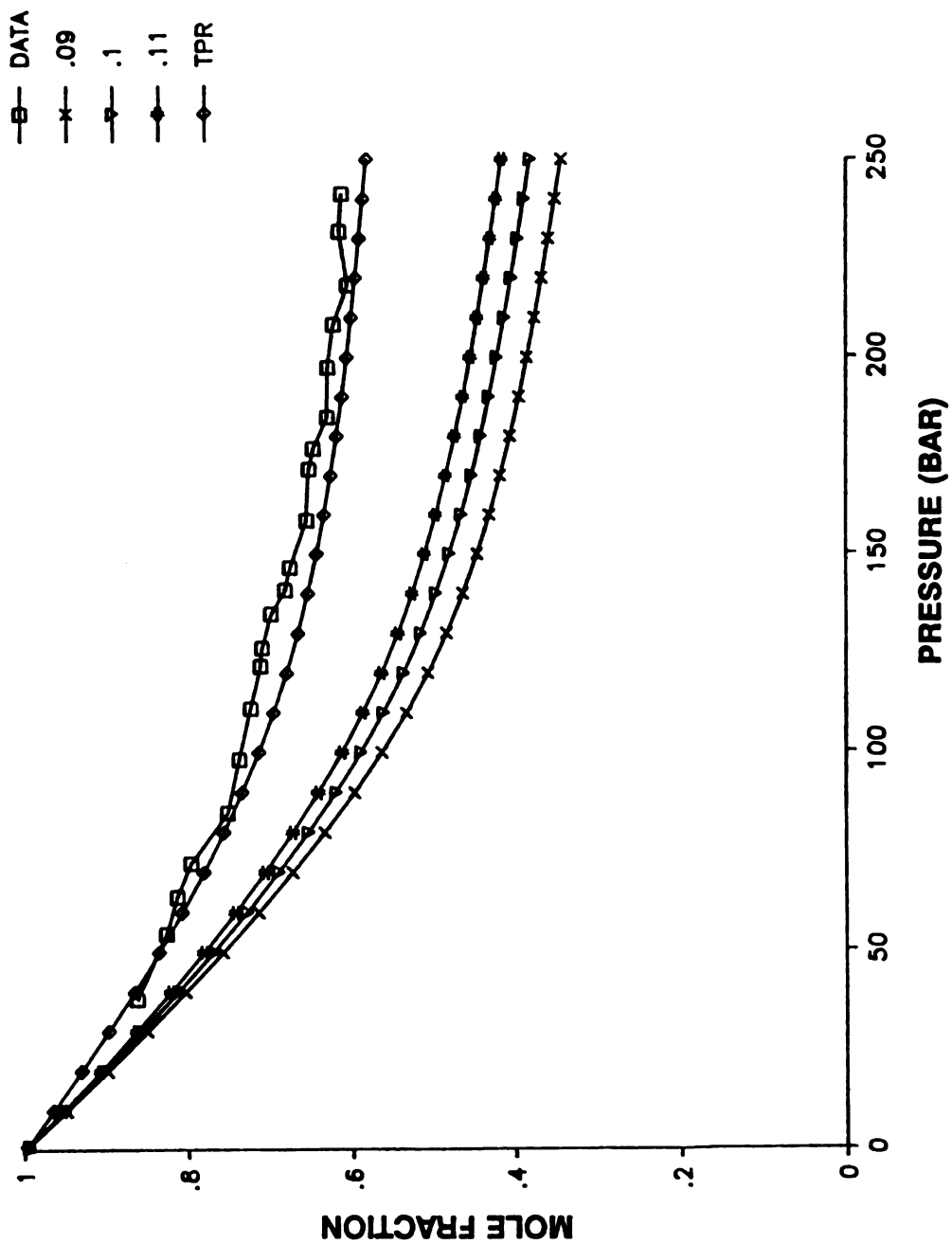


Figure G.6 Comparison of fits to the P-x-y plot along the SLV line for the CO_2 +phenanthrene system.

APPENDIX H

RAW COMPOSITION DATA

Naphthalene/CO₂ SAMPLES AT 67.6°C AND 990 PSIA

v CO ₂	7.9	7.1	16.2	15.9	
T	295.35	296.15	297.15	297.15	
P (mbar)	976.5	977	988	988	
n ₂	.0003141	.0002817	.0006478	.0006358	
n ₁	.0000052	.0000010	.0000022	.0000014	
y ₁	.0164296	.0033620	.0033371	.0022516	
v CO ₂	3.4	3.5	3.9	1.95	3.15
T	302.65	303.55	298.15	300.65	300.55
P (mbar)	982.5	981	994	985	986
n ₂	.0001328	.0001360	.0001564	.0000768	.0001243
n ₁	.0002096	.0002004	.0000175	.0001838	.0001679
x ₁	.6122554	.5956496	.1008058	.7051679	.5746179

Naphthalene/CO₂ SAMPLES AT 60.3°C AND 1860 PSIA

v CO ₂	19.2	28.9	30.6	28.9	
T K	305.15	305.15	303.85	303.7	
P (mbar)	983	984	986	989	
n ₂	.0007439	.0011209	.0011943	.0011319	
n ₁	.0000310	.0000172	.0000152	.0000167	
y ₁	.0399596	.0151443	.0125646	.0145349	
v CO ₂	6.7	5.35	4.25	4.85	
T K	302.45	300.85	299.05	300.05	
P (mbar)	989	984.5	987	987	
n ₂	.0002635	.0002106	.0001687	.0001919	
n ₁	.0002376	.0002334	.0002333	.0002339	
x ₁	.4741195	.5256883	.5803339	.5493904	

Naphthalene/CO₂ SAMPLES AT 59.2°C AND 2060 PSIA

v CO ₂	34.6	36	35.1	34.8
T K	301.15	302.15	302.75	302.95
P (mbar)	990	996	994	994
n ₂	.0013680	.0014273	.0013861	.0013733
n ₁	.0000317	.0000349	.0000316	.0000330
y ₁	.0226256	.0238798	.0223050	.0234720
v CO ₂	4.95	16.1	19.75	14.05
T K	303.15	301.55	300.85	300.45
P (mbar)	996	990	988.5	988.5
n ₂	.0001956	.0006357	.0007805	.0005560
n ₁	.0002089	.0000418	.0002493	.0000334
x ₁	.5164461	.0616995	.2420597	.0566894

Naphthalene/CO₂ SAMPLES AT 58.9°C AND 2310 PSIA

v CO ₂	36.25	36.7	37	34.7	30.7
T K	302.05	303.85	303.05	300.25	300.4
P (mbar)	985.5	979	976	984.5	982
n ₂	.0014225	.0014222	.0014332	.0013685	.0012070
n ₁	.0000090	.0000683	.0000564	.0000892	.0001370
y ₁	.0062721	.0457978	.0378335	.0612223	.1018996
v CO ₂	6.65	7.95	4.8		
T K	300.15	300.45	299.65		
P (mbar)	989	984	988		
n ₂	.0002635	.0003132	.0001904		
n ₁	.0002384	.0002333	.0001733		
x ₁	.4749060	.4268998	.4764898		

Naphthalene/CO₂ SAMPLES AT 59.2°C AND 3060 PSIA

v CO ₂	36.2	29.7	35.7
T °C	24.6	25	25.9
T K	297.75	298.15	299.05
P (mbar)	992	992	990.5
n ₂	.0014506	.0011885	.0014222
n ₁	.0001385	.0002724	.0000721
y ₁	.0871762	.1864481	.0482565
v CO ₂	17.8		
T °C	25		
T K	298.15		
P (mbar)	993		
n ₂	.0007130		
n ₁	.0000172		
x ₁	.0236169		

Naphthalene/CO₂ SAMPLES AT 59.5°C AND 3220 PSIA

v CO ₂	10.15	38.6	9.75	10.3	39.45
T °C	23.8	24	25.1	25.5	25.3
T K	296.95	297.15	298.25	298.65	298.45
P (mbar)	971.5	972	973	973	973
n ₂	.0003994	.0015186	.0003826	.0004036	.0015469
n ₁	.0000817	.0001217	.0000731	.0000787	.0001143
y ₁	.1697813	.0742057	.1604873	.1631413	.0687821

v CO ₂	10.4	37.45	37.4
T °C	23.75	25.4	24.3
T K	296.9	298.55	297.45
P (mbar)	970	981	985
n ₂	.0004087	.0014800	.0014896
n ₁	.0002002	.0003528	.0003249
x ₁	.3287950	.1924657	.1790669

Naphthalene/CO₂ SAMPLES AT 59.2°C AND 3060 PSIA

v CO ₂	10.4	10.5	9.75	10
T K	298.45	298.95	299.05	299.25
P (mbar)	979	988	988.5	988.5
n ₂	.0004103	.0004174	.0003876	.0003973
n ₁	.0001746	.0001742	.0001784	.0001803
y ₁	.2985180	.2944604	.3151282	.3121935

v CO ₂	33.95	37.6	37.55	30.4
T K	298.15	298.05	298.25	298.15
P (mbar)	988	987	987	987.5
n ₂	.0013531	.0014976	.0014946	.0012110
n ₁	.0002062	.0001125	.0001224	.0001364
x ₁	.1322403	.0698925	.0756983	.1012106

Naphthalene/CO₂ SAMPLES AT 60.2°C AND 1860 PSIA

v CO ₂	17.8
T K	298.15
P (mbar)	993
n ₂	.0007130
n ₁	.0002327
x ₁	.2460513

Naphthalene/CO₂ SAMPLES AT 59.7°C AND 3620 PSIA

v CO ₂	34.2	30	33.05	28
T K	296.35	299.45	299.05	299.05
P (mbar)	973	974	972.5	970
n ₂	.0013505	.0011736	.0012927	.0010923
n ₁	.0000266	.0002627	.0001939	.0003062
y ₁	.0193117	.1828982	.1304249	.2189216
v CO ₂	11.6	12	12.3	12.35
T K	300.45	299.65	299.45	299.05
P (mbar)	982	979	977	975.5
n ₂	.0004560	.0004715	.0004827	.0004845
n ₁	.0001673	.0001676	.0001617	.0001537
x ₁	.2683557	.2622537	.2509556	.2408517

Biphenyl/CO₂ SAMPLES AT 58.3°C AND 630 PSIA

v CO ₂	5	4.9	4.9	1.15	2.15
T °C	23.4	23.3	23.35	23	23.25
T K	296.55	296.45	296.5	296.15	296.4
P (mbar)	993.5	996	995.5	999	999.5
n ₂	.0002015	.0001980	.0001979	.0000467	.0000872
n ₁	.0000039	.0000025	.0000015	.0001269	.0000089
y ₁	.0187998	.0122260	.0075816	.7310929	.0926092
v CO ₂	5.1	2.1	2.05		
T °C	25.5	23.2	23.4		
T K	298.65	296.35	296.55		
P (mbar)	980	999	999.5		
n ₂	.0002013	.0000851	.0000831		
n ₁	.0000133	.0000087	.0000122		
x ₁	.0619944	.0924913	.1281251		

Biphenyl/CO₂ SAMPLES AT 48.65°C AND 1400 PSIA

v CO ₂	36.2	30.7	34.7
T K	297.75	300.4	300.25
P (mbar)	992	982	984.5
n ₂	.0014506	.0012070	.0013685
n ₁	.0000212	.0000042	.0000013
y ₁	.0143832	.0034539	.0009380
v CO ₂	17.8		
T K	298.15		
P (mbar)	993		
n ₂	.0007130		
n ₁	10.31381		
x ₁	.9999309		

Naphthalene/Biphenyl Ternary at 410 psia and 42.20 °C

MOLES N	.0000003	.0000030	3.822e-8	.0000001	.0000004
MOLES B	.0000012	.0000101	.0000002	.0000074	.0000001

ml GAS	4.3	6.3	3	3.2	4.4
P (mbar)	978	1001	1001	1001	979
T K	296.95	294.15	294.55	294.35	301.35
MOLES CO ₂	.0001703	.0002579	.0001226	.0001309	.0001719
TOTAL MOL	.0001719	.0002710	.0001229	.0001385	.0001724

y N	.0018001	.0110240	.0003110	.0010727	.0022143
y B	.0072236	.0374451	.0019849	.0537719	.0004481

MOLES N	.0000887	.0000962
MOLES B	.0002158	.0002376
ml GAS	1.9	1.6
P (mbar)	986	982
T K	301.35	301.35
MOLES CO ₂	.0000748	.0000627
TOTAL MOL	.0003792	.0003965

x N	.2338357	.2426674
x B	.5689920	.5991919

Naphthalene/Biphenyl Ternary at 1070 psia and 32.65 °C

MOLES N	.0000070	.0000067	.0000066	.0000057
MOLES B	.0000126	.0000072	.0000094	.0000085
ml GAS	38.5	38.2	38.9	37.75
P (mbar)	983	982	982	976
T K	295.55	295.55	295.55	295.45
MOLES CO ₂	.0015401	.0015266	.0015545	.0014999
TOTAL MOL	.0015597	.0015405	.0015705	.0015141

y N	.0044871	.0043737	.0041860	.0037845
y B	.0080567	.0046523	.0059753	.0055918

MOLES N	.0000550	.0000969	.0000859	.0000752
MOLES B	.0001526	.0002367	.0002235	.0001973
ml GAS	5	5.7	5.7	5.5
P (mbar)	982.5	984	975	975
T K	294.95	295.55	295.35	295.25
MOLES CO ₂	.0002003	.0002282	.0002263	.0002184
TOTAL MOL	.0004079	.0005618	.0005357	.0004910

x N	.1348403	.1724022	.1604208	.1532426
x B	.3740594	.4213144	.4171199	.4018509

Naphthalene/Biphenyl Ternary at 760 psia and 52.80 °C

MOLES N	.0000003	.0000047	.0000003	.0000002
MOLES B	.0000005	.0000019	.0000001	.0000001
ml GAS	5.7	5.7	5.8	5.6
P (mbar)	992	986	986.5	986
T °C	23.6	22.9	23.4	23.9
T K	296.75	296.05	296.55	297.05
MOLES CO ₂	.0002292	.0002283	.0002321	.0002236
TOTAL MOL	.0002300	.0002350	.0002324	.0002238

y N	.0013907	.0199467	.0013185	.0007561
y B	.0022198	.0082989	.0003153	.0004202

MOLES N	.0002384	.0002335	.0002213	.0002377
MOLES B	.0000897	.0000354	.0000860	.0000909
ml GAS	2.4	2.4	2.45	2.3
P (mbar)	989	990	986	986
T °C	22.9	23	23.6	23.6
T K	296.05	296.15	296.75	296.75
MOLES CO ₂	.0000964	.0000965	.0000979	.0000919
TOTAL MOL	.0004245	.0003654	.0004052	.0004206

x N	.5616530	.6390803	.5461984	.5652421
x B	.2112060	.0968728	.2121431	.2162126

Naphthalene/Biphenyl Ternary at 1180 psia and 42.20 °C

MOLES N	0	0	0
MOLES B	0	0	0
ml GAS	38.7	36.6	38.8
P (mbar)	979	978	976.5
T K	300.25	300.25	300.25
MOLES CO ₂	.0015177	.0014339	.0015177
TOTAL MOL	0	0	0

y N	0	0	0
y B	0	0	0

MOLES N	.0001861	.0001979
MOLES B	.0000853	.0000358
ml GAS	6.9	6.6
P (mbar)	984	979
T K	297.25	299.75
MOLES CO ₂	.0002747	.0002593
TOTAL MOL	.0005462	.0004929

x N	.3408213	.4014298
x B	.1561708	.0725979

Naphthalene/Biphenyl Ternary at 780 psia and 32.65 °C

MOLES N	.00000002	.00000002	.00000001	.00000001
MOLES B	.00000002	.00000003	.00000001	.00000001
ml GAS	6.3	6.1	7.1	7.1
P (mbar)	986	987	982.5	983
T °C	23.3	23.2	23.3	23.3
T K	296.45	296.35	296.45	296.45
MOLES CO ₂	.0002520	.0002443	.0002830	.0002832
TOTAL MOL	.0002524	.0002448	.0002833	.0002833

y N	.0008844	.0007259	.0003567	.0002270
y B	.0006461	.0010683	.0005155	.0003651

MOLES N	.0001056	.0000988	.0000074	.0000661	.0000986
MOLES B	.0002150	.0002068	.0000150	.0001263	.0002034
ml GAS	3.25	2.9	2.3	3.05	3.05
P (mbar)	981	981	981	981.5	983
T °C	22	23.4	23.4	23.4	23.3
T K	295.15	296.55	296.55	296.55	296.45
MOLES CO ₂	.0001299	.0001154	.0000915	.0001214	.0001216
TOTAL MOL	.0004506	.0004210	.0001139	.0003138	.0004236

x N	.2344290	.2345902	.0650834	.2105704	.2327820
x B	.4772334	.4913301	.1315398	.4025639	.4800779

Naphthalene/Biphenyl Ternary at 1080 psia and 32.65 °C

MOLES N	.0000146	.0000137	.0000049	.0000046	.0000062
MOLES B	.0000070	.0000066	.0000024	.0000021	.0000030
ml GAS	36.6	36.4	24.9	24.65	23.55
P (mbar)	985	985.5	985.5	986	987
T K	296.5	296.45	296.35	296.45	296.45
MOLES CO ₂	.0014624	.0014554	.0009959	.0009861	.0009430
TOTAL MOL	.0014840	.0014757	.0010032	.0009928	.0009522

y N	.0098458	.0093007	.0048765	.0046034	.0064661
y B	.0047249	.0044559	.0024031	.0021353	.0031917

MOLES N	.0001516	.0001631	.0001653	.0001702
MOLES B	.0001324	.0001368	.0001347	.0001319
ml GAS	5	5.4	5.7	5.9
P (mbar)	984	984	984	985
T K	296.45	296.45	296.35	296.45
MOLES CO ₂	.0001996	.0002156	.0002276	.0002358
TOTAL MOL	.0004836	.0005155	.0005277	.0005379

x N	.3134186	.3164753	.3133110	.3164466
x B	.2737992	.2653291	.2553180	.2452202

Naphthalene/Biphenyl Ternary at 920 psia and 32.65 °C

MOLES N	.0000027	.0000025	.0000003	.0000002	.0000004
MOLES B	.0000023	.0000021	.0000024	.0000002	.0000005
ml GAS	9.6	9.6	9.7	9.9	9.8
P (mbar)	986	987	987.5	987.5	987.5
T K	296.65	297.15	296.15	296.05	296.1
MOLES CO ₂	.0003838	.0003835	.0003890	.0003972	.0003931
TOTAL MOL	.0003888	.0003881	.0003917	.0003976	.0003940

y N	.0068918	.0063497	.0006450	.0006216	.0010928
y B	.0059256	.0055100	.0061550	.0004148	.0011683

MOLES N	.0001492	.0000018	.0000002	.0001608	.0001688
MOLES B	.0001620	.0000016	.0000024	.0001493	.0001560
ml GAS	3.3	4.4	4.8	3.95	3.75
P (mbar)	988	987.5	987.5	987	987.5
T K	297.15	296.05	296.25	296.05	296.05
MOLES CO ₂	.0001320	.0001765	.0001924	.0001584	.0001504
TOTAL MOL	.0004431	.0001800	.0001951	.0004686	.0004752

x N	.3365973	.0101909	.0011540	.3432574	.3551726
x B	.3655872	.0089817	.0124725	.3187095	.3282578

Naphthalene/Biphenyl Ternary at 920 psia and 32.65 °C
(continued)

MOLES N	.0001698	.0001658
MOLES B	.0001552	.0001536
ml GAS	3.9	4.2
P (mbar)	987	988
T K	295.95	295.9
MOLES CO ₂	.0001564	.0001687
TOTAL MOL	.0004814	.0004881
x N	.3526569	.3397802
x B	.3223811	.3146356

BIBLIOGRAPHY

BIBLIOGRAPHY

- Adachi, Y., H. Sugie, and B. C.-Y. Lu, Fluid Phase Equilib., 28:119 (1986)
- Beckman, E. J., J. L. Fulton, D. W. Matson, and R. D. Smith, ACS Symp. Ser. 406, p. 184 (1989)
- Brennecke, J. F., and C. A. Eckert, ACS Symp. Ser. 406, p. 14 (1989)
- Brunner, G., and S. Peter, Chem. -Ing. -Tech., 53:529 (1981)
- Büchner, E. G., Z. Phys. Chem., 56:257 (1906)
- Chai, C. P, Ph.D. Diss., Univ. of Delaware (1981)
- Chao, K. C., and J. D. Seader, AIChE J., 7:598 (1961)
- Charpentier, B. A., and M. R. Sevenants, ACS Symposium Series 366, American Chemical Society, Washington DC (1988)
- Cheong, P. L., D. Zhang , and K. Ohgaki, B.C.-Y. Lu, Fluid Phase Equilib., 29:555 (1986)
- Deiters, U. and G. M. Schneider, Ber. Bunsenges. Phys. Chem., 80:1316 (1976)
- Diepen, G. A. M., and F. E. C. Scheffer, J. Am. Chem. Soc., 70:4081 (1948)
- Diepen, G. A., and J. A. M. van Hest, in "The Physics and Chemistry of High Pressures", Symp. Soc. of Chem. Ind., London, 10 (1963)
- Dymond, J. H., E. B. Smith, The Virial Coefficients of Pure Gasses and Mixtures, Clarendon Press, Oxford (1980)
- "England Symposium", J. Fluid Phase Equilib., Vol. 10 (1983)
- Fall, D. J., and K. D. Luks, J. Chem. Eng. Data, 29:413 (1984)
- Gopal, J. S., G. D. Holder, and E. Kosal, IEC Proc. Des. Dev., 24:697 (1985)

Gruberski, T, Bull. Acad. Polon. Sci, Sér. sci. chim., 10:561 (1961)

Hannay, J. B., and J. Hogarth, Proc. R. Soc. London, 29:324 (1879) Hannay, J. B., and J. Hogarth, Proc. R. Soc. London, 30:484 (1880)

Henley, E. J., and J. D. Seader, Equilibrium-Stage Separation Operations in Chemical Engineering, John Wiley & Sons, New York (1981)

Hess, B. S., J. G. van Alsten, and C. A. Eckert, paper 147d presented at the 1986 AIChE annual meeting, Miami Beach, FL

Hong, G. T., M. Modell, and J. W. Tester, in Chemical Engineering at Supercritical Fluid Conditions, M. E. Paulaitis, J. M. L. Penninger, R. D. Gray, and P. Davidson eds., Ann Arbor Science: Ann Arbor, MI, p. 263 (1983)

Irani, C. A., and E. W. Funk, in CRC Handbook: Recent Developments in Separations Science, vol. 3, Part A, 171, CRC Press, Boca Raton, FL (1977)

Jangkamolkulchai, A., M. M. Arbuckle, and K. D. Luks, Fluid Phase Equilib., 40:235 (1988)

Johnston, K. P., and C. A. Eckert, AIChE J., 27:773 (1981)

Johnston, K. P., G. J. McFann, and R. M. Lemert, ACS Symp. Ser. 406, p. 140 (1989)

Johnston, K. P., in Encyclopedia of Chemical Technology, 3rd ed., Suppl. vol, p. 872, John Wiley & Sons, New York (1984)

Johnston, K. P., and J. M. L. Penninger, eds., ACS Symposium Series 406, American Chemical Society, Washington, DC (1989)

Johnston, K.P., D. H. Ziger, and C. A. Eckert, Ind. Eng. Chem. Fundam, 21:191 (1982)

King, M. B., D. A. Alderson, F. H. Fallah, D. M. Kassim, K. M. Kassim, J. R. Sheldon, and R. S. Mahmud, in Chemical Engineering at Supercritical Fluid Conditions, M. E. Paulaitis, J. M. L. Penninger, R. D. Gray, and P. Davidson eds., Ann Arbor Science: Ann Arbor, MI (1983)

Klochko-Zhovnir, Y. C., Zhurnal Prikladnoi Khimii, 22:484 (1949)

Kohn, J. P., Ph.D. Thesis, Univ. Kansas, Lawrence (1956)

Kohn, J. P., E. S. Andris, K. D. Luks, J. D. Colmenares, J. Chem. Eng. Data, 25:348 (1980)

- Kohn, J. P., K. D. Luks, P. H. Liu, and D. L. Tiffin, J. Chem. Eng. Data, 22:419 (1977)
- "Königstein Symposium", Ber. Bunsenges. Phys. Chem., Vol. 88 (1984)
- Krukonis, V. J., M. A. McHugh, A. J. Seckner, J. Phys. Chem., 88:2687 (1984)
- Krukonis, V. J., and R. T. Kurnik, J. Chem. Eng. Data, 30:247 (1985)
- Kuebler, G. P., and C. McKinley, Adv. Cryog. Eng., 21:509 (1976)
- Kulkarni, A. A., Ph.D. Thesis, University of Notre Dame, Indiana (1974)
- Kulkarni, A. A., B. Y. Zarah, K. D. Luks, and J. P. Kohn, J. Chem. Eng. Data, 19:92 (1974)
- Kurnik, R. T., S. J. Holla, and R. C. Reid, J. Chem. Eng. Data, 26:47 (1981)
- Kurnik, R. T., and R. C. Reid, Fluid Phase Equilib., 8:93 (1982)
- Lee, H. H., and J. C. Warner, J. Am. Chem. Soc., 57:318 (1935)
- Legret, D., D. Richon, H. Renon, AIChE. J., 27:203 (1981)
- Lemert, R. M., private communication to Dr. C. T. Lira (1988)
- Lemert, R. M., and K. P. Johnston, Fluid Phase Equilib., 45:265 (1989)
- Lentz, H., Rev. Sci. Instrum., 40:371 (1969)
- Lu, B. C.-Y., and D. Zhang, Pure & Applied Chem., 61:1065 (1989)
- Luks, K. D., Fluid Phase Equilib., 29:209 (1986)
- Mackay, M. E., and M. E. Paulaitis, Ind. Eng. Chem. Fund., 18:149 (1979)
- McHugh, M. A., Ph.D. Thesis, University of Delaware, (1981)
- McHugh, M. A., and V. J. Krukonis, Supercritical Fluid Extraction, Butterworths, Boston (1986)
- McHugh, M. A., and T. J. Yogan, J. Chem. Eng. Data, 29:112 (1984)

- McHugh, M. A., J. J. Watkins, B. T. Doyle, V. J. Krukonis, IEC Res., 27:1025 (1988)
- McHugh, M. A., A. J. Seckner, and T. J. Yogan, IEC Fundam., 23:493 (1984)
- Miller, M. M., and K. D. Luks, Fluid Phase Equilib., 44:295 (1989)
- Miller, M. M., A. Jangkamolkulchai, and K. D. Luks, Fluid Phase Equilib., 50:189 (1989)
- Paul, P. M. F., and W. S. Wise, The Principles of Gas Extraction, Mills and Boon Ltd., London (1971)
- Paulaitis, M. E., V. J. Krukonis, R. T. Kurnik, and R. C. Reid, Rev. Chem. Eng., 1:179 (1983a)
- Paulaitis, M. E., M. A. McHugh, and C. P. Chai, in Chemical Engineering at Supercritical Fluid Conditions, M. E. Paulaitis, J. M. L. Penninger, R. D. Gray, and P. Davidson eds., Ann Arbor Science: Ann Arbor, MI (1983)
- Paulaitis, M. E., J. M. L. Penninger, R. D. Gray Jr., and P. Davidson, eds., Chemical Engineering at Supercritical Fluid Conditions, Ann Arbor, MI, Ann Arbor Science (1983b)
- Peneloux, E., and E. Rauzy, Fluid Phase Equilib., 8:7 (1982)
- Peng, D. Y., and D. B. Robinson, Eng. Chem. Fundam., 15:59 (1976)
- Penninger, J. M. L., M. Radosz, M. A. McHugh, and V. J. Krukonis, eds., Process Technology Proceedings, vol. 3, Elsevier, New York (1985)
- Prausnitz, J. M., and P. R. Benson, AIChE J., 5:161 (1959)
- Prins, A., Proc. Acad. Sci., Amsterdam 17:1095 (1915)
- Randall, L. G., Sep. Sci. Tech., 17:1 (1982)
- Rastogi, R. P., K. T. R. Varma, J. Chem. Soc., :2097 (1956)

Rodrigues, A. B., and J. P. Kohn, J. Chem. Eng. Data, 12:191 (1967)

Schmitt, W. J., PhD. Diss., Massachusetts Institute of Technology

Schneider, G. M., E. Stahl, and G. Wilke, eds, Extraction with Supercritical Gases, Verlag Chemie, Weinheim, W. Germany (1980)

Sherman, W. F., and A. A. Stadtmuller, Experimental Techniques in High-Pressure Research, John Wiley & Sons LTD, New York (1987)

Simnick, J. J., C. C. Lawson, H. H. Lin, and K. C. Chao, AIChE J., 23:469 (1977)

Smith, R. D., J. P. Blitz, and J. L. Fulton, ACS Symp. Ser. 406, p. 165 (1989)

Smits, A., Proc. Roy. Acad. Sci. Amsterdam, 6:171 (1903-04a)

Smits, A., Proc. Roy. Acad. Sci. Amsterdam, 6:484 (1903-04b)

Smits, A., Proc. Roy. Acad. Sci. Amsterdam, 7:177 (1904-05)

Smits, A., Proc. Roy. Acad. Sci. Amsterdam, 8:196 (1905-06a)

Smits, A., Proc. Roy. Acad. Sci. Amsterdam, 8:568 (1905-06b)

Smits, A., Proc. Roy. Acad. Sci. Amsterdam, 12:231 (1909-10)

Smits, A., and J. P. Treub, Proc. Roy. Acad. Sci. Amsterdam, 14:183 (1911-12a)

Smits, A., and J. P. Treub, Proc. Roy. Acad. Sci. Amsterdam, 14:189 (1911-12b)

Soave, G., Chem. Eng. Sci., 27:1197 (1972)

Streett, W. B., and J. L. E. Hill, J. Chem. Phys., 54:5088 (1971)

Streett, W. B., and A. L. Erickson, Phys. Earth Planet Interiors, 5:357 (1972)

Tiffin, D. L., J. P. Kohn, and K. D. Luks, J. Chem. Eng. Data, 24:98 (1979a)

Tiffin, D. L., J. P. Kohn, and K. D. Luks, J. Chem. Eng. Data, 24:306 (1979b)

- Tsang, C. Y., and W. B. Streett, Chem. Eng. Sci., 36:993 (1981a)
- Tsang, C. Y., and W. B. Streett, Fluid Phase Equilib., 6:261 (1981b)
- Tsang, C. Y., P. Clancy, and W. B. Streett, Chem. Eng. Comm., 6:365 (1980)
- Valertis, R. L., Birmingham Univ. Chem. Eng., 17:38 (1966)
- van Gunst, C. A. E., F. E. C. Scheffer, and G. A. M. Diepen, J. Phys. Chem., 57:578 (1953a)
- van Gunst, C. A. E., F. E. C. Scheffer, and G. A. M. Diepen, J. Phys. Chem., 57:581 (1953b)
- van Gunst, C. A. E., "De Oplosbaarheid van Mengsels van Vaste Stoffen in Superkritische Gassen", Dissertation, Delft (1950)
- Van Leer, R. A., and M. E. Paulaitis, J. Chem. Eng. Data, 25:257 (1980)
- van Welie, G. S. A., and G. A. M. Diepen, Rec. Trav. Chim., 80:659 (1961a)
- van Welie, G. S. A., and G. A. M. Diepen, Rec. Trav. Chim., 80:666 (1961b)
- van Welie, G. S. A., and G. A. M. Diepen, Rec. Trav. Chim., 80:673 (1961c)
- van Welie, G. S. A., and G. A. M. Diepen, Rec. Trav. Chim., 80:683 (1961d)
- van Welie, G. S. A., and G. A. M. Diepen, Rec. Trav. Chim., 80:693 (1961e)
- Verchoyle, T. T. A., Phil. Trans. R. Soc. London, ser. A, 230:189 (1931)
- Villard, P., J. Phys., 5:455 (1896)
- Williams, D. F., Chem. Eng. Sci., 36:1769 (1981)
- White, G. L., C. T. Lira, ACS Symp. Ser. 406, p. 111 (1989)
- Yamamoto, S., K. Ohgaki, and T. Katayama, J. Supercritical Fluids, 2:63 (1989)
- Zarah, B. Y., K. D. Luks, and J. P. Kohn, AIChE Symp. Ser. No. 140, 70:91 (1974)

Zhang, D., Y. Adachi, and B. C.-Y. Lu, Proc. Int. Symp. Supercritical Fluids, Nice, France, Oct. 1988; Tome 1, p.19

Ziger, D. H., and C. A. Eckert, Ind. Eng. Chem. Process Des. Dev., Vol. 22:582 (1983)

MICHIGAN STATE UNIV. LIBRARIES



31293009063581